



HAL
open science

Approches physiopathologiques et pharmacologiques de la fonction microvasculaire dans la Sclérodermie systémique

Florence Gaillard-Bigot

► **To cite this version:**

Florence Gaillard-Bigot. Approches physiopathologiques et pharmacologiques de la fonction microvasculaire dans la Sclérodermie systémique. Médecine humaine et pathologie. Université Grenoble Alpes, 2017. Français. NNT : 2017GREAS032 . tel-01719381

HAL Id: tel-01719381

<https://theses.hal.science/tel-01719381>

Submitted on 28 Feb 2018

HAL is a multi-disciplinary open access archive for the deposit and dissemination of scientific research documents, whether they are published or not. The documents may come from teaching and research institutions in France or abroad, or from public or private research centers.

L'archive ouverte pluridisciplinaire **HAL**, est destinée au dépôt et à la diffusion de documents scientifiques de niveau recherche, publiés ou non, émanant des établissements d'enseignement et de recherche français ou étrangers, des laboratoires publics ou privés.

THÈSE

Pour obtenir le grade de

DOCTEUR DE LA COMMUNAUTE UNIVERSITE GRENOBLE ALPES

Spécialité : **Biotechnologie, instrumentation, signal et Imagerie
pour la biologie, la médecine et l'environnement**

Arrêté ministériel : 25 mai 2016

Présentée par

Florence GAILLARD-BIGOT

Thèse dirigée par le **Pr Jean-Luc CRACOWSKI**, Unité de
pharmacologie Clinique Inserm CIC1406

préparée au sein du **Laboratoire HP2 – Inserm U1042**
dans **l'École Doctorale Ingénierie pour la Santé, la Cognition et
l'Environnement**

Approches physiopathologiques et pharmacologiques de la fonction microvasculaire dans la Sclérodermie systémique

Thèse soutenue publiquement le **mercredi 11 octobre 2017**
devant le jury composé de :

Pr Olivier BLIN

Aix Marseille Université, Président du Jury

Pr Jean-Luc CRACOWSKI

Université Grenoble Alpes, Membre

Dr Guillaume MAHÉ

Université de Rennes, Rapporteur

Dr Guillaume WALTHER

Université d'Avignon et des pays de Vaucluse, Rapporteur

Dr Matthieu ROUSTIT

Université Grenoble Alpes, Membre

Dr Sophie BLAISE

Université Grenoble Alpes, Membre



Remerciements

Je remercie mon directeur de thèse et mentor, Monsieur Jean-Luc Cracowski, pour m'avoir encadré depuis le tout début de ce cursus scientifique. Ta joie et ta bonne humeur n'ont d'égale que ta curiosité et ta passion. Tu m'as transmis la flamme du chercheur et je garde précieusement en mémoire ma première expérience scientifique avec toi, lorsque nous avons dégonflé ce brassard lors du protocole EETY. Merci encore de cet apprentissage, ce soutien, ces moments de joie et de passion.

Je tiens à remercier également toute l'équipe du Centre d'Investigation Clinique du CHU de Grenoble. Ce fut un immense plaisir de travailler toutes ces années à vos côtés. Et notamment aux côtés de mes très chères Anne et Dominique (sans oublier mes débuts avec Nicole et son célèbre tempérament). Merci à vous tous: Matthieu, Kella, Johanne, Nicolas, Adeline, Christophe et tous les autres; vos personnalités et votre travail pour la recherche sont précieux et motivant.

Je remercie enfin tout particulièrement Claire, qui fut sans nulle doute un autre modèle personnel et professionnel pour moi. Ta douceur et ta gentillesse n'ont d'égale que ta clairvoyance et ta ténacité.

Je souhaite également remercier l'équipe de médecine vasculaire du Pr Carpentier et tout particulièrement Sophie, qui continue à nous honorer très régulièrement de sa présence lors de nos célèbres rendez-vous du « club microcirculation ». Ta rigueur m'a toujours servi d'exemple et tu sais entretenir un lien permanent entre recherche et clinique ; j'espère pouvoir en faire autant dans le futur !

Une pensée pour tous mes pairs de la psychiatrie, et notamment Monsieur Bougerol, Amandine, et récemment Monsieur Kara, Françoise et Virginie; qui m'ont permis indirectement de mener à bien ce cursus et également de me faire découvrir une passionnante spécialité, dévorante, inlassable, gratifiante et épanouissante pour moi.

Mes remerciements vont maintenant à l'Association des Sclérodermiques de France et à l'ensemble des patients atteints de sclérodermie pour m'avoir accordés une bourse d'études et participés activement à la réalisation de ce travail . Ce travail n'aurait jamais pu aboutir sans votre aide et votre implication. J'ai également pu faire la connaissance de personnalités extraordinaires à l'occasion des manifestations organisés par l'Association.

Je remercie également chaleureusement la Société Française de Pharmacologie et de Thérapeutique pour m'avoir accordée une bourse d'étude, et le laboratoire HP2 pour avoir permis cette collaboration pendant plus de 6 ans.

Une pensée à tous les étudiants qui sont passés au CIC pendant mon cursus, et qui pour certains sont maintenant bien lancés dans la recherche (Marcin, en plus d'être pleins de ressources, tu es également un sacré farceur, pour avoir fait croire à Jean-Luc que les étudiants ERASMUS étaient travailleurs, curieux, intéressants et motivés...).

Je remercie bien sûr ma belle-famille : Jacqueline, Gilbert, Sonia et Julien (et maintenant Basile...). Vous êtes la famille que je n'ai plus, qui me soutient et m'épaulé à toutes les étapes d'une vie.

Merci enfin à toi, Boris. Les mots de notre langue sont bien trop fades pour résumer ce que je voudrais écrire. Alors comme Grenouille de Süskind, imagine que le langage recèle autant de nuances pour te décrire ma gratitude pour ton soutien, ton courage, ta passion et mon amour pour toi.

Que tous ceux qui comptent pour moi et que j'ai inexorablement oubliés, mais qui se reconnaîtrons, me pardonnent.

Résumé

Approches physiopathologiques, pharmacologiques et thérapeutiques de la microcirculation cutanée

La microcirculation cutanée a été proposée comme modèle d'étude de la dysfonction microvasculaire globale dans les maladies cardiovasculaires. Par ailleurs, elle est spécifiquement atteinte dans la sclérodemie systémique (SSc), qui est une maladie dysimmunitaire rare, particulièrement invalidante, caractérisée par une fibrose cutanée et viscérale associée à une atteinte microvasculaire diffuse et la présence d'auto anticorps dirigés contre des antigènes cellulaires. L'exploration de la fonction microvasculaire cutanée suscite donc un réel intérêt, même s'il n'existe pas de technique standardisée pour l'étude de la fonction microvasculaire, en particulier endothéliale.

La première partie de ce travail a porté sur l'étude physiologique de la microcirculation cutanée chez le volontaire sain, en utilisant les méthodes les plus récentes adaptées à l'étude fonctionnelle de la microcirculation (tests de réactivité vasculaire couplés à l'enregistrement du flux sanguin cutané par *laser speckle contrast imaging*). Dans une seconde partie, nous avons étudié la pathologie de la microcirculation cutanée dans la sclérodemie systémique, en utilisant les mêmes d'étude fonctionnelle de la microcirculation. La dernière partie de cette thèse a été consacrée à l'étude d'une nouvelle approche pharmacologique et thérapeutique dans la prise en charge des manifestations vasculaires cutanées périphériques identifiées chez les patients. Nous avons évalué l'effet vasodilatateur du tréprostinil, analogue de la prostacycline, sur le flux sanguin cutané de divers zones anatomiques, chez le volontaire sain, le patient atteint de SSc, le patient diabétique et lors d'un refroidissement local dans la SSc.

Mots-clés : microcirculation – flux sanguin cutané – sclérodemie systémique – *laser speckle contrast imaging* – hyperhémie post-occlusive – tréprostinil – iontophorèse – refroidissement local.

Summary

Physiopathological, pharmacological and therapeutic approaches of cutaneous microcirculation

Cutaneous microcirculation has been proposed as a model to study the global microvascular dysfunction occurring in cardiovascular diseases. Furthermore, it is specifically impaired in systemic sclerosis (SSc), which is a rare and particularly invalidating auto-immune disease, characterized by a cutaneous and visceral fibrosis, associated with a diffuse microvascular impairment and auto-antibodies targeting some cellular antigens. The study of cutaneous microvascular function provides a real interest despite the lack of available standardized techniques, particularly to explore endothelial microvascular function.

In the first part of this work, we aimed to study the physiology of cutaneous microcirculation in healthy volunteers, using the more recent methods in this field, adapted to functional study of microcirculation (vascular reactivity tests coupled with cutaneous blood flow recording by laser speckle contrast imaging). The second part of our work aimed to study the pathology of cutaneous microcirculation in SSc volunteers, by using the same functional exploration methods. The last part of this work has been dedicated to a new pharmacologic and therapeutic approach for the management of peripheral cutaneous vascular manifestations in patients, using innovating technics as cutaneous iontophoresis. We studied the vasodilator effect of treprostinil, a prostacycline analogue, on cutaneous blood flow in several anatomic regions in healthy subject, SSc patient and diabetic patient, and also during a local cooling in SSc.

Keywords: microcirculation, cutaneous blood flow, systemic sclerosis, laser speckle contrast imaging, post-occlusive reactive hyperemia, treprostinil, iontophoresis, local cooling.

Cette thèse a été préparée au sein de l'unité Inserm U1042 - Laboratoire HP2
Institut Jean Roget, Faculté de Médecine et de Pharmacie de Grenoble
38042 Grenoble, France

Les études cliniques se sont déroulées dans l'unité de Pharmacologie clinique du Centre
d'Investigation Clinique – Inserm CIC 1406, CHU de Grenoble
38043 Grenoble, France

Tables des matières

Remerciements	2
Résumé	4
Summary	5
Liste des abréviations	9
Introduction	11
Partie I. Approche physiologique de la microcirculation cutanée	17
1. Les médiateurs vasculaires de la microcirculation	18
2. L'hyperhémie post-occlusive	24
3. La microdialyse cutanée	27
Première étude: Faisabilité de la microdialyse cutanée associée au Laser Speckle Contrast Imaging pour évaluer la réactivité microvasculaire (titre court: EETY, étude préliminaire)	30
Deuxième étude : Rôle des acides époxy-eicosatriénoïques (EETs) dans l'hyperhémie post-occlusive (titre court : EETY)	40
Troisième étude : Rôle des cyclo-oxygénases (COX) dans l'hyperhémie post-occlusive (titre court : EETY, étude ancillaire)	51
Partie II. Approche de la pathologie de la microcirculation cutanée : exemple de la sclérodémie systémique	61
Quatrième étude : Intérêt du laser SPEckle Contrast Imaging dans la détection de la dysfonction microvasculaire cutanée de la Sclérodémie systémique (titre court : SPECIES)	66
Partie III. Approches pharmacologiques et thérapeutiques de l'iontophorèse de tréprosténil appliquée à la microcirculation cutanée	76
1. La thérapeutique de la sclérodémie systémique	77
2. Principes de l'iontophorèse	81
3. L'iontophorèse thérapeutique dans la SSc : synthèse des études cliniques et précliniques menées par l'équipe depuis 2009	87
Cinquième étude : Iontophorèse de Tréprosténil, une étude Pharmacodynamique et Pharmacocinétique, preuve de concept (titre court: TIPPS)	90

Sixième étude : Efficacité de l'iontophorèse de tréprostinil sur un biomarqueur intermédiaire, test de refroidissement cutané local (titre court: TIPPS, étude ancillaire)	100
Septième étude : Effets vasculaires de l'iontophorèse cutanée de tréprostinil sur la jambe, le doigt et le pied : escalade de doses (titre court : TIPPS, étude ancillaire)	108
Huitième étude : Effet vasculaires de l'iontophorèse cutanée de tréprostinil chez le diabétique (titre court : TIPPS, étude ancillaire)	117
Perspectives et conclusion	126
1. Perspectives physiopathologiques de l'étude de la microcirculation cutanée	127
2. Perspectives thérapeutiques de l'iontophorèse de tréprostinil appliquée à la microcirculation cutanée	130
Références	133

Liste des abréviations

AA : acide arachidonique

AMPc ou cAMP : adénosine monophosphate cyclique

ATP : adénosine triphosphate

AUC ou ASC : aire sous la courbe

BKCa : canaux calciques à conduction rapide activés par le potassium

Ca²⁺ : ion calcique

COX : cyclo-oxygénase

CVC : conductance vasculaire cutanée

CYP450 : cytochrome P450

EDHF : facteur hyperpolarisant dérivé de l'endothélium

EETs : acides époxy-eicosatriénoïques

eNOS : isoforme endothéliale de la NO synthase

GMPc ou cGMP : guanosine monophosphate cyclique

GTP : guanosine triphosphate

H₂O₂ : peroxyde d'hydrogène

IP₃ : inositol triphosphate

K⁺ : ion potassique

K_{Ca} : canaux potassiques activés par le calcium

L-NAME : N(G)-nitro-L-arginine-méthyl ester

L-NMMA : N(G)- monométhyl-L-arginine

LDF : *laser Doppler flowmetry*, fluxmétrie par laser Doppler

LDI : *laser Doppler imaging*, imagerie par laser Doppler

LSCI : *laser speckle contrast imaging*, imagerie de granularité

LTH : *local thermal hyperemia*, hyperhémie thermique locale

mmHg : millimètre(s) de mercure

NADP : nicotinamide adénine dinucléotide phosphate

NO : monoxyde d'azote

NOS : NO synthase

pH : potentiel hydrogène

pO₂ : pression partielle d'oxygène

PORH : *postocclusive reactive hyperemia*, hyperémie post-occlusive

PGI₂ : prostacycline

RE : réticulum endoplasmique

ROI : *region of interest*, région d'intérêt

SNP : nitroprussiate de sodium

SOD : superoxyde dismutase

SSc : sclérodémie systémique

TEA : chlorure de tétra-éthyl-ammonium

UD : ulcère digital

Introduction

La microcirculation désigne historiquement l'ensemble des vaisseaux non visibles à l'œil nu, c'est-à-dire approximativement de diamètre inférieur à 150 μm , parmi les artérioles, les veinules, les "shunts" artério-veineux et les capillaires. La microcirculation ne représente qu'une petite part du volume corporel (environ moins de 10%), mais elle est organisée pour être distribuée de façon ubiquitaire (1).

De par son rôle fondamental de nutrition et d'élimination des déchets de pratiquement toutes les cellules du corps humain, la microcirculation joue un rôle fondamental au bon fonctionnement tissulaire. Par ailleurs, les artérioles jouent un rôle central dans la régulation des résistances périphériques, afin de protéger les capillaires en cas d'élévation trop importante de la pression artérielle et de permettre une distribution optimale de l'oxygène et nutriments aux tissus (2).

La microcirculation joue également un rôle clé dans la régulation thermique. La réactivité microvasculaire cutanée est régulée de façon fine par des mécanismes centraux ainsi que par des facteurs locaux sensibles aux variations de température (3).

La microcirculation cutanée présente l'avantage d'être facilement accessible à l'exploration de par sa situation superficielle, permettant son étude de façon non invasive (4). Son implication est maintenant bien connue dans certaines pathologies comme la sclérodémie systémique (SSc), où sa dysfonction grève en partie le pronostic fonctionnel.

Des méthodes d'évaluation précises et sensibles de la dysfonction microvasculaire chez l'homme sont donc un élément clé pour permettre sa détection précoce, quantifier la sévérité de l'atteinte, ainsi que pour étudier la physiopathologie de cette atteinte (5,6). Contrairement à la méthode d'étude de la dilatation débit-dépendante de l'artère humérale, examen de référence pour l'étude de la dilatation endothéliale-dépendante des vaisseaux de conductance (7), il n'existe pas de technique standardisée pour l'étude de la fonction microvasculaire, en particulier endothéliale. La fonction microvasculaire cutanée peut être étudiée en routine chez l'homme à l'aide de techniques d'imagerie laser (8), particulièrement adaptées pour des maladies impliquant le tissu cutané, telles que la sclérodémie.

Les techniques d'imagerie dérivées du laser Doppler sont basées sur la réflexion d'un faisceau de lumière monochromatique (faisceau laser), qui subit un effet Doppler comparable à celui décrit initialement pour les ondes sonores.

Le signal obtenu est corrélé au flux microvasculaire, et ce, de façon linéaire. Cet effet laser Doppler est à la base de deux techniques courantes rappelées ci-dessous (LDF et LDI).

La technique de *fluxmétrie par laser Doppler* (LDF) fut l'une des premières techniques utilisées pour explorer le flux de la microcirculation cutanée. Ce système a l'avantage d'une grande résolution temporelle (enregistrement continu) mais présente parallèlement une très mauvaise résolution spatiale (analyse via un seul faisceau laser), réhibitoire pour une utilisation clinique en dehors de certains sites (9,10). Cette mauvaise résolution spatiale peut être améliorée à l'aide de sondes comportant plusieurs fibres émettrices/réceptrices.

À la suite, s'est développée la technique *d'imagerie par laser Doppler* (Laser Doppler Imaging ou LDI), conçue pour améliorer la résolution spatiale de la LDF. Elle consiste en bref à balayer par un faisceau laser – en général par l'intermédiaire d'un miroir – une surface définie au préalable. Cependant, le gain très net en termes de résolution spatiale est contrebalancé par la durée nécessaire au balayage de la surface étudiée par le faisceau laser, ce qui altère fortement la résolution temporelle et ne permet donc pas d'étudier des phénomènes de cinétique rapide (11).

Plus récemment, est apparu une nouvelle technique d'imagerie laser, qui n'utilise pas l'effet Doppler. Il s'agit de *l'imagerie laser par analyse de la granularité* du faisceau (*Laser Speckle Contrast Imaging* ou LSCI). Ce système, constitué d'une source laser et d'une caméra de haute résolution, permet l'acquisition d'images à très grande vitesse. La variation d'intensité de chaque granularité (que l'on peut comprendre comme étant les variations d'intensité d'un pixel à un autre pixel dont les coordonnées spatiales sont identiques d'une image à l'autre) permet de calculer la vitesse des éléments responsables de cette variation. Cette méthode permet de combiner une haute résolution temporelle à une haute résolution spatiale et apparaît très prometteuse et reproductible pour étudier le flux sanguin de la microcirculation cutanée (12).

Enfin, lors de l'étude du flux sanguin de la microcirculation cutanée en LDF, LDI ou LSCI, des tests de provocation (ou tests de réactivité vasculaire) peuvent être réalisés soit par hyperhémie post-occlusive (hyperhémie post-ischémique), soit par chauffage cutané local (hyperhémie thermique), soit par passage de molécules par voie transdermique (iontophorèse), soit par passage de drogues vaso-actives par voie intradermique (microdialyse).

La sclérodermie systémique est une maladie dysimmunitaire rare (prévalence de 50 à 300 patients par million d'habitants, soit un total de 9 000 à 12 000 patients en France), caractérisée par une atteinte vasculaire et une fibrose cutanée pouvant engager le pronostic vital. La thérapeutique est limitée car aucun traitement étiologique n'existe et la prise en charge est de fait axée sur les traitements symptomatiques des différentes atteintes. La dysfonction vasculaire est un élément clé dans la pathogénie de cette maladie et concerne à la fois la microcirculation et les artères de conductance. La microcirculation présente des anomalies de structure et de fonction, qui sont interdépendantes. Cette microangiopathie est caractérisée sur un plan structural par une raréfaction capillaire, le développement de mégacapillaires, et une oblitération vasculaire (13,14). Sur un plan fonctionnel, la dysfonction microvasculaire est un évènement précoce dans la pathogénie de la maladie (15). Les principaux symptômes de ce dysfonctionnement sont représentés d'une part par un phénomène de Raynaud secondaire à la sclérodermie, qui est une source de gêne fonctionnelle sévère, et d'autre part, par des ulcérations digitales, qui sont fréquentes et extrêmement invalidantes, pouvant par exemple conduire à l'amputation d'un ou de plusieurs segments de doigts et représentent la première source de handicap fonctionnel chez ces patients. Actuellement, la prise en charge thérapeutique de ces manifestations vasculaires périphériques est limitée et au mieux partiellement efficace (16).

La dysfonction de la microcirculation est également impliquée dans le développement de complications de nombreuses pathologies, notamment vasculaires (17), suggérant la possible implication d'une dysfonction microvasculaire généralisée dans l'origine de ces pathologies (18–20). Il n'est de fait pas étonnant que la peau ait été – et soit encore – utilisée en tant que modèle pour explorer la fonction microvasculaire dans de nombreuses maladies (19, 21–25).

Enfin, chez le sujet âgé, la microcirculation cutanée est tout particulièrement impliquée dans la genèse et le traitement des escarres, qui sont souvent un des aspects centraux du pronostic fonctionnel voire vital en milieu hospitalier pour cette population fragile.

Ainsi que nous venons de la résumer, l'exploration de la microcirculation cutanée présente à la fois un intérêt comme marqueur d'une dysfonction microvasculaire globale dans de nombreuses pathologies vasculaires, mais aussi dans l'amélioration de la caractérisation de la dysfonction locale – enjeu majeur dans les atteintes acrales au cours de la SSc – et enfin pour le développement de nouvelles perspectives thérapeutiques.

Schéma organisationnel des études (Figure 1)

La première partie de ce travail de thèse porte sur l'étude physiologique de la microcirculation cutanée chez le volontaire sain, en utilisant les méthodes les plus récentes adaptées à l'étude fonctionnelle de la microcirculation.

La deuxième partie de ce travail aborde l'approche de la pathologie de la microcirculation cutanée avec l'exemple de la sclérodémie systémique, en utilisant les méthodes les plus récentes adaptées à l'étude fonctionnelle de la microcirculation.

La troisième partie est consacrée à l'étude d'une nouvelle approche pharmacologique et thérapeutique dans la prise en charge des manifestations vasculaires cutanées périphériques.

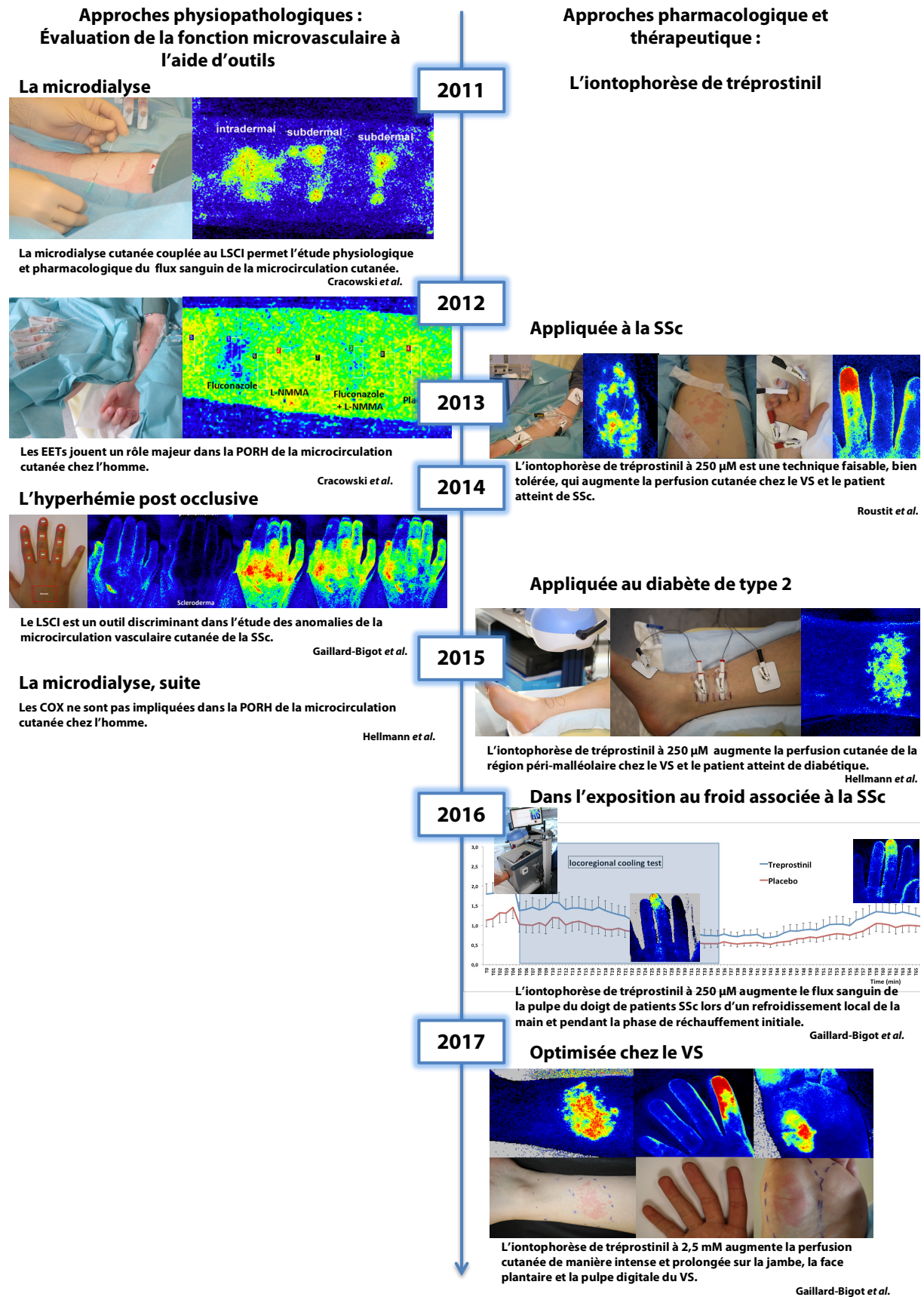


Figure 1. Schéma organisationnel des études.

LSCI : *laser speckle contrast imaging*. EETs : acides époxy-eicosatriénoïques. PORH : *postocclusive reactive hyperemia*. COX : cyclo-oxygénase. SSc : sclérodémie systémique. VS : volontaire sain.

Partie I. Approche physiologique de la microcirculation cutanée

1. Les médiateurs vasculaires de la microcirculation

L'endothélium est, d'un point de vue histologique, un épithélium simple pavimenteux – c'est à dire une monocouche de cellules appelées endothéliales, qui forment l'intima – reposant sur une lame basale et connectées avec leurs voisines par différents types de jonctions. Parmi les trois tuniques vasculaires de l'arbre vasculaire (composées de l'intima, de la media – dans des proportions variables – et de l'adventice), l'endothélium est la couche la plus interne de tous les vaisseaux sanguins, en contact avec le sang. Deux particularités structurales sont remarquables au sein des plus petits vaisseaux cutanés, les capillaires : d'une part, l'absence de media – qui permet de favoriser les échanges – et, d'autre part, la présence de péricytes – dont les rôles sont encore mal connus et comprendraient une fonction de vasoconstriction locale et des fonctions métaboliques. L'endothélium représente une surface d'échange évaluée entre 280 et 350 m² (26) et près de 1 à 2 % de la masse corporelle totale (27). Occupant une position stratégique à l'interface entre le sang et les tissus, l'endothélium n'est pas une simple barrière inerte mais un organe dynamique qui possède une grande variété de fonctions. Longtemps assimilé à une simple « enveloppe » impliquée dans le processus de l'hémostase, l'endothélium est actuellement considéré aussi comme une glande endocrine ainsi que comme un intégrateur des processus tissulaires sous-jacents. Il réagit aux modifications chimiques, physiques et humorales qui surviennent dans son environnement, par la synthèse et la libération de nombreux facteurs impliqués dans la modulation de l'angiogenèse, l'inflammation, l'hémostase, la vasomotricité et la perméabilité vasculaire (28). L'endothélium maintient ainsi un équilibre entre vasoconstriction et vasodilatation, inhibition et promotion de la prolifération et de la migration des cellules musculaires lisses sous-jacentes, prévention et stimulation de l'adhésion et de l'agrégation plaquettaire, thrombose et fibrinolyse.

Il contribue donc de façon majeure à l'homéostasie du système cardiovasculaire (29,30) et les mécanismes précis contrôlant cette homéostasie sont complexes et résultent d'interactions entre le sang, l'endothélium et les cellules musculaires lisses.

L'endothélium module le tonus et la vasomotricité des cellules musculaires lisses sous-jacentes en libérant de nombreux facteurs de relaxation et de contraction. Dans les conditions normales, la libération des facteurs de relaxation prévaut sur celle des facteurs de contraction (Figure 2). L'endothélium contrôle le tonus vasculaire par la libération de monoxyde d'azote (NO), de prostaglandines vasodilatatrices, comprenant notamment la prostacycline (PGI_2), et de facteurs hyperpolarisants dérivés de l'endothélium (EDHF).

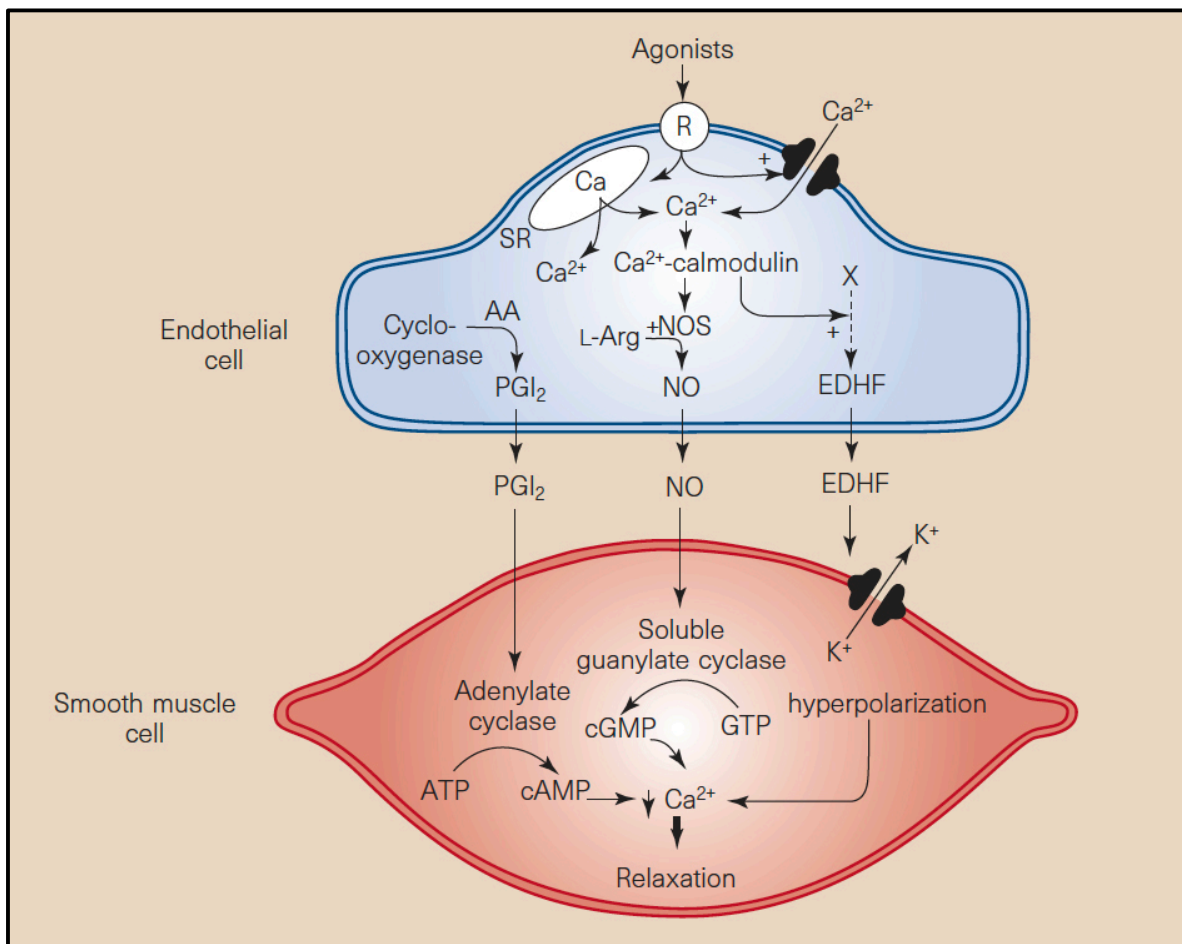


Figure 2. Libération de facteurs de relaxation d'origine endothéliale. L'activation des récepteurs endothéliaux induit un flux de calcium dans le cytoplasme des cellules endothéliales. Lorsque les agonistes activent les cellules endothéliales, une augmentation de l'inositol triphosphate (IP_3) pourrait contribuer à l'augmentation du Ca^{2+} cytoplasmique en induisant sa libération par le réticulum endoplasmique (RE). Après interaction avec la calmoduline (calmodulin), le Ca^{2+} active la NO synthase (NOS) et entraîne la libération de facteur endothélial hyperpolarisant (EDHF). L'augmentation du Ca^{2+} accélère également la formation de prostacycline (PGI_2) à partir de l'acide arachidonique (AA) par la voie de la cyclo-oxygénase. Le NO provoque la relaxation en activant la formation de guanosine monophosphate cyclique (cGMP) à partir de la guanosine triphosphate (GTP). La prostacycline provoque la relaxation en activant la formation d'adénosine monophosphate cyclique (cAMP) à partir de l'adénosine triphosphate (ATP). L'EDHF provoque l'hyperpolarisation et la relaxation en ouvrant les canaux K^+ . (D'après Vanhoutte, Nature 1998).

Endothélium et régulation du tonus vasodilatateur

La voie du NO (Figure 2).

Dans les cellules endothéliales, le NO est obtenu par oxydation NADPH-dépendante et oxygène-dépendante de la L-arginine sous l'action de la NO synthase (NOS), libérant également de la L-citrulline (31). La NOS est une oxydoréductase qui existe au moins sous trois isoformes, codées par des gènes distincts (32–35) ; l'isoforme endothéliale (eNOS) est celle qui est considérée dans le cadre de ce travail. Très labile, le NO diffuse d'une part vers la lumière vasculaire, où il exerce un rôle antiagrégant et anti-adhérent sur les plaquettes circulantes et, d'autre part, vers le pôle basal de l'endothélium, où il provoque une relaxation des cellules musculaires lisses en augmentant le taux intracellulaire de GMP cyclique (GMPc ou cGMP) (36).

La voie de l'EDHF (Figure 2).

Le facteur endothélial hyperpolarisant (EDHF), dont la nature chimique n'est toujours pas connue et qui suscite toujours de nombreuses controverses (37), stimule l'ouverture des canaux potassiques des cellules musculaires lisses entraînant ainsi leur hyperpolarisation et leur relaxation (38). On distingue actuellement l'EDH (hyperpolarisation musculaire lisse liée à une hyperpolarisation de l'endothélium) des EDHFs (libération de molécules provenant de l'endothélium induisant une hyperpolarisation des cellules musculaires lisses sans hyperpolarisation endothéliale). Il semble exister plusieurs EDHFs, qui pourraient correspondre dans certains vaisseaux aux acides époxy-eicosatriénoïques (EETs), métabolites formés à partir de l'acide arachidonique (AA) par l'action du cytochrome P450 (39).

La voie des prostacyclines (Figure 2).

La prostacycline (PGI_2), dérivée de l'acide arachidonique, exerce son action vasodilatatrice en élevant le taux intracellulaire d'AMP cyclique (AMPc ou cAMP). Les effets de la PGI_2 sont intimement liés à ceux du NO. La PGI_2 facilite la libération endothéliale de NO, qui, en retour, potentialise l'action de la PGI_2 au niveau musculaire lisse par inhibition de la phosphodiesterase (40). Toutefois, la contribution de la PGI_2 à la relaxation endothélium-dépendante est beaucoup moins importante que celle du NO (41).

Endothélium et régulation du tonus vasodilatateur

La vasoconstriction endothélium-dépendante résulte de la libération de substances telles que la prostaglandine H_2 , les radicaux libres dérivés de l'oxygène, l'angiotensine II, le thromboxane A_2 , et l'endothéline-1.

La voie des EETs: une nouvelle approche des facteurs impliqués dans la relaxation endothéliale-dépendante (Figure 3)

Dans les cellules endothéliales des artères de conductance, des agonistes tels que la bradykinine ou le stress de cisaillement (*shear stress*) augmentent la concentration calcique intracellulaire qui active la phospholipase A_2 pour produire de l'acide arachidonique. Sa métabolisation par le cytochrome P450 génèrerait des acides époxy-eicosatriénoïques (EETs) (42–44).

Les EETs stimuleraient alors les petits et gros canaux potassiques calcium-dépendants (K_{Ca}) des cellules endothéliales et des cellules musculaires lisses, ainsi que les jonctions gap entre ces deux types cellulaires. D'une part, le passage de potassium dans l'interstitium activerait un courant potassique rectifiant entrant (K^+_{IR}) ainsi que la pompe Na/K-ATPase des cellules musculaires lisses et provoquerait l'hyperpolarisation. D'autre part, le passage d'AMP cyclique par les jonctions gap aboutirait également à l'hyperpolarisation des cellules musculaires lisses. Parallèlement, dans les cellules endothéliales, les mêmes signaux activeraient la NOS permettant la production d'ions superoxydes que la superoxyde dismutase (SOD) métaboliserait en peroxyde d'hydrogène (H_2O_2). Celui-ci pourrait, par les mêmes voies que les EETs, provoquer l'hyperpolarisation des cellules musculaires lisses. Ces voies sont mises en évidence lors de l'inhibition des deux voies endothéliales principales que sont celle de la production endothéliale de NO par l'eNOS (voie du GMPc), et celle de la synthèse endothéliale de prostacyclines (PGI_2) par les cyclo-oxygénases (COX) endothéliales (voie de l'AMPc).

Cependant, il faut souligner que ces interactions (Figure 3) ne sont pas encore démontrées au niveau de la microcirculation.

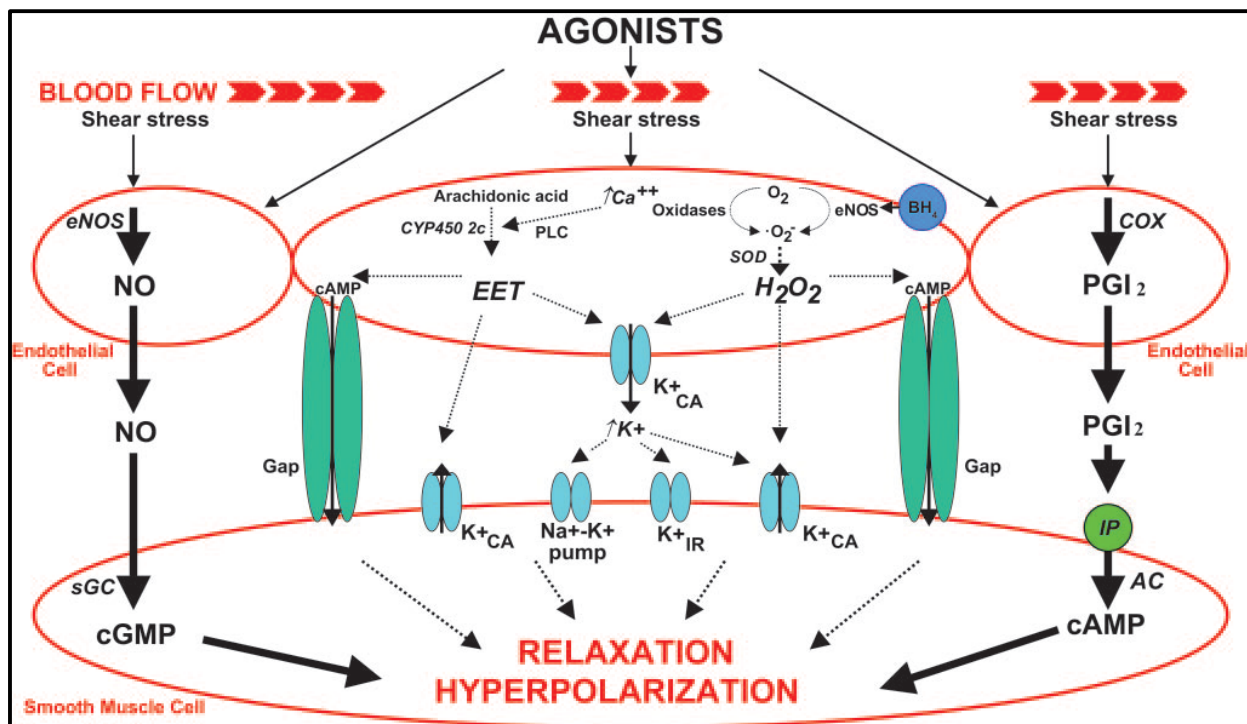


Figure 3. Représentation schématique des mécanismes de dilatation endothéliale. Au centre, ceux liés à l'hyperpolarisation des cellules musculaires lisses. (Schéma de Quyyumi, Hypertension 2006).

Outils pharmacologiques utilisés

Actuellement, des méthodes pharmacologiques d'étude de la microcirculation se développent, mais elles sont essentiellement utilisées au niveau des artères de conductance. Les outils suivants sont classiquement utilisés dans les études physiopathologiques :

- Le L-NMMA et le L-NAME sont des inhibiteurs des NOS, d'intérêt expérimental et permettant d'inhiber la première des deux voies principales ;
- L'aspirine et les anti-inflammatoires non stéroïdiens permettent d'inhiber la voie des cyclo-oxygénases ;
- Le fluconazole est un inhibiteur du CYP2C9 et CYP2C19, et inhibe l'époxydation de l'acide arachidonique et limite donc la libération des EETs ;
- Le chlorure de tétraéthyl-ammonium (TEA) est un antagoniste non sélectif des canaux K_{Ca} ;

- Le nitroprussiate de sodium (SNP) est un donneur de NO qui réagit avec les groupes sulfhydryl tissulaires dans des conditions physiologiques, pour produire directement du NO. Il induit ainsi une relaxation des cellules musculaires lisses, de manière égale sur toutes les cellules musculaires lisses, artérielles et veineuses. Il est donc à l'origine d'une vasodilatation endothélium-indépendante (45).
- Le mélange équimassique de lidocaïne et prilocaïne permet l'abolition du réflexe axonal lors de l'hyperhémie thermique au niveau de la microcirculation sous-cutanée (46).

2. L'hyperhémie post-occlusive

L'hyperhémie post-occlusive (PORH), parfois aussi appelée hyperhémie post-ischémique, fait référence à l'augmentation du flux sanguin cutané au-dessus de la valeur basale de ce flux, suite à la résolution brutale d'une courte occlusion artérielle (8). Elle est en général obtenue en distalité (au niveau de la main, par exemple) en gonflant un brassard situé au niveau de l'artère humérale homolatérale à 50 mmHg au-dessus de la pression artérielle systolique du sujet pendant 5 minutes, avant de le dégonfler brutalement.

La réponse hyperhémique post-occlusive se décompose en deux phases : un pic initial, survenant dès les premières secondes après l'arrêt de l'occlusion artérielle, suivi d'une phase hyperhémique davantage prolongée. L'enregistrement de cette réponse de vasodilatation post-occlusion artérielle permet d'en apprécier l'amplitude, mais aussi la cinétique (Figure 4).

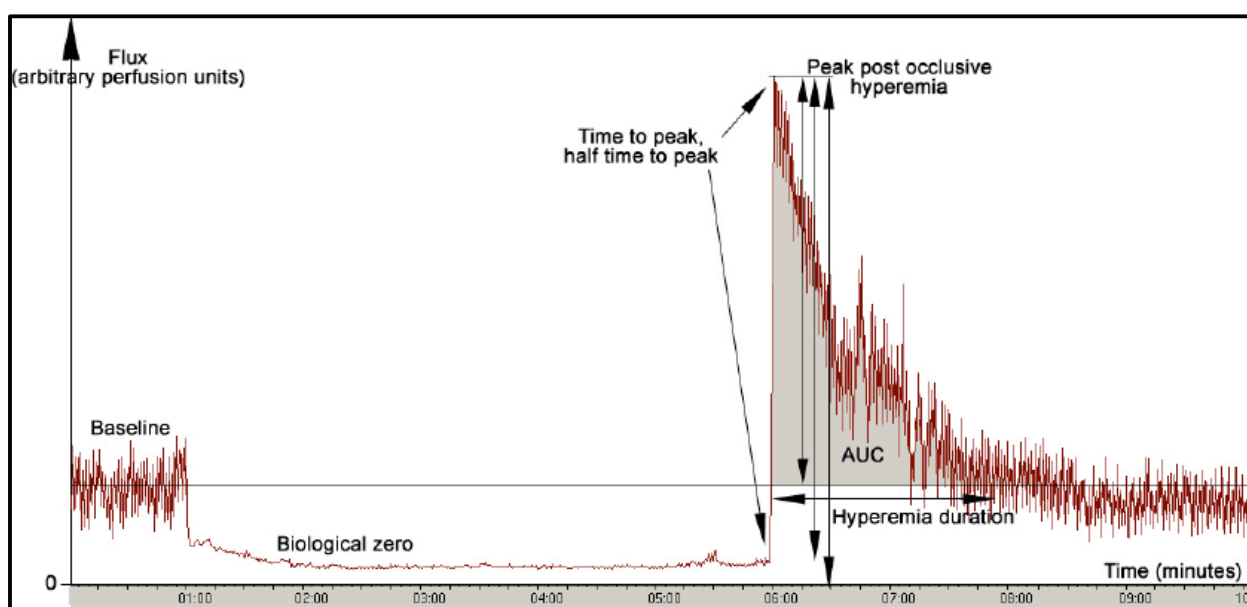


Figure 4. Tracé typique d'hyperhémie post-occlusive après 5 minutes d'occlusion de l'artère humérale chez un sujet sain. Le zéro biologique correspond au signal laser Doppler en l'absence de flux. Il existe différentes modalités d'expression du pic d'hyperhémie (d'après Cracowski, Trends Pharmacol Sci 2006).

Les mécanismes exacts de l'hyperhémie post-occlusive au niveau de la microcirculation cutanée ne sont pas encore totalement élucidés. Quatre facteurs seraient impliqués dans l'hyperhémie post-occlusive : des vasodilatateurs dits métaboliques (adénosine, canaux potassiques ATP-dépendants, pH, pO₂), des vasodilatateurs dits endothéliaux, la réponse myogénique et le réflexe axonal.

Parmi les vasodilatateurs endothéliaux, ce sont les prostaglandines qui apparaîtraient avoir le rôle le plus important (47), avec cependant des résultats contradictoires (48–50). Le système nerveux périphérique, par un phénomène appelé réflexe axonal, est partiellement impliqué (51,52). La réponse myogénique, quant à elle, ferait appel à des neuromédiateurs locaux impliquant les canaux calciques à conduction rapide activés par le potassium (BKCa), qui semblent jouer un rôle majeur (51), suggérant aussi une implication de l'EDHF. La contribution du NO est discutée, avec des résultats divergents (50,53,54), sauf sur la pulpe du doigt où la réponse semble partiellement NO-dépendante (55).

De par les mécanismes mis en jeu lors de sa réalisation, la PORH pourrait ne pas seulement être considérée comme un test de réactivité vasculaire de la fonction endothéliale, mais aussi comme un potentiel marqueur de modification de la fonction microvasculaire. De multiples paramètres peuvent être utilisés pour exprimer le flux vasculaire secondaire à l'occlusion artérielle (Figure 5). L'un des plus utilisés est le pic initial, survenant dès les premières secondes après la fin de l'occlusion artérielle. Il peut être exprimé soit en valeur brute, soit par rapport à la ligne de base. Dans ce dernier cas, le pic peut être soit exprimé comme la différence entre la valeur du pic et la valeur de la ligne de base, soit exprimé comme aire sous la courbe, ou encore exprimé en pourcentage de changement relatif (par le calcul : $[(\text{valeur au pic} - \text{valeur à la ligne de base}) / \text{valeur à la ligne de base}] \times 100$). Le pic initial peut également être exprimé par sa valeur relative à l'échelle de la « vasodilatation maximale » ; cette-dernière étant obtenue lorsque la peau est chauffée à 42°C ou plus (3). La phase hyperhémique prolongée, suivant le pic initial, est un autre paramètre quantifiable lors de la réalisation d'une PORH, mais sa signification physiologique comme marqueur de la réactivité microvasculaire cutanée reste à établir.

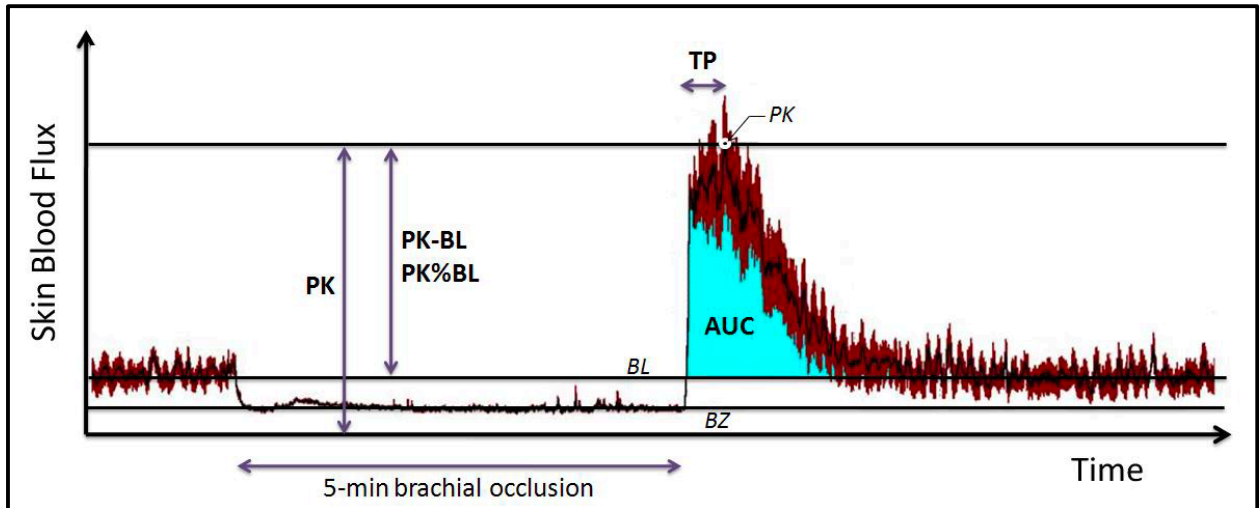


Figure 5. Exemple d'une hyperhémie post-occlusive (PORH) enregistrée sur l'avant-bras par fluxmétrie laser doppler (LDF). L'hyperhémie peut être exprimée soit en valeur brute (PK), soit par soustraction à la ligne de base (PK-BL), soit par pourcentage d'augmentation par rapport à la ligne de base (PK%BL), soit sous forme d'aire sous la courbe (AUC), soit encore en pourcentage par rapport à la vasodilatation maximale qui est obtenue en chauffant la peau localement à une température de 42 à 44 °C. La cinétique de la réponse hyperhémique est parfois exprimée en temps écoulé avant le pic hyperhémique (TP, time to peak). BL : ligne de base. BZ : zéro biologique (d'après Roustit, *Microcirculation* 2011).

Le meilleur outil permettant d'étudier le flux vasculaire de l'HPO était historiquement la fluxmétrie par laser Doppler (LDF), mais cette technique est limitée par sa reproductibilité dans le temps (dite inter-jour) qui varie en fonction du site cutané choisi, de la manière d'exprimer les données, et de la température cutanée de base (9, 56). Récemment, Roustit *et al.* ont montré une excellente reproductibilité de l'imagerie par *laser-speckle* (LSCI) dans l'évaluation de la PORH, ainsi qu'une bien meilleure résolution spatiale que la LDF, utilisée jusqu'alors (12).

3. La microdialyse cutanée

Comme nous l'avons vu, l'étude du flux sanguin de la microcirculation cutanée en LDF, LDI ou LSCI peut être couplée à des tests de réactivité vasculaire tel que l'hyperhémie post-occlusive, l'hyperhémie thermique, l'iontophorèse cutanée ou encore la microdialyse.

Le passage de drogues vaso-actives par voie intradermique est rendu possible par la technique de microdialyse qui consiste à insérer des fibres de microdialyse par voie intradermique (Figure 6) et à délivrer des ions, molécules ou agents pharmacologiques d'intérêt, dans une région restreinte de la peau. Ceci permet d'observer un effet local en limitant les effets systémiques, tout en donnant la possibilité d'analyser l'effluent dans le dialysat. Les substances libérées du fait de l'action pharmacologique dans le dialysat peuvent également être quantifiées (57).



Figure 6. Mise en place d'une sonde de microdialyse dermo-hypodermique (clichés personnels).

Gauche : Mise en place à travers une aiguille 21 Gauges (800 μ m de largeur x 4 cm de longueur). Droite : Après retrait de l'aiguille : la membrane est insérée à la jonction dermo-hypodermique, une pompe de microdialyse en amont permet l'écoulement de solution en intradermique et l'analyse de l'effluent recueilli dans le dialysat situé en aval sur les compresses.

Après insertion des fibres de microdialyse, le flux microvasculaire du tissu cutané situé au-dessus de la sonde est classiquement mesuré par fluxmétrie laser Doppler (Figure 7), ce qui permet de quantifier l'effet pharmacodynamique local des agents pharmacologiques délivrés (8). Cette technique a par exemple été utilisée pour évaluer le rôle du NO dans l'hyperhémie thermique (53, 58–61). L'utilisation d'un fluxmètre laser Doppler (LDF) permet une étude du flux dans une demi-sphère de 1 mm³. Par conséquent, le positionnement de la sonde sur le trajet de la fibre est très important. L'écart par rapport à la fibre peut en effet conduire à observer des effets moins prononcés du produit injecté, avec une grande hétérogénéité spatiale et donc une grande variabilité (45). L'imageur laser Doppler (LDI) utilise le même principe physique mais étudie une surface délimitée au préalable. Il est ainsi possible en utilisant l'imageur de s'affranchir totalement de la variabilité liée au positionnement de la sonde. Enfin, bien que le LSCI n'utilise pas l'effet Doppler, il est tout aussi possible de s'affranchir des mêmes contraintes liées à la LDF.

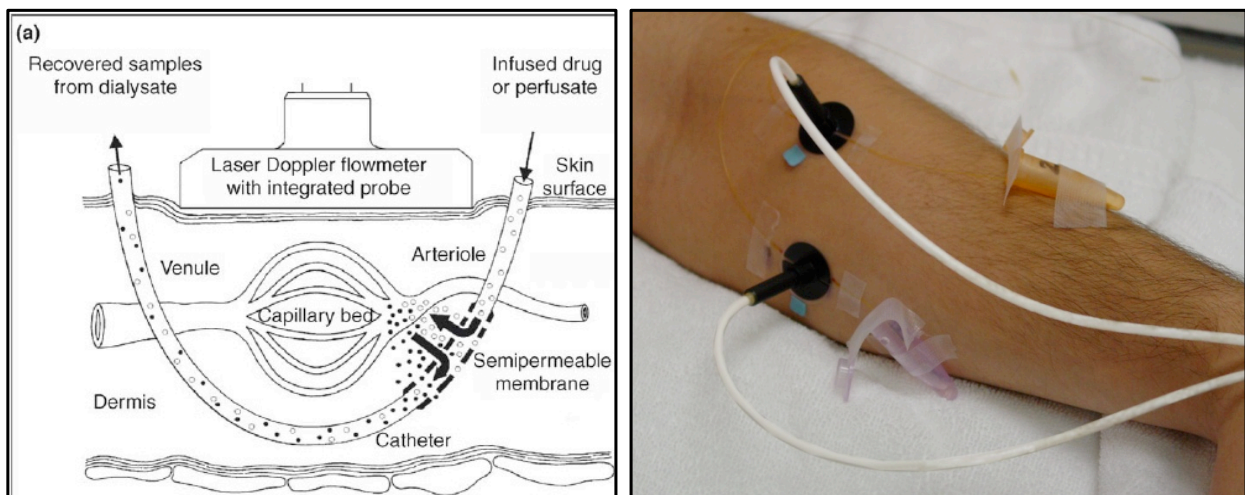


Figure 7. Représentation schématique (gauche) et photo (droite) de la combinaison de microdialyse intradermique et de fluxmètre laser Doppler (d'après Cracowski, Trends Pharmacol Sci 2006).

Première étude: Faisabilité de la microdialyse cutanée associée au Laser Speckle Contrast Imaging pour évaluer la réactivité microvasculaire (titre court: EETY, étude préliminaire)

Le *laser speckle contrast imaging* (LSCI) peut être utilisée pour l'étude en « temps réel » du flux sanguin de la microcirculation cutanée. Couplé à la technique modérément invasive de microdialyse cutanée, ces deux techniques pourraient permettre l'étude du passage de drogues vaso-actives et des voies impliquées dans la réponse microvasculaire suivant des tests de réactivité cutanée.

L'objectif principal de cette étude préliminaire était de déterminer quelle profondeur d'insertion des fibres de microdialyse (entre le derme superficiel et le derme profond) permettrait l'étude du flux sanguin de la microcirculation cutanée par LSCI sans en altérer son interprétation lors de tests de réactivité cutanée tels que l'hyperhémie post-occlusive (PORH) ou l'hyperhémie thermique (LTH).

De façon aléatoire, nous avons procédé à l'insertion d'une fibre dans le derme profond et deux fibres dans le derme superficiel chez 6 volontaires sains. Nous avons ensuite réalisé consécutivement un test d'hyperhémie post-occlusive suivi d'une administration (par la fibre de microdialyse) de nitroprussiate de sodium (SNP) et un test d'hyperhémie thermique suivi d'une administration (toujours par microdialyse) de SNP. Pendant toute la procédure, le flux sanguin de la microcirculation cutanée a été enregistré par LSCI et exprimé en conductance vasculaire cutanée (CVC).

Deux heures après l'insertion des fibres, la CVC au niveau des sites d'insertion dermique superficielle ne différait pas de celle de leur zone contrôle respective, tandis que la CVC du site d'insertion dermique profonde restait significativement plus élevée par rapport à sa zone contrôle. Le pic et l'AUC observés pendant la PORH étaient similaires à tous les sites d'insertion ainsi qu'à leur zone contrôle respective et l'augmentation de la CVC consécutivement à l'administration de SNP ou à l'hyperhémie thermique était également comparable entre tous les sites et leur zone contrôle respective.

En conclusion, cette étude préliminaire a permis la mise au point et la validation de la microdialyse cutanée couplée au LSCI dans l'étude de la microcirculation cutanée et montre que l'étude physiologique et pharmacologique de la microcirculation cutanée par cette technique sont faisables, reproductibles et permettent une source d'informations bidimensionnelle.

Article publié: *[Skin microdialysis coupled with laser speckle contrast imaging to assess](#)*

[microvascular reactivity](#). Cracowski JL, Gaillard-Bigot F, Cracowski C, Roustit M, Millet C. *Microvasc Res.* 2011

Nov;82(3):333-8.



Skin microdialysis coupled with Laser Speckle Contrast Imaging to assess microvascular reactivity

J.L. Cracowski^{a,b,c,*}, F. Gaillard-Bigot^{a,b}, C. Cracowski^a, M. Roustit^{a,b,c}, C. Millet^b

^a Clinical Pharmacology Department, Inserm CIC3, University Hospital, Grenoble, France

^b Inserm U1042, Grenoble, France

^c University Joseph Fourier, Grenoble, France

ARTICLE INFO

Article history:

Accepted 26 September 2011

Available online 6 October 2011

ABSTRACT

Objective: Laser Speckle Contrast Imaging (LSCI) can be used to assess real-time responses of skin microcirculation to pharmacological interventions. The main objective of this study was to determine whether intra-dermal or subdermal microdialysis fiber insertion, coupled with skin flux recording using LSCI, can be used to assess baseline cutaneous flux and the post-occlusive reactive hyperemic response. The microdialysis sites were compared to control area without microdialysis fibers.

Methods: One dermal and two subdermal microdialysis fibers were randomly inserted in the right forearm skin of six healthy volunteers. We performed consecutively tests of post-occlusive hyperemia, infusion of 29 mM sodium nitroprusside (SNP), local thermal hyperemia at 43 °C and a second 29 mM SNP infusion at the end of the experiment.

Results: Two hours after fiber insertion, cutaneous vascular conductances (CVC) at the subdermal fiber sites were not different from their respective control regions of interest, while at the dermal site CVC remained higher (0.48 ± 0.15 versus 0.37 ± 0.1 PU.mm Hg⁻¹, P=0.003). The peak CVC and area under the curve observed during post-occlusive reactive hyperemia were similar at all fiber sites and their respective controls. We observed a similar increase in CVC using 29 mM SNP infusion, 40 min local heating at 43 °C, and their combination. Finally, physiological and pharmacological responses of the subdermal sites were reproducible in terms of amplitude, whether expressed as raw CVC or as %CVCmax.

Conclusions: We showed that studying skin microvascular physiological or pharmacological responses using inserted subdermal microdialysis fibers coupled with LSCI is feasible and reproducible, and provides two-dimensional information. This technique will be useful for future mechanistic studies of skin microcirculation.

© 2011 Elsevier Inc. All rights reserved.

Introduction

Ultrasonography of the brachial or radial artery is routinely used to assess the function of conductance arteries. Its most frequent use is to quantify flow-mediated dilation in the study of endothelial function in case controlled studies, for which there are detailed published guidelines (Thijssen et al., 2011). However, most mechanistic studies require the catheterization of the intra-brachial artery to inject pharmacological agents, which has the major advantage of enabling high concentrations of drugs to be delivered locally with few systemic effects. Such a procedure has been used to study the role of NO or Endothelial Derived Hyperpolarizing Factors for example (Bellien et al., 2006; Mullen et al., 2001).

When studying microcirculation, the conventional approach is to study blood flow in the forearm using strain-gauge venous

plethysmography in order to assess skeletal muscle microvasculature (Joannides et al., 2006). Here again, intra-brachial artery catheterization is required to deliver drugs. Skin is a more easily accessible tissue. Skin microvascular function can be readily assessed using laser Doppler flowmetry or imaging, or the more recent Laser Speckle Contrast Imaging (LSCI). Physiological studies may require injecting locally pharmacological agents as the oral or intravenous route is not optimal given the systemic effect of the drug and the difficulty in demonstrating that the drug diffuses to the skin. The preferred approach is to use skin microdialysis fibers to deliver drugs of interest to the interstitial space (Cracowski et al., 2006). Fibers are used to deliver pharmacological agents to a small area of the skin avoiding confounding systemic effects, and furthermore, the effluent fluid can be simultaneously sampled. Skin blood flux over the fiber is measured using laser Doppler Flowmetry, with the probes located on the skin. This approach has been used for example, to assess the role of NO in skin post-occlusive and thermal hyperemia (Minson et al., 2001; Wong et al., 2003). However, while single-point laser Doppler flowmetry shows good temporal resolution, it shows poor spatial resolution, and poor reproducibility in low capillary density skin areas (Roustit et al., 2010a). This latter issue can be

* Corresponding author at: Clinical Pharmacology Department, Inserm CIC3, Centre d'Investigation Clinique de Grenoble, CHU de Grenoble, 38043 Grenoble Cedex 09, France. Fax: +33 4 76 76 92 62.

E-mail address: Jean-Luc.Cracowski@ujf-grenoble.fr (J.L. Cracowski).

overcome by using either integrated probes with several transmitting and/or receiving fibers, or full field techniques such as laser Doppler imaging (LDI). LDI shows excellent spatial resolution but poor temporal resolution and is therefore not suitable to assess rapid changes in skin blood flow, such as during post-occlusive reactive hyperemia.

The recently developed Laser Speckle Contrast Imaging (LSCI) is a technique based on speckle contrast analysis that provides an index of blood flow (Briers, 2001). High frame rate LSCI produces the same spectral information as LDI (Thompson and Andrews, 2010). Skin blood flux measured with LSCI is linearly related to the LDI signal over a wide range of perfusion (Millet et al., 2011), and shows good spatial and temporal resolution, as well as excellent reproducibility (Rousseau et al., 2011; Roustit et al., 2010b). Therefore, LSCI could be used to assess real-time responses to local pharmacological interventions such as those performed using skin microdialysis.

The main objective of this study was to describe the effect of intradermal or subdermal microdialysis fiber insertion, coupled with skin flux recording using LSCI, on baseline cutaneous vascular conductance and post-occlusive reactive hyperemia. Each microdialysis sites was compared to a control area without microdialysis fibers. We also described the 2 dimensional diffusion of injected sodium nitroprusside (SNP), and compared the maximal hyperemia obtained using SNP, local 43 °C thermal hyperemia or their combination. Finally, we assessed the intra-individual reproducibility of the subdermal skin microdialysis technique.

Materials and methods

Study population

This was a pilot study, enrolling ten healthy subjects recruited through the Clinical Research Center Volunteer database. Inclusion criteria were age 18 years or older, no significant medical history. For women of child bearing age, the possibility of pregnancy was excluded by urine tests at the beginning of the visit. For all subjects, non-inclusion criteria included any allergies to local anesthetics, cigarette smoking or a dermatological disease affecting the arms. Grenoble

Institutional Review Board (IRB n°6705) approval was obtained and each subject gave written informed consent before participation. The first 4 volunteers underwent the same protocol but were enrolled to improve the technical skills and the learning curve of the operators, and their data were not used for data analysis; the main objective being assessed on the 6 subsequent subjects.

Experimental procedure

Subjects attended an initial enrollment visit (V1) where inclusion and non-inclusion criteria were checked by a physician, and full information given. Seven \pm 2 days later, they came back for the experimental visit.

Upon arrival at the laboratory between 8 and 9 a.m., subjects were placed in a temperature-controlled room (24 ± 1 °C). After checking for visible veins, lidocaine/prilocaine cream (10 g) was applied on the ventral face of the right forearm for 40 min, and an occlusive transparent dressing was placed over the cream. We previously showed that lidocaine/prilocaine cream, when applied for 40 min, induces a significant 75% decrease in pain following skin needle insertion, but does not modify skin post-occlusive and thermal hyperemia 2 h after cream removal (Cracowski et al., 2007). The subjects were supine for the whole duration of the experiments.

After lidocaine/prilocaine cream removal, we randomly chose 3 skin sites, 3 to 5 cm apart, on the ventral side of the right upper forearm, avoiding veins checked previously (see Fig. 1 for experimental setup). Local asepsia was performed using chlorhexidine gluconate soap (Hibiscrub® 4%, Regent Medical, Manchester, UK), followed by applying chlorhexidine gluconate and benzalkonium chloride (Biseptine®, Bayer, Gaillard, France). Two sterile fields were placed on the lateral and median face of the forearm. Then, a sterile 21 G, 50 mm needle was inserted into the skin over a length of 1.5 to 2 cm. The 3 needles were randomly placed intradermally (1 out of 3) and at the dermal–subdermal interface (called “subdermal” fibers, 2 out of 3) separated by 3 to 4 cm. A CMA 66® linear microdialysis catheter with a 1 cm long, 500 μ m diameter, 20,000 Da cut-off membrane (CMA Microdialysis, Solna, Sweden), previously rinsed with sterile

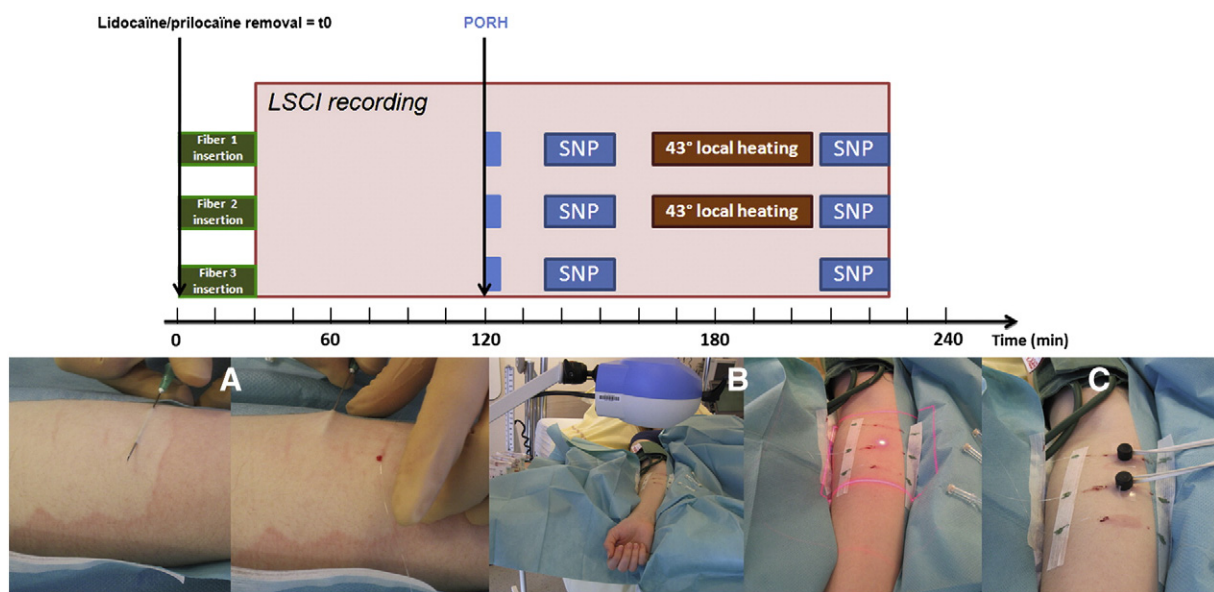


Fig. 1. The top image shows the experimental setup, with detailed views below. A sterile 21 G, 50 mm needle was inserted in the skin over a length of 1.5 to 2 cm (A). The 3 needles were randomly placed intradermally (1 out of 3) or at the dermal–subdermal interface (2 out of 3, such as in A) and separated by 3 to 4 cm. A microdialysis fiber was inserted, and connected to a portable pump. As soon as the last fiber was inserted, cutaneous blood flux was recorded using Laser Speckle Contrast Imaging (B). Two hours after lidocaine/prilocaine removal, we occluded blood flow for 5 min. Ten min after release of the cuff, sodium nitroprusside was infused at all sites simultaneously for 15 min. Then, sodium nitroprusside was stopped, and two heating probes were placed on the intradermal fiber and on one of the two deep skin microdialysis fibers (chosen at random) and set at 43 °C for 40 min (C). When the probes were removed sodium nitroprusside was infused simultaneously at all sites for 15 min. PORH: post occlusive reactive hyperemia. SNP: sodium nitroprusside.

NaCl 0.9%, was immediately inserted through the needle. Then the fiber was connected to a portable battery driven syringe pump (CMA 107 Microdialysis Pump®, CMA Microdialysis, Solna, Sweden). Once the cover was closed, the pump started a 5 min flush sequence at 15 $\mu\text{L}/\text{min}$ and then automatically decreased to the preset flow rate that we adjusted it to, 2 $\mu\text{L}/\text{min}$, similar to that used previously (McCord et al., 2006).

As soon as the last fiber was inserted, the arm was placed on a vacuum cushion to decrease artifacts associated with arm movements, and cutaneous blood flow was measured with LSCI (PeriCam PSI System, Perimed, Järfälla, Sweden). The laser speckle contrast imager wavelength was 785 nm and the laser head was placed 15 cm above the skin (with a resolution of approximately 6944 pixels/cm²). The image size was 12 × 5 to 7 cm and the acquisition rate was 3 s⁻¹, and increased to 8 s⁻¹ during the post-occlusive reactive hyperemia (PORH).

Two hours after lidocaine/prilocaine removal, blood flow was occluded for 5 min by inflating a cuff placed on the right arm to 50 mm Hg above the systolic blood pressure. Ten minutes after releasing the cuff, 29 mM sodium nitroprusside was infused at all sites simultaneously for 15 min. Ten minutes after SNP was stopped, two heating probes (P457, Perimed, Järfälla, Sweden) were placed above the intradermal fiber and on one of the two deep skin microdialysis fibers chosen randomly, and set at 43 °C for 40 min. Then the probes were removed and 3 min later 29 mM sodium nitroprusside was again infused at all sites simultaneously for 15 min.

Blood pressure was recorded continuously throughout the experiment (Nexfin monitor, Bmeye B.V., Amsterdam, The Netherlands) on the contralateral hand.

The volunteer's forearm was examined 7 days later to assess any potential side effects.

Drugs

Sodium nitroprusside was purchased from Serb, Paris, France (Nitriate®). One vial containing 50 mg of SNP was diluted in 8 mL of 0.9% NaCl solution (Aguettant, Lyon, France) to obtain 29 mM SNP. All solutions were prepared extemporaneously, and discarded the same day. Lidocaine/prilocaine cream was purchased from Pierre

Fabre (5 g tubes containing 125 mg lidocaine and 125 mg prilocaine, Anesderm®, Pierre Fabre, Boulogne, France).

Data analysis

Skin blood flux was averaged over regions of interest area of 60 mm², i.e. 12 mm long and 5 mm large rectangles surrounding the microdialysis fiber, excluding the insertion points (Fig. 2). One 60 mm² control area was chosen for each microdialysis fiber site, 1 to 3 cm apart on the lateral or median site of the forearm. Data were digitized, stored on a computer, and analyzed off-line with signal processing software (PimSoft 1.1.1; Perimed, Järfälla, Sweden). Data were subsequently expressed as cutaneous vascular conductance (CVC; PU.mm Hg⁻¹), which is the flux in perfusion units (PU) divided by the mean arterial pressure (MAP) in mm Hg. For the post-occlusive hyperemia, we also calculated the area under the curve (AUC) of the CVC expressed as PU.sec.mm Hg⁻¹. The PORH AUC (total hyperemic response) was = raw PORH AUC over 6 min – (baseline CVC × 360 s). CVC values were averaged over 4 min periods for the baseline, the SNP and the thermal hyperemia recordings. Peak blood flow was defined as the highest blood flow value after release of the pressure cuff, and peak PORH was averaged over 20 s around this peak. The SNP hyperemic area was calculated as follows: three 2D images were transferred from Pimsoft to ImageJ 1.44 (NIH software, in the public domain), where it was modified to a gray scale image. Then, for each image, the mean value of a control area was used as a cutoff for determining the hyperemic area due to SNP. We were therefore able to extract simultaneously the hyperemic area of the 3 fiber sites.

Statistical analysis

Quantitative data were expressed as mean and standard deviation, and were analyzed by one way anova for repeated measures followed by Bonferroni's post hoc test; or by paired *t*-tests for paired analyses, with each subject serving as his/her own control. *P* values less than 0.05 were considered statistically significant. Intra-subject reproducibility was expressed as within-subject coefficients of variation (CV), the CV being the square root of the residual mean square in the analysis of variance table divided by the mean, expressed as percentage

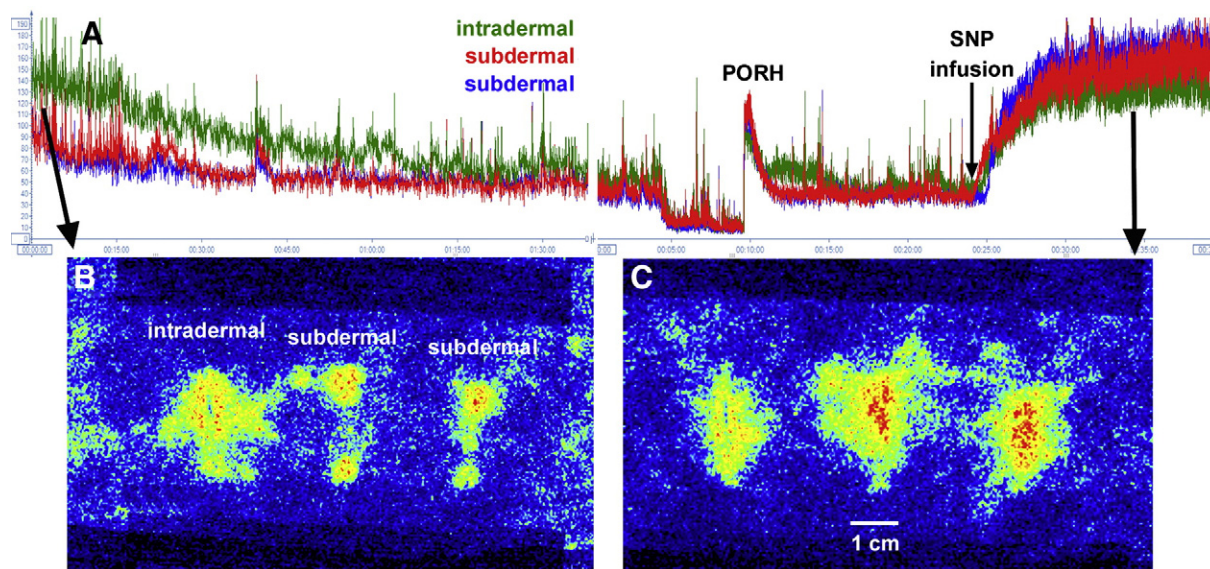


Fig. 2. Figure A shows the recording of the experiment over 60 mm² regions of interest from the first minutes after skin microdialysis fiber insertion until 15 min after 29 mM SNP infusion. Figure B shows an initial LSCI image where an axon reflex can be seen over the 3 fiber insertions. Figure C shows the effect of an infusion of sodium nitroprusside (29 mM) on the same area.

(Bland, 2000). Statistical analysis was performed using SPSS 13.0 for Windows (SPSS Inc, Chicago IL, USA).

Results

Study population

Ten Caucasian subjects were enrolled in the protocol (5 males and 5 females). Their age was 22.6 ± 1.6 years, their body mass index was 23.1 ± 3.4 kg/m², their systolic/diastolic arterial pressure was 127 ± 11 mm Hg/ 69 ± 14 mm Hg. Fibers were inserted in the forearms of the volunteers as described. The mean peak pain score was 1.3 ± 0.5 . No adverse events occurred either on the experimental day or 7 days later. For all subjects the whole sequence of LSCI recording was performed without any significant artifacts. Enrollment of the first 4 subjects enabled to improve the technical skills and the learning curve of the operators, and the following objectives were assessed on the 6 subsequent subjects (3 males, 3 females).

Effect of intradermal or subdermal microdialysis fiber insertion on baseline and PORH cutaneous vascular conductance

Fiber insertion induced immediate hyperemia at all sites compared to the respective control region of interest (Fig. 3). We also observed weak hyperemia at all the control sites compared to the baseline values before PORH. Two hours after fiber insertion, CVC at the subdermal fiber sites were not different from controls. In contrast, CVC at the intradermal fiber site was significantly higher than at the control site and at both subdermal sites (Fig. 3). The peak CVC observed during PORH was similar at all sites and their respective controls (Fig. 4).

Likewise, the PORH AUC did not significantly differ between the sites and their respective control regions of interest. The PORH AUC for the intradermal fiber site was 61.6 ± 18.7 PU.s.mm Hg⁻¹, compared to its control of 66.2 ± 29.8 PU.s.mm Hg⁻¹ (NS). The AUC of the two subdermal fibers were 71.8 ± 31.7 PU.s.mm Hg⁻¹, control 75 ± 28 PU.s.mm Hg⁻¹ (NS); and 65 ± 34.3 PU.s.mm Hg⁻¹, control 71.8 ± 31.7 PU.s.mm Hg⁻¹ (NS).

Comparison of SNP induced hyperemia, local thermal hyperemia (LTH) and their combination

SNP induced significant hyperemia at all sites, with a stable plateau obtained after 5 to 10 min. The hyperemia observed 40 min after local

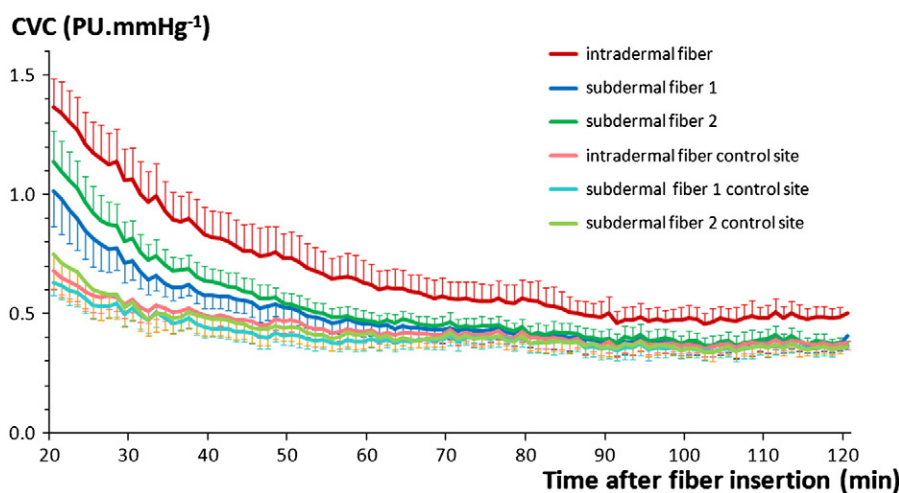


Fig. 3. Cutaneous vascular conductance (CVC, PU.mm Hg⁻¹) recorded during 100 min using LSCI 20 min after intradermal or subdermal microdialysis fiber insertion together with their respective control regions of interest (n=6).

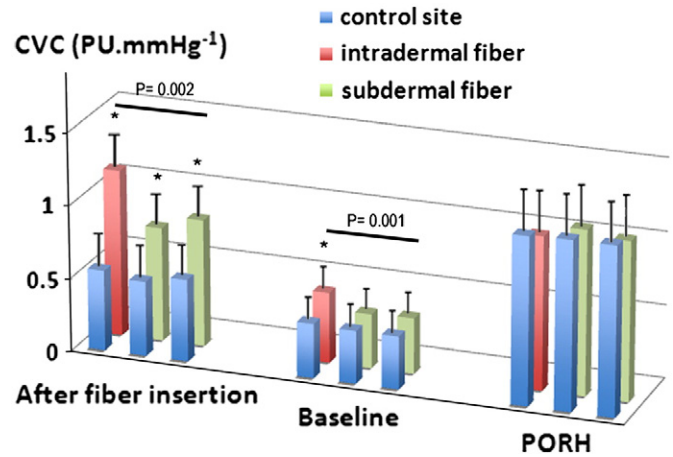


Fig. 4. Cutaneous vascular conductance (CVC, PU.mm Hg⁻¹) recorded after the 3 microdialysis fibers had been inserted (one intradermal and 2 subdermal), 2 h after (baseline), and during PORH. * P<0.01 versus control site (n=6). CVC values were averaged over 4 min periods 30 min after fiber insertion and 2 h after, and over 20 s for the peak PORH.

heating at 43 °C was not significantly different. Similarly, the addition of SNP at the end of the local heating period did not modify skin vascular conductance (Fig. 5).

SNP induced hyperemia extended over an area of 633 ± 266 mm² at the intradermal site; and 682 ± 593 mm² and 714 ± 387 mm² at the first and second subdermal sites respectively (NS).

Spatial within subject coefficient of variation

The within subject coefficient of variation for the subdermal microdialysis fiber insertion sites are given in Table 1, expressed as raw values (PU.mm Hg⁻¹) or as a percentage of CVCmax (29 mM SNP).

Discussion

We have shown that studying skin microvascular physiological or pharmacological responses using inserted skin microdialysis fibers coupled with LSCI is feasible and reproducible. Subdermal placement using 21 G introducing needles is the best choice compared with

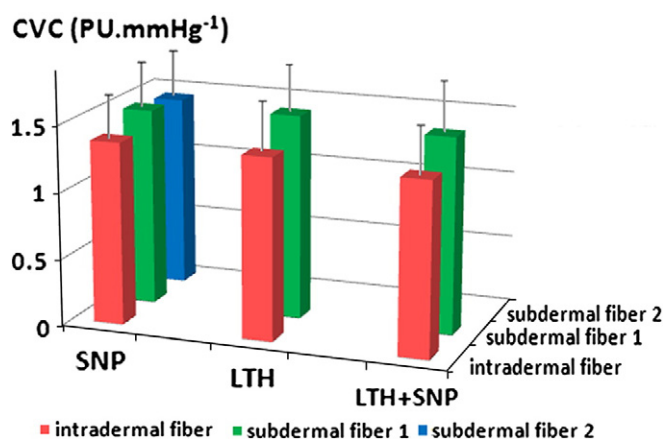


Fig. 5. Maximal CVC (PU.mm Hg⁻¹) recorded at the end of 15 min 29 mM SNP infusion through microdialysis; 40 min local hyperemia; or 40 min local hyperemia followed with 15 min 29 mM SNP infusion (n = 6).

intra-dermal placement, and both 29 mM SNP and 43 °C local heating lead to a maximal skin vasodilatation.

We used CMA 66 linear microdialysis fibers approved by the European Community (CE) according to the Medical Device Directive 93/42/EEC. This is to date the only linear fiber that can be used in Europe in clinical research and it meets Good Manufacturing Practice requirements. Unlike microdialysis probes used by US research teams, the introducing needle is slightly larger since the diameter of the fiber is 500 μm. In the initial experiments on 4 volunteers (data not shown), we observed that the use of a 21-G introducing needle intradermally was associated with sustained inflammation and increased basal skin blood flux several hours later. Therefore, we chose subsequently to insert 1 intra-dermal fiber, and 2 subdermal fibers, and not to test the reproducibility of the intra-dermal insertion. The order of fiber insertion was randomized so that the delay between fiber insertion and initial recording could not explain the observed difference between superficial and deeper fibers. We previously showed that lidocaine/prilocaine cream, applied for 40 min, did not alter skin PORH compared to control sites (Cracowski et al., 2007) and enabled painless insertion of fibers in the present protocol. An important issue concerning microdialysis fibers was to determine whether intra-dermal fiber placement is mandatory. Intra-dermal placement is relatively easy using small 25-G introducing needles (McCord et al., 2006), and is also feasible using 23-G needles (Wong and Fieger, 2010). However, in the present experiment,

the 21-G introducing needle induced local trauma that was not resolved 2 h after fiber insertion. Therefore, our technique cannot be used intra-dermally. We observed that when we inserted the microdialysis fiber at the derma-hypoderma interface the CVC returned to control values 80 to 90 min after fiber insertion. In addition, SNP induced hyperemia was not significantly different in terms of the amplitude and hyperemic area between the dermal or subdermal fibers, suggesting that subdermal placement is the best choice for skin pharmacological and physiological studies using our protocol, with a good diffusion of injected drugs. We have shown for the first time the 2D diffusion of SNP induced hyperemia when it is injected through a microdialysis fiber. Diffusion of SNP covers a skin area between 633 and 714 mm². Assuming that such an area is circular, this means that when injected into the microdialysis fiber, SNP diffuses up to 14 to 15 mm. The high frame rate mapping of SNP diffusion confirms that fibers can be inserted 3 cm apart without overlap of the hyperemia.

We observed similar increases in CVC using 29 mM SNP infusion, 40 min local heating at 43 °C, and their combination. This means that in order to obtain maximal CVC, either SNP infusion or local heating can be used, as is commonly done in microdialysis protocols coupled with laser Doppler flowmetry. However, 60 to 70% of the local heating plateau depends on NO (Brunt and Minson, 2011), and is mediated through TRPV1 (Wong and Fieger, 2010) and adenosine receptor stimulation (Fieger and Wong, 2010); while reactive oxygen species produced by angiotensin II may modulate this response (Medow et al., 2011). Therefore, SNP has the advantage of inducing direct smooth muscle relaxation, and is less sensitive to pathological conditions susceptible to alter these pathways.

Using LSCI improves the reproducibility of the technique compared with laser Doppler flowmetry (Rousseau et al., 2011; Roustit et al., 2010a,b). The coefficients of variation we observed in the present study were very close to the intersite coefficient of variation we found previously using another group of healthy subjects (Roustit et al., 2010b). Furthermore, in the presence of a microdialysis fiber, we also observed excellent intra-individual coefficients of variation, whether data were expressed as raw value or as a percentage of CVCmax, suggesting that LSCI coupled with microdialysis fiber insertion is a promising tool for physiological and pharmacological studies of the skin, where one drug could be injected in one fiber and a placebo in the second. It has a major advantage over the conventional laser Doppler flowmetry method, as there is a double control for each experiment. Indeed, the first control would be the adjacent fiber containing placebo, and using LSCI we are able to make simultaneous recordings of an adjacent region of interest without microdialysis fiber as a second control. In the present study, local heating was not performed on one dermal fiber as a quality control to ensure that skin CVC did not plateau after we stopped SNP. Therefore, the LTH coefficient of variation needs to be checked in future experiments.

In conclusion, we have shown that studying skin microvascular physiological or pharmacological responses using inserted microdialysis fibers coupled with LSCI is feasible and reproducible, and provides two-dimensional information. Subdermal placement is the best choice using or protocol compared with intra-dermal placement. In order to express data as a percentage of maximal CVC, both 29 mM SNP or 43 °C local heating can be used, SNP infusion requiring microdialysis fibers while LTH is non invasive but potentially altered in disease states. Such a technique will be useful for future mechanistic studies of skin microcirculation.

Conflict of interest

Pr Jean-Luc Cracowski and Dr Matthieu Roustit have received research grants from Actelion, Glaxo-Smith Kline, Boiron and Pfizer, for other studies. Pr Jean-Luc Cracowski reports being a consultant for Actelion. All authors report that they do not have any conflict of interest with CMA Microdialysis or Dipyron Medical.

Table 1

Within subject coefficient of variation of the different LSCI measurements for the subdermal fiber sites and their adjacent control sites (n = 6).

	Fiber sites	Adjacent control sites
CVC (PU.mm Hg ⁻¹)		
CVC immediately following the insertion procedure	10%	13%
Baseline CVC 2 h after the procedure	8%	3%
Peak PORH	10%	3%
29 mM SNP plateau	8%	NA
CVC (%CVCmax)		
CVC immediately following the insertion procedure	13%	NA
Baseline CVC 2 h after the procedure	11%	NA
Peak PORH	12%	NA
PORH AUC (PU.sec.mm Hg ⁻¹)	22%	17%
SNP diffusion area (mm ²)	32%	NA

NA: Not applicable as SNP infusion was not possible at the adjacent control sites. CVC: cutaneous vascular conductance; PORH: post-occlusive thermal hyperemia; SNP: sodium nitroprusside; PU: perfusion units. % CVCmax : percentage of the 29 mM SNP plateau.

Acknowledgments

We thank the Clinical research department of Grenoble University Hospital for funding. We also thank Dr Marcin Hellmann for help with technical measurements and Dr Alison Foote for editing the manuscript.

References

- Bellien, J., et al., 2006. Crucial role of NO and endothelium-derived hyperpolarizing factor in human sustained conduit artery flow-mediated dilatation. *Hypertension* 48, 1088–1094.
- Bland, M., 2000. An introduction to medical statistics. Third Edition, Oxford University press Chapter 15.2 Repeatability and measurement error, pp. 269–272.
- Briers, J.D., 2001. Laser Doppler, speckle and related techniques for blood perfusion mapping and imaging. *Physiol. Meas.* 22, R35–R66.
- Brunt, V., Minson, C., 2011. Cutaneous thermal hyperemia: more than skin deep. *J. Appl. Physiol.* 111 (1), 5–7.
- Cracowski, J.L., et al., 2006. Methodological issues in the assessment of skin microvascular endothelial function in humans. *Trends Pharmacol. Sci.* 27, 503–508.
- Cracowski, J.L., et al., 2007. Effects of local anaesthesia on subdermal needle insertion pain and subsequent tests of microvascular function in human. *Eur. J. Pharmacol.* 559, 150–154.
- Fieger, S.M., Wong, B.J., 2010. Adenosine receptor inhibition with theophylline attenuates the skin blood flow response to local heating in humans. *Exp. Physiol.* 95, 946–954.
- Joannides, R., et al., 2006. Clinical methods for the evaluation of endothelial function – a focus on resistance arteries. *Fundam. Clin. Pharmacol.* 20, 311–320.
- McCord, G.R., et al., 2006. Prostanoids contribute to cutaneous active vasodilation in humans. *Am. J. Physiol. Regul. Integr. Comp. Physiol.* 291, R596–R602.
- Medow, M.S., et al., 2011. Reactive oxygen species (ROS) from NADPH and xanthine oxidase modulate the cutaneous local heating response in healthy humans. *J. Appl. Physiol.* 111 (1), 20–26.
- Millet, C., et al., 2011. Comparison of laser speckle contrast imaging and laser Doppler imaging to assess skin blood flow in humans. *Microvasc. Res.* 82 (2), 147–151.
- Minson, C.T., et al., 2001. Nitric oxide and neurally mediated regulation of skin blood flow during local heating. *J. Appl. Physiol.* 91, 1619–1626.
- Mullen, M.J., et al., 2001. Heterogenous nature of flow-mediated dilatation in human conduit arteries in vivo: relevance to endothelial dysfunction in hypercholesterolemia. *Circ. Res.* 88, 145–151.
- Rousseau, P., et al., 2011. Increasing the “region of interest” and “time of interest”, both reduce the variability of blood flow measurements using laser speckle contrast imaging. *Microvasc. Res.* 82, 88–91.
- Roustit, M., et al., 2010a. Reproducibility and methodological issues of skin post-occlusive and thermal hyperemia assessed by single-point laser Doppler flowmetry. *Microvasc. Res.* 79, 102–108.
- Roustit, M., et al., 2010b. Excellent reproducibility of laser speckle contrast imaging to assess skin microvascular reactivity. *Microvasc. Res.* 80, 505–511.
- Thijssen, D.H., et al., 2011. Assessment of flow-mediated dilation in humans: a methodological and physiological guideline. *Am. J. Physiol. Heart Circ. Physiol.* 300, H2–H12.
- Thompson, O.B., Andrews, M.K., 2010. Tissue perfusion measurements: multiple-exposure laser speckle analysis generates laser Doppler-like spectra. *J. Biomed. Opt.* 15, 027015.
- Wong, B.J., Fieger, S.M., 2010. Transient receptor potential vanilloid type-1 (TRPV-1) channels contribute to cutaneous thermal hyperaemia in humans. *J. Physiol.* 588, 4317–4326.
- Wong, B.J., et al., 2003. Nitric oxide synthase inhibition does not alter the reactive hyperemic response in the cutaneous circulation. *J. Appl. Physiol.* 95, 504–510.

Deuxième étude : Rôle des acides époxy-eicosatriénoïques (EETs) dans l'hyperhémie post-occlusive (titre court : EETY)

Il n'existe pas de technique standardisée pour l'étude de la fonction endothéliale des microvaisseaux, contrairement aux artères de conductance, et les interactions mises en évidence dans la relaxation endothéliale-dépendante ne sont pas actuellement démontrées au niveau de la microcirculation.

L'objectif principal de cet essai de preuve de concept était d'étudier la contribution spécifique des acides époxy-eicosatriénoïques (EETs) dans l'hyperhémie post-occlusive (PORH) au niveau de la microcirculation cutanée chez l'homme.

Pour cela, nous avons utilisé un test de provocation – l'hyperhémie post-occlusive – couplé d'une part à un enregistrement par imagerie en *laser speckle contrast imaging* (LSCI) pour étudier de façon non invasive le flux sanguin de la microcirculation cutanée, et couplé d'autre part à la technique de microdialyse cutanée pour mettre en évidence le passage des drogues vaso-actives utilisées. Huit volontaires sains ont été inclus dans deux expériences contrôlées contre placebo (du NaCl à 0,9%).

Dans la première expérience, nous avons étudié les effets séparés et combinés du fluconazole, administré à une concentration de 6,5 mM à l'aide de fibres de microdialyse, et du mélange équimassique de lidocaïne/prilocaine sur la peau, après une PORH faisant suite à 5 minutes d'occlusion artérielle.

Dans la deuxième expérience, nous avons étudié les effets séparés et combinés du fluconazole à 6,5 mM et de N(G)-monométhyl-L-arginine (L-NMMA) à 10 mM. Le flux sanguin cutané a été exprimé en conductance vasculaire cutanée maximale (CVCmax) obtenue après l'administration de nitroprussiate de sodium (SNP) à 29 mM.

Comparativement au site placebo, le pic de la PORH était significativement abaissé au site du fluconazole, de la lidocaïne-prilocaine, et au site combinant le fluconazole et la lidocaïne-prilocaine. L'effet du fluconazole était celui qui était le plus prononcé sur la phase hyperhémique prolongée.

Dans la deuxième expérience, par rapport au site placebo, la valeur du pic de la PORH était significativement abaissée au site du fluconazole, mais pas au site du L-NMMA ni au site combinant les deux.

En conclusion, en plus du réflexe axonal, les métabolites de la cytochrome P450 époxygénase – les EETs – jouent un rôle majeur dans la PORH de la microcirculation cutanée chez l'homme, avec un effet plus prononcé sur la phase hyperhémique prolongée que sur le pic initial.

Article publié: *Involvement of cytochrome epoxygenase metabolites in cutaneous postocclusive hyperemia in humans.* Cracowski JL, Gaillard-Bigot F, Cracowski C, Sors C, Roustit M, Millet C. *J Appl Physiol* (1985). 2013 Jan 15;114(2):245-51.

Involvement of cytochrome epoxygenase metabolites in cutaneous postocclusive hyperemia in humans

Jean-Luc Cracowski,^{1,2,3} Florence Gaillard-Bigot,^{1,2} Claire Cracowski,¹ Claire Sors,^{1,2} Matthieu Roustit,^{1,2,3} and Claire Millet²

¹Clinical Pharmacology Department, Institut National de la Santé et de la Recherche Médicale CIC3, University Hospital, Grenoble, France; ²Institut National de la Santé et de la Recherche Médicale U1042, Grenoble, France; and ³University Joseph Fourier, Grenoble, France

Submitted 5 September 2012; accepted in final form 19 November 2012

Cracowski J, Gaillard-Bigot F, Cracowski C, Sors C, Roustit M, Millet C. Involvement of cytochrome epoxygenase metabolites in cutaneous postocclusive hyperemia in humans. *J Appl Physiol* 114: 245–251, 2013. First published November 21, 2012; doi:10.1152/jappphysiol.01085.2012.—Several mediators contribute to postocclusive reactive hyperemia (PORH) of the skin, including sensory nerves and endothelium-derived hyperpolarizing factors. The main objective of our study was to investigate the specific contribution of epoxyeicosatrienoic acids in human skin PORH. Eight healthy volunteers were enrolled in two placebo-controlled experiments. In the first experiment we studied the separate and combined effects of 6.5 mM fluconazole, infused through microdialysis fibers, and lidocaine/prilocaine cream on skin PORH following 5 min arterial occlusion. In the second experiment we studied the separate and combined effects of 6.5 mM fluconazole and 10 mM *N*^G-monomethyl-L-arginine (L-NMMA). Skin blood flux was recorded using two-dimensional laser speckle contrast imaging. Maximal cutaneous vascular conductance (CVC_{max}) was obtained following 29 mM sodium nitroprusside perfusion. The PORH peak at the placebo site averaged 66 ± 11% CVC_{max}. Compared with the placebo site, the peak was significantly lower at the fluconazole (47 ± 10% CVC_{max}; *P* < 0.001), lidocaine (29 ± 10% CVC_{max}; *P* < 0.001), and fluconazole + lidocaine (30 ± 10% CVC_{max}; *P* < 0.001) sites. The effect of fluconazole on the area under the curve was more pronounced. In the second experiment, the PORH peak was significantly lower at the fluconazole site, but not at the L-NMMA or combination site, compared with the placebo site. In addition to sensory nerves cytochrome epoxygenase metabolites, putatively epoxyeicosatrienoic acids, play a major role in healthy skin PORH, their role being more important in the time course rather than the peak.

epoxyeicosatrienoic acids; cytochrome *P*-450; nitric oxide; endothelium; reactive hyperemia; microdialysis; skin; microcirculation; laser speckle contrast imaging

FOLLOWING BRIEF ARTERIAL occlusion, marked vasodilation associated with a transient rise in blood flow to the postischemic tissues has been described since the 1950s. This transient increase in blood flow, called postocclusive reactive hyperemia (PORH) or reactive hyperemia, has been observed in most vascular beds (7, 30, 34, 36). It is used as a trigger for the study of flow-mediated dilation in conductance vessels such as the brachial or radial arteries (31). In such vessels, one of the mediators implicated in the response to a 5-min occlusive episode was initially suggested to be nitric oxide (NO), to a greater or lesser extent depending on whether the artery ob-

served was, respectively, proximal or distal to the site of arterial occlusion (28). More recently, Bellien et al. showed that a cytochrome-related endothelium-derived hyperpolarizing factor (EDHF) was involved in the flow-mediated dilatation of the human radial artery (3). Moreover, the effect was synergistic with NO, suggesting a functional interaction between NO and cytochrome-related EDHF pathways.

In human skin, following the end of arterial occlusion an immediate and significant transient increase in cutaneous flux is observed that lasts a few minutes (15). Several mediators contribute to this PORH. Local anesthesia using lidocaine/prilocaine cream partially alters the PORH (22), suggesting that a local axon reflex involving sensory nerves is implicated. The implication of sensory nerves has been consistently described thereafter (14, 24). In contrast to skeletal muscle where both NO and cyclooxygenase (COX) metabolites play a role (18), the inhibition of NO production does not alter PORH in the skin of the forearm (36). Furthermore, PORH occurs through mechanisms that are not associated with a measurable increase in local NO concentrations (38). Interestingly, Medow et al. confirmed that the blockade of NO synthase exerts no effects on PORH but that the inhibition of COX unmasks the NO dependence of PORH (26). Results are conflicting concerning the implication of prostaglandins, but there is no strong evidence that prostanoids participate in PORH. One study showed that 1 g of acetylsalicylic acid decreased the PORH peak (6), while another group showed no effect of a 900-mg intravenous lysine acetylsalicylate injection (16) and a slight reduction in PORH duration without effect on the peak response following the ingestion of 1 g acetylsalicylic acid (1). Using the nonspecific COX inhibitor ketorolac (10 mM) and a cutaneous microdialysis fiber system, one group found a higher PORH peak following COX blockade (26), but no effect was found in a subsequent study (24).

Apart from NO and prostacyclin, the third major endothelial-dependent dilation mechanism involves the EDHF (17). The classical EDHF pathway initiates endothelial cell hyperpolarization through activation of endothelial small- and intermediate-conductance calcium-activated potassium channels, leading to vascular myocyte hyperpolarization through potassium or gap junctions (17). A second category of EDHF pathways does not require endothelial cell hyperpolarization and involves the endothelial release of various molecules, including arachidonic acid metabolites (17). Endothelial cells metabolize arachidonic acid via three distinct enzymatic pathways [COX, lipoxygenase, and cytochrome *P*-450 (CYP)]. CYP epoxygenases add oxygen across the double bonds of arachidonic acid to produce the four regioisomers *cis*-epoxides

Address for reprint requests and other correspondence: Jean-Luc Cracowski, Clinical Pharmacology Dept., Inserm CIC3, Centre d'Investigation Clinique de Grenoble, CHU de Grenoble, 38043 Grenoble Cedex 09, France (e-mail: Jean-Luc.Cracowski@ujf-grenoble.fr).

14,15-, 11,12, 8,9-, and 5,6-epoxyeicosatrienoic acids (EETs), each of these existing as two stereoisomers S,R and R,S. In human endothelial cells, these epoxygenases are CYP2C8/2C9 and CYP2J2 (37). In conductance arteries, EDHF produced by endothelial CYP epoxygenase accounts for two-thirds of the flow-mediated vasodilation during prolonged hyperemic stimulation (3, 19), whereas in forearm microcirculation, it contributes to resting microvascular dilator tone (29). Using the nonspecific large-conductance calcium-activated potassium channel blocker tetraethylammonium, Lorenzo and Minson showed that such channels play a major role in the EDHF component of PORH, in part independent of the axon reflex (24). However, the exact nature of the EDHF implicated in human skin PORH remains unknown.

The main objective of our study was to investigate the specific contribution of EETs in human skin PORH. Secondary objectives were to identify any potential interaction with the axon reflex and the NO pathways. We hypothesized that an inhibition of EETs production through CYP epoxygenase inhibition by fluconazole would decrease the PORH in the skin microcirculation, assessed using the recently described skin microdialysis technique coupled with laser speckle contrast imaging (LSCI) (13).

MATERIALS AND METHODS

Study Population

We enrolled eight healthy subjects recruited through the Clinical Research Center Volunteer database. Inclusion criteria were age 18 years or older and no significant medical history. For women of child-bearing age, the possibility of pregnancy was excluded by urine tests at the beginning of each study visit. For all subjects, noninclusion criteria included any allergies to local anesthetics, cigarette smoking, and any dermatological pathology affecting the arms. Grenoble Institutional Review Board (IRB no. 6705) approval was obtained, and each volunteer gave written informed consent before participation.

Experimental Set-Up

Subjects attended an initial enrollment visit where inclusion and noninclusion criteria were checked by a physician, and full information was given. Later (7 ± 3 days), they returned for the first experimental visit, then 14 ± 4 days later, for the second experimental visit. For women, experimental visits were performed during the menstrual phase.

On arrival at the laboratory between 8:00 and 9:00 A.M., subjects were placed in a temperature-controlled room ($24 \pm 1^\circ\text{C}$). After checking for visible veins, lidocaine/prilocaine cream (10 g) was applied to the ventral face of the right forearm for 40 min, with an occlusive transparent dressing placed over the cream (14). The subjects were supine for the whole duration of the experiments.

Microdialysis fiber insertion was performed as previously described (13). After the removal of lidocaine/prilocaine cream, we randomly chose four skin sites, 2–3 cm apart, on the ventral side of the right upper forearm, avoiding veins. Local asepsia was performed using chlorhexidine gluconate soap (4% Hibiscrub; Regent Medical, Manchester, UK), followed by swabbing with chlorhexidine gluconate and benzalkonium chloride (Biseptine; Bayer, Gaillard, France). Two sterile fields were placed on the lateral and median face of the forearm. Next, sterile 21-gauge, 50-mm needles were inserted into the skin over a length of 1.5–2 cm, and a CMA 66 linear microdialysis catheter with a 1-cm long, 500- μm diameter, 20,000-Dalton cut-off membrane (CMA Microdialysis, Solna, Sweden), previously rinsed with sterile 0.9% NaCl, was immediately inserted through the needle. The fiber was immediately connected to a portable

battery-driven syringe pump (CMA 107 Microdialysis Pump; CMA Microdialysis). Once closed, the pump started a 5-min flush sequence at 15 $\mu\text{l}/\text{min}$ and then automatically decreased to the preset flow rate of 2 $\mu\text{l}/\text{min}$, as used previously (25). The insertion procedure was immediately repeated with four microdialysis fibers spaced at 2- to 3-cm intervals.

Fiber sites were randomized to receive any of the four potential experimental combinations, i.e., placebo, fluconazole, placebo + lidocaine/prilocaine skin application, or fluconazole + lidocaine/prilocaine skin application in *experiment 1*; and placebo, fluconazole, N^G -monomethyl-L-arginine (L-NMMA), or fluconazole + L-NMMA in *experiment 2*. All drugs and syringes were blinded by an independent pharmacist working in a separate preparation room.

The arm was then placed on a vacuum cushion to decrease artifacts associated with arm movements, and cutaneous blood flow was measured with LSCI (PeriCam PSI System; Perimed, Järfälla, Sweden). The LSCI wavelength was 785 nm, and the laser head was placed 15 cm above the skin (with a resolution of $\sim 6,944$ pixels/cm²). The image size was 12×5 -7 cm, and the acquisition rate was 3/s during the whole procedure.

Two hours after lidocaine/prilocaine removal, blood flow was occluded for 5 min by inflating a cuff placed on the right upper arm to 50 mmHg above the volunteer's systolic blood pressure. At the end of all experiments, 29 mM sodium nitroprusside (SNP) was perfused at all sites simultaneously for 15 min to obtain maximal cutaneous vascular conductance (CVC_{max}), as previously described for this protocol (13).

Blood pressure was recorded continuously throughout the experiment (Nexfin monitor; Bmeye, Amsterdam, The Netherlands) on the contralateral hand.

Experiments

Protocol 1: EETs and sensory nerve inhibition. We investigated the effects of fluconazole (a CYP2C9 and -2C19 inhibitor used to block EETs production) and lidocaine/prilocaine cream (a Na^+ channel blocker used to inhibit sensory nerve activity) alone and in combination on skin PORH. One site was perfused with 6.5 mM fluconazole for 100 min. At another site lidocaine/prilocaine cream was applied for 100 min. At a third site both fluconazole (6.5 mM) perfusion and lidocaine/prilocaine cream were used, and the fourth site was perfused with placebo only (0.9% NaCl).

Protocol 2: EETs and NO inhibition. In this experiment we investigated the effects of fluconazole and L-NMMA (a NO synthase inhibitor used to inhibit NO production) alone and in combination on skin PORH. One site was perfused with 6.5 mM fluconazole for 100 min. At another site, 10 mM L-NMMA was perfused for 100 min. At a third site both fluconazole (6.5 mM) and L-NMMA (10 mM) were perfused together, and the fourth site was perfused with placebo (0.9% NaCl). The choice of L-NMMA as an inhibitor of NO synthase was based on previous work on conductance arteries to facilitate comparison between studies (2).

Drugs

Fluconazole (2 mg/ml) was purchased from Panpharma (Beaucé, France). The choice of drug concentration was determined from a pilot study in our laboratory in which we observed the effect of the perfusion of fluconazole at 650 μM and 6.5 mM on skin PORH. We tested only two concentrations, since 6.5 mM is the highest concentration commercially available for human use. We performed 5 min PORH in four subjects and observed a systematic inhibition of PORH at 6.5 mM, with a lower nonsystematic inhibition at 650 μM .

L-NMMA (250 mg/vial) was purchased from Clinalfa Basic (Bachem Distribution Services, Weil am Rhein, Germany). L-NMMA (10 mM) systematically blunted the NO-dependent local thermal hyperemia plateau in a pilot study in four subjects. SNP (Nitriate) was purchased from Serb (Paris, France). One vial containing 50 mg of

SNP was diluted in 8 ml of 0.9% NaCl solution (Aguettant, Lyon, France) to obtain 29 mM SNP. All solutions were prepared extemporaneously and discarded the same day. Lidocaine/prilocaine cream was purchased from Aguettant (5-g tubes containing 125 mg lidocaine and 125 mg prilocaine).

Data Analysis

Skin blood flux was averaged over four regions of interest area of 60 mm². For each region of interest, an additional region of interest was used as a quality control, but not used for data analysis. Data were digitized, stored, and analyzed off-line with signal-processing software (PimSoft 1.1.1; Perimed). The biological zero, recorded during the 5-min occlusion, was subtracted from all raw values, and data were subsequently expressed as cutaneous vascular conductance [CVC, perfusion units (PU)/mmHg], which is the flux in PU divided by the mean arterial pressure in millimeters mercury and as a percentage of CVC_{max} (29 mM SNP infusion). The area under the curve (AUC) for CVC expressed as PU·s⁻¹·mmHg⁻¹ was also calculated. CVC values were averaged over 4-min periods for the baseline and SNP and over 20 s for the peak PORH. The PORH AUC (total hyperemic response) was given by: raw PORH AUC over 6 min – (baseline CVC × 360 s).

Statistical Analysis

Quantitative data are expressed as mean and SD and were analyzed by one-way ANOVA for repeated measurements followed by Bonferroni's post hoc test or by paired *t*-tests for paired analyses, with each subject serving as his/her own control. *P* values <0.05 were considered statistically significant. Statistical analysis was performed using SPSS 13.0 for Windows (SPSS, Chicago, IL).

RESULTS

Study Population

Four Caucasian males and 4 females were enrolled in the study. Their mean age was 23 ± 3 yr, their body mass index was 23 ± 3 kg/m², and their systolic/diastolic arterial pressure was 123 ± 11/71 ± 4 mmHg. The mean pain scores on insertion of the microdialysis fibers assessed on a 10-point visual analogic scale were 1.5 ± 0.9 and 1.6 ± 0.7 for protocols 1 and 2, respectively. One volunteer presented a vasovagal malaise after fiber insertion during protocol 2 and spontaneously recovered within 10 min. Five days after protocol 2, another volunteer presented with a 2-mm-diameter noninflammatory papula at the entry site of the proximal fiber that spontaneously disappeared within 7 days.

EET and Sensory Nerve Inhibition

There was no significant difference between treatment sites in absolute CVC_{max} values obtained following 29 mM SNP infusion at the end of the experiment (placebo: 1.9 ± 0.4 PU/mmHg; fluconazole: 1.9 ± 0.5; lidocaine: 2.1 ± 0.6; fluconazole + lidocaine: 2 ± 0.7). We observed a nonsignificant trend toward lower baseline flux values at the lidocaine/prilocaine-treated site (12.8 ± 4% CVC_{max}) vs. placebo (14 ± 3% CVC_{max}), fluconazole (16.1 ± 3% CVC_{max}), and fluconazole + lidocaine/prilocaine (16.4 ± 4) sites.

The mean PORH peak at the placebo site was 66 ± 11% CVC_{max}. Compared with the placebo site, it was significantly lower at the fluconazole (47 ± 10% CVC_{max}; *P* < 0.001), lidocaine (29 ± 10% CVC_{max}; *P* < 0.001), and fluconazole + lidocaine (30 ± 10% CVC_{max}; *P* < 0.001) sites

(ANOVA *P* < 0.001, Fig. 1). The PORH peak was also significantly lower at the combination site compared with the fluconazole alone site (*P* = 0.003). The PORH AUC was lower than placebo (4,477 ± 2,410% CVC_{max}/s) at the fluconazole (2,451 ± 1,417% CVC_{max}/s; *P* = 0.008), lidocaine (2,247 ± 1,851% CVC_{max}/s; *P* = 0.001), and fluconazole + lidocaine (1,683 ± 1,015% CVC_{max}/s; *P* = 0.01) sites (ANOVA *P* < 0.001, Fig. 1).

In a post hoc analysis, we tested whether the effect of fluconazole and lidocaine/prilocaine was different on PORH peak and AUC. Data were expressed as a percentage of placebo peak and AUC. Fluconazole effect on PORH peak was significantly smaller than on AUC (–29 ± 11 vs. –45 ± 19%, respectively, *P* = 0.015). Lidocaine/prilocaine effect did not differ on PORH peak vs. AUC [–57 ± 11 and –52 ± 29%, respectively, not significant (NS)]. The effect of the combination did not differ on PORH peak vs. AUC (–54 ± 15 and –59 ± 29%, respectively, NS).

EETs and NO Synthase Inhibition

There was no significant difference in absolute CVC_{max} values between treatment sites (placebo: 1.9 ± 0.5 PU/mmHg; fluconazole: 1.9 ± 0.6; L-NMMA: 1.9 ± 0.5; fluconazole + L-NMMA: 1.9 ± 0.6). Similarly, there was no significant difference in baseline flux values between treatment sites (placebo: 16 ± 6% CVC_{max}; fluconazole: 18 ± 6% CVC_{max}; L-NMMA: 14 ± 4% CVC_{max}; and fluconazole + L-NMMA: 14 ± 6% CVC_{max}).

The PORH peak at the placebo site averaged 64 ± 9% CVC_{max} and was significantly reduced at the fluconazole site only (49 ± 11% CVC_{max}; *P* = 0.001) (ANOVA *P* < 0.001, Fig. 2). The PORH peak was significantly lower at the combination site compared with the L-NMMA site (*P* = 0.008). The PORH AUC was lower than placebo (4,317 ± 993% CVC_{max}/s) at the fluconazole site only (2,318 ± 691% CVC_{max}/s; *P* = 0.008) (ANOVA *P* = 0.002, Fig. 2).

In a post hoc analysis, when data were expressed as a percentage of placebo peak and AUC, fluconazole effect on PORH peak was significantly smaller than on AUC (–23 ± 12 vs. –43 ± 24%, respectively, *P* = 0.043).

DISCUSSION

Using two-dimensional LSCI coupled with skin microdialysis, we show that, in addition to sensory nerves, cytochrome epoxygenase metabolites play a major role in skin PORH.

To assess the role of EDHF in skin PORH, we used fluconazole as an inhibitor of cytochrome epoxygenases. Lorenzo and Minson previously showed that 50 mM tetraethylammonium decreases PORH peak and AUC (24), suggesting that an EDHF is implicated in skin PORH. However, tetraethylammonium ions, especially at high concentrations, may block different types of potassium channels with varying degrees of effectiveness, targeting ATP-dependent potassium and delayed-rectifier channels (21). We tested the hypothesis that the EETs pathway, one of the EDHF pathways, is involved in skin PORH. Like tetraethylammonium, fluconazole did not affect baseline CVC (24), suggesting that cytochrome epoxygenase metabolites do not regulate basal skin vascular tone. Similarly to Lorenzo and Minson, we were unable to demonstrate an effect of fluconazole at the lidocaine/prilocaine-treated sites, suggesting that

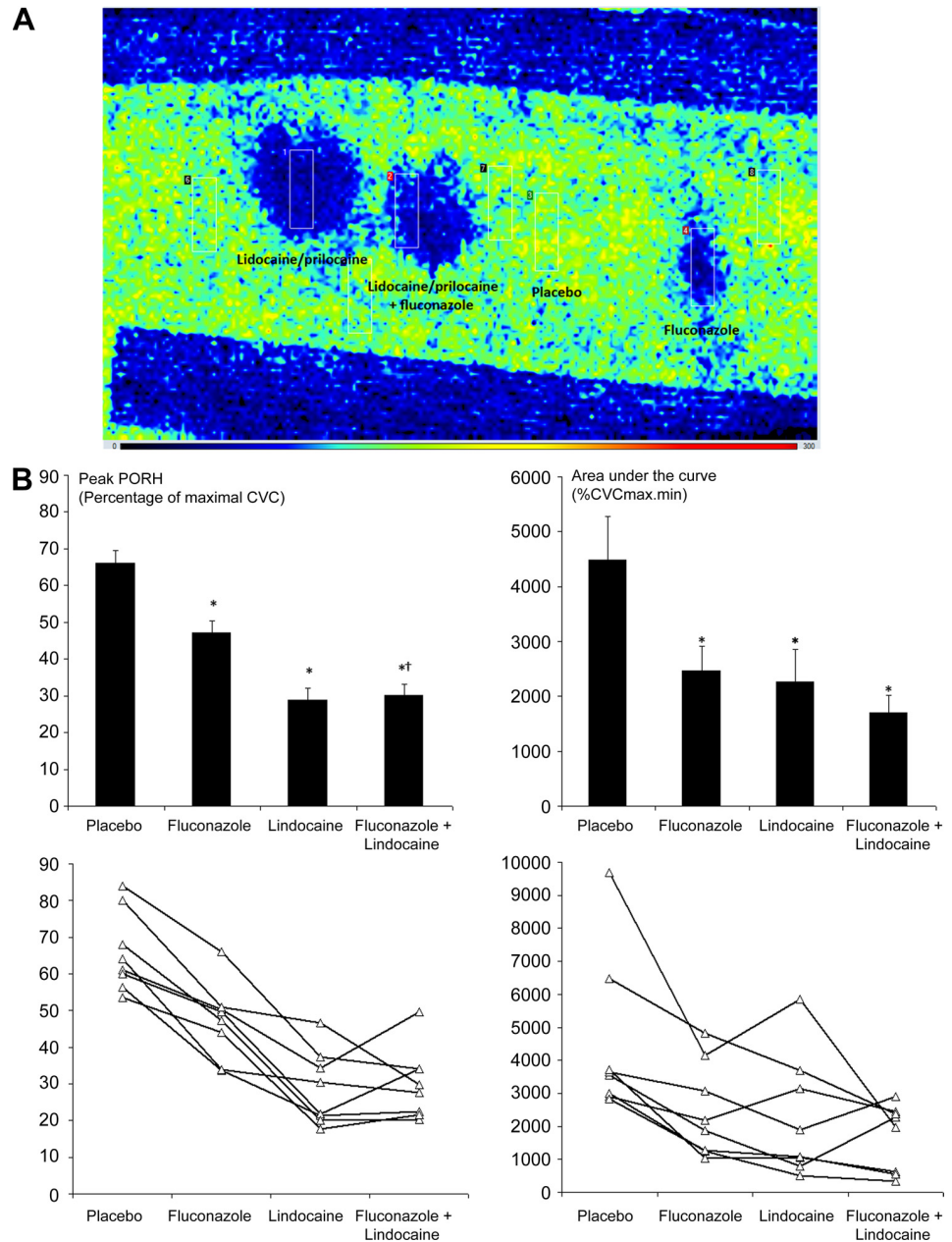


Fig. 1. *A*: representative laser speckle contrast image (LSCI) over the 4 microdialysis fibers during the peak of postocclusive reactive hyperemia (region of interest 1 to 4 and their respective controls 5 to 8, the latter were used only for quality control during the recording and not used for data analysis) where the effect of fluconazole, lidocaine/prilocaine, and the combination can be observed. *B*: mean \pm SE effect of placebo, fluconazole, lidocaine/prilocaine, and the combination on peak post-occlusive reactive hyperemia (*left*) and area under the curve (AUC, *right*). PORH, post-occlusive reactive hyperemia; CVC, cutaneous vascular conductance; CVCmax, maximal CVC. * $P < 0.001$ (peak) and < 0.01 (AUC) vs. placebo. † $P = 0.003$ vs. fluconazole. Corresponding individual data are on *bottom*.

while both pathways contribute to skin PORH, they do not act synergistically and that cytochrome epoxygenase metabolites are involved in the downstream actions of sensory nerves. A potential limitation is that, in addition to sodium channels, local anesthetics may block potassium channels, whether voltage sensitive or not, as well as Ca^{2+} channels, yet with a low affinity (33). Therefore, while unlikely, we cannot rule out a direct effect of lidocaine/prilocaine on calcium-activated potassium channels. Recent data suggest that CYP metabolites play a role in local thermal hyperemia in skin (9). In the latter study, CYP2C9 was blocked using sulfaphenazole, which has the advantage of being highly specific but the disadvantage of being insoluble in water, and requires dimethyl sulfoxide, making experiments more complex. We chose fluconazole since it preferentially inhibits CYP2C9 and -2C19 (35), is

soluble in water, is available for perfusion in humans, and has been used previously as a reference for EETs inhibition in studies on flow-mediated dilation in conductance arteries, where an inhibition of EETs production was demonstrated (2, 4). Furthermore, with the use of intra-arterial fluconazole injections in patients with essential hypertension, an impaired contribution of EETs to the flow-mediated dilation in the radial artery can be demonstrated (4). Interestingly, the inhibitory effect of fluconazole was more pronounced on the PORH AUC than on the peak, suggesting that EETs are mostly involved in the time course rather than the peak response.

Previous *in vitro* studies clearly indicate that an endothelium-dependent non-NO, nonprostanoid mechanism of relaxation is involved in human subcutaneous microvessels mounted on pressure myographs (10, 12). Indeed, EDHF was the major

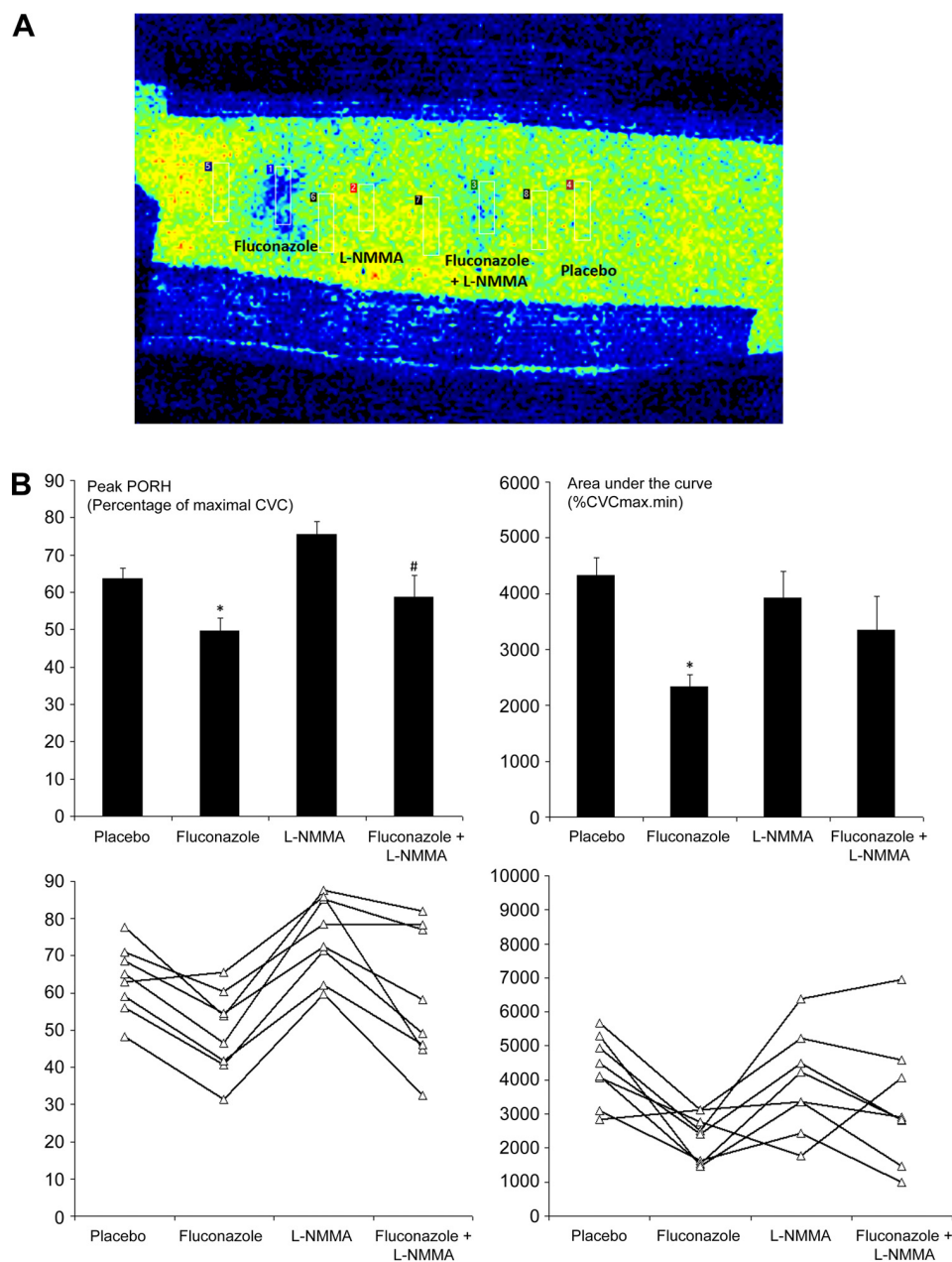


Fig. 2. A: representative LSCI image over the 4 microdialysis fibers during the peak of postocclusive reactive hyperemia where the effect of fluconazole, N^G -monomethyl-L-arginine (L-NMMA), and the combination can be observed (region of interest 1–4 and their respective controls 5–8, the latter were used only for quality control during the recording and not used for data analysis). B: mean \pm SE effect of placebo, fluconazole, L-NMMA, and the combination on peak postocclusive reactive hyperemia (left) and AUC (right). * $P = 0.001$ (peak) and 0.002 (AUC) vs. placebo. # $P = 0.008$ vs. L-NMMA. Corresponding individual data are on bottom.

contributor to the acetylcholine-dependent endothelium vasorelaxation, and in these arteries a product of CYP metabolism of arachidonic acid was likely to be EDHF, as shown by the concentration-dependent inhibition obtained using the nonspecific CYP inhibitor ketoconazole (12). However, heterogeneity of CYP inhibitors is observed, since acetylcholine relaxation of human subcutaneous microvessels was unaffected by 17-octadecynoic acid, a CYP inhibitor, whereas econazole induced a small but significant rightward shift of the concentration-dependent curves (10). In contrast, Lenasi et al. showed that inhibition of CYP2C9 through skin microinjections did not modify acetylcholine iontophoresis-induced vasodilation of human forearm skin, whereas combined NO and COX blockade altered the response (23). However, to fully compare such data and avoid the confounding effect of current-induced vasodilation, acetylcholine and the

blockers used should be infused intradermally through microdialysis fibers rather than via the less reproducible iontophoresis and microinjection techniques.

Multiple CYPs can metabolize arachidonic acids to EETs. Mammalian CYP1A, CYP2B, CYP2C, CYP2D, CYP2G, CYP2J, CYP2N, and CYP4A subfamilies have been shown to be capable of EET biosynthesis in vitro (37), but only the CYP2C and CYP2J isoforms appear to contribute to EETs formation in human endothelial cells (5). In our study it is likely that fluconazole exerted its effect through the inhibition of EETs production. However, it was not feasible to quantify EETs in the dialysate. Indeed, plasma EET concentrations are very low, ~ 10 ng/ml (4). EETs are strongly bound to proteins (95%), and the quantity available for diffusion through a microdialysis membrane is therefore very low. In addition, quantification by skin microdialysis

would not be optimal given that EETs production would be transient over the 5-min PORH, while it takes ~60 min to obtain a sufficient volume of dialysate to run an assay using LC-MS MS. LSCI coupled with the use of inserted microdialysis fibers has the advantage of providing easy visual analysis throughout the protocol, with low within-subject coefficients of variation for skin PORH (13).

The human skin microcirculation is able to release NO, as suggested in the plateau phase of local thermal hyperemia (27) or following acetylcholine perfusion (38). In the present study we showed that infusion of a NO synthase inhibitor, L-NMMA, does not affect skin PORH. This is consistent with three previous studies where NO synthase inhibition using *N*^G-nitro-L-arginine methyl ester (L-NAME) or nitro-L-arginine perfusion through microdialysis fibers did not alter skin PORH (24, 26, 36). Similarly, L-NAME injected intradermally did not decrease peak skin PORH in a fourth study (11). Lastly, skin PORH was not associated with a detectable rise in NO concentrations (38). Therefore, there is large evidence that NO does not participate in skin PORH and that the effects of EDHFs are more important than NO in this microcirculation (32). However, when L-NMMA was infused together with fluconazole, the inhibitory effect of fluconazole on skin PORH was partially reversed and did not differ from placebo. An interaction between NO and EET had already been described in human peripheral conductance arteries, where either fluconazole or L-NMMA infusion decreased the flow-mediated dilation of radial arteries induced by heating skin of the hand, but their combination potentiated their effects (3). The general belief is that the effects of NO predominate in large vessels while EDHFs are more important in the microcirculation (32). However, both NO and EDHFs contribute to the flow-mediated vasodilatation in human conductance arteries (3). An important question that remains unanswered is why would PORH stimulate the skin endothelium to release EDHFs and EETs but not NO? A possible response is the nature of the stimulus. When PORH is studied using the flow-mediated dilation of the brachial artery or forearm strain gauge plethysmography, quick increases in shear stress are the major initial mechanisms leading to endothelial cell activation. Indeed, Koller and Bagi showed in vitro that, in isolated skeletal muscle arterioles (20), a reactive dilatation resembling that of in vivo PORH can be generated. The factors implicated in the response were deformation, stretch, pressure, and shear stress. However, such physical factors differ when studying PORH of the skin because of its specific microvascular architecture: it is organized as a horizontal arteriovenous plexus at the dermal-hypodermal interface, from which ascending arterioles arise and connect directly to a superficial horizontal arteriovenous plexus in the papillary dermis, from which the nutritive capillary loops arise (8). Contrary to the flow-mediated dilatation of the brachial artery, skin PORH cannot be elicited above the pressure cuff (unpublished observations). Therefore, it is likely that a similar method (brachial artery occlusion) will not induce the same physical stimulus and will not activate the same endothelial mechanisms, but this hypothesis remains to be tested.

In conclusion, we have shown that cytochrome epoxygenase metabolites, putatively EETs, play a major role in healthy skin PORH, in addition to sensory nerves. Their effect seems to be more important in the time course rather than the peak. Whether alteration of this pathway can explain the modified

skin PORH observed in diseases such as diabetes and scleroderma remains to be tested.

ACKNOWLEDGMENTS

We thank the "Direction de la Recherche Clinique et des Innovations" of Grenoble University Hospital for funding. We also thank Dr. Adeline Paris and Elodie Troccaz for performing the blinded randomization and Dr. Alison Foote for editing the manuscript.

DISCLOSURES

Jean-Luc Cracowski and Dr. Matthieu Roustit have received research grants from Actelion, Glaxo-Smith Kline, Boiron and Pfizer, for other studies.

AUTHOR CONTRIBUTIONS

Author contributions: J.-L.C., M.R., and C.M. conception and design of research; J.-L.C., F.G.-B., C.C., and C.S. performed experiments; J.-L.C., F.G.-B., C.C., and M.R. analyzed data; J.-L.C., F.G.-B., C.S., M.R., and C.M. interpreted results of experiments; J.-L.C. prepared figures; J.-L.C. drafted manuscript; J.-L.C., F.G.-B., C.C., C.S., M.R., and C.M. edited and revised manuscript; J.-L.C., F.G.-B., C.C., C.S., M.R., and C.M. approved final version of manuscript.

REFERENCES

1. Addor G, Delachaux A, Dischl B, Hayoz D, Liaudet L, Waeber B, Feihl F. A comparative study of reactive hyperemia in human forearm skin and muscle. *Physiol Res* 57: 685–692, 2008.
2. Bellien J, Favre J, Iacob M, Gao J, Thuillez C, Richard V, Joannides R. Arterial stiffness is regulated by nitric oxide and endothelium-derived hyperpolarizing factor during changes in blood flow in humans. *Hypertension* 55: 674–680, 2010.
3. Bellien J, Iacob M, Gutierrez L, Isabelle M, Lahary A, Thuillez C, Joannides R. Crucial role of NO and endothelium-derived hyperpolarizing factor in human sustained conduit artery flow-mediated dilatation. *Hypertension* 48: 1088–1094, 2006.
4. Bellien J, Iacob M, Remy-Jouet I, Lucas D, Monteil C, Gutierrez L, Vendeville C, Dreano Y, Mercier A, Thuillez C, Joannides R. Epoxyeicosatrienoic acids contribute with altered nitric oxide and endothelin-1 pathways to conduit artery endothelial dysfunction in essential hypertension. *Circulation* 125: 1266–1275, 2012.
5. Bellien J, Joannides R, Richard V, Thuillez C. Modulation of cytochrome-derived epoxyeicosatrienoic acids pathway: a promising pharmacological approach to prevent endothelial dysfunction in cardiovascular diseases? *Pharmacol Ther* 131: 1–17, 2011.
6. Binggeli C, Spiekler LE, Corti R, Sudano I, Stojanovic V, Hayoz D, Luscher TF, Noll G. Statins enhance postischemic hyperemia in the skin circulation of hypercholesterolemic patients: a monitoring test of endothelial dysfunction for clinical practice? *J Am Coll Cardiol* 42: 71–77, 2003.
7. Blair DA, Glover WE, Roddie IC. The abolition of reactive and post-exercise hyperaemia in the forearm by temporary restriction of arterial inflow. *J Physiol* 148: 648–658, 1959.
8. Braverman IM. The cutaneous microcirculation. *J Invest Dermatol Symp Proc* 5: 3–9, 2000.
9. Brunt VE, Minson CT. KCa channels and epoxyeicosatrienoic acids: major contributors to thermal hyperaemia in human skin. *J Physiol* 590: 3523–3534, 2012.
10. Buus NH, Simonsen U, Pilegaard HK, Mulvany MJ. Nitric oxide, prostanoid and non-NO, non-prostanoid involvement in acetylcholine relaxation of isolated human small arteries. *Br J Pharmacol* 129: 184–192, 2000.
11. Cankar K, FINDERLE Z, Struel M. The effect of alpha-adrenoceptor agonists and L-NMMA on cutaneous postocclusive reactive hyperemia. *Microvasc Res* 77: 198–203, 2009.
12. Coats P, Johnston F, MacDonald J, McMurray JJ, Hillier C. Endothelium-derived hyperpolarizing factor: identification and mechanisms of action in human subcutaneous resistance arteries. *Circulation* 103: 1702–1708, 2001.
13. Cracowski JL, Gaillard-Bigot F, Cracowski C, Roustit M, Millet C. Skin microdialysis coupled with laser speckle contrast imaging to assess microvascular reactivity. *Microvasc Res* 82: 333–338, 2011.

14. Cracowski JL, Lorenzo S, Minson CT. Effects of local anaesthesia on subdermal needle insertion pain and subsequent tests of microvascular function in human. *Eur J Pharmacol* 559: 150–154, 2007.
15. Cracowski JL, Minson CT, Salvat-Melis M, Halliwill JR. Methodological issues in the assessment of skin microvascular endothelial function in humans. *Trends Pharmacol Sci* 27: 503–508, 2006.
16. Dalle-Ave A, Kubli S, Golay S, Delachaux A, Liaudet L, Waeber B, Feihl F. Acetylcholine-induced vasodilation and reactive hyperemia are not affected by acute cyclo-oxygenase inhibition in human skin. *Microcirculation* 11: 327–336, 2004.
17. Edwards G, Feletou M, Weston AH. Endothelium-derived hyperpolarising factors and associated pathways: a synopsis. *Pflugers Arch* 459: 863–879, 2010.
18. Engelke KA, Halliwill JR, Proctor DN, Dietz NM, Joyner MJ. Contribution of nitric oxide and prostaglandins to reactive hyperemia in human forearm. *J Appl Physiol* 81: 1807–1814, 1996.
19. Fischer D, Landmesser U, Spiekermann S, Hilfiker-Kleiner D, Hospely M, Muller M, Busse R, Fleming I, Drexler H. Cytochrome P450 2C9 is involved in flow-dependent vasodilation of peripheral conduit arteries in healthy subjects and in patients with chronic heart failure. *Eur J Heart Fail* 9: 770–775, 2007.
20. Koller A, Bagi Z. On the role of mechanosensitive mechanisms eliciting reactive hyperemia. *Am J Physiol Heart Circ Physiol* 283: H2250–H2259, 2002.
21. Langton PD, Nelson MT, Huang Y, Standen NB. Block of calcium-activated potassium channels in mammalian arterial myocytes by tetraethylammonium ions. *Am J Physiol Heart Circ Physiol* 260: H927–H934, 1991.
22. Larkin SW, Williams TJ. Evidence for sensory nerve involvement in cutaneous reactive hyperemia in humans. *Circ Res* 73: 147–154, 1993.
23. Lenasi H. The role of nitric oxide- and prostacyclin-independent vasodilatation in the human cutaneous microcirculation: effect of cytochrome P450 2C9 inhibition. *Clin Physiol Funct Imaging* 29: 263–270, 2009.
24. Lorenzo S, Minson CT. Human cutaneous reactive hyperaemia: role of BKCa channels and sensory nerves. *J Physiol* 585: 295–303, 2007.
25. McCord GR, Cracowski JL, Minson CT. Prostanoids contribute to cutaneous active vasodilation in humans. *Am J Physiol Regul Integr Comp Physiol* 291: R596–R602, 2006.
26. Medow MS, Taneja I, Stewart JM. Cyclooxygenase and nitric oxide synthase dependence of cutaneous reactive hyperemia in humans. *Am J Physiol Heart Circ Physiol* 293: H425–H432, 2007.
27. Minson CT. Thermal provocation to evaluate microvascular reactivity in human skin. *J Appl Physiol* 109: 1239–1246, 2010.
28. Mullen MJ, Kharbanda RK, Cross J, Donald AE, Taylor M, Vallance P, Deanfield JE, MacAllister RJ. Heterogenous nature of flow-mediated dilatation in human conduit arteries in vivo: relevance to endothelial dysfunction in hypercholesterolemia. *Circ Res* 88: 145–151, 2001.
29. Ozkor MA, Murrrow JR, Rahman AM, Kavtaradze N, Lin J, Manatunga A, Quyyumi AA. Endothelium-derived hyperpolarizing factor determines resting and stimulated forearm vasodilator tone in health and in disease. *Circulation* 123: 2244–2253, 2011.
30. Patterson GC. The role of intravascular pressure in the causation of reactive hyperaemia in the human forearm. *Clin Sci (Lond)* 15: 17–25, 1956.
31. Pyke KE, Tschakovsky ME. The relationship between shear stress and flow-mediated dilatation: implications for the assessment of endothelial function. *J Physiol* 568: 357–369, 2005.
32. Quyyumi AA, Ozkor M. Vasodilation by hyperpolarization: beyond NO. *Hypertension* 48: 1023–1025, 2006.
33. Scholz A. Mechanisms of (local) anaesthetics on voltage-gated sodium and other ion channels. *Br J Anaesthesia* 89: 52–61, 2002.
34. Tagawa T, Imaizumi T, Endo T, Shiramoto M, Harasawa Y, Takeshita A. Role of nitric oxide in reactive hyperemia in human forearm vessels. *Circulation* 90: 2285–2290, 1994.
35. Venkatakrishnan K, von Moltke LL, Greenblatt DJ. Effects of the antifungal agents on oxidative drug metabolism: clinical relevance. *Clin Pharmacokinet* 38: 111–180, 2000.
36. Wong BJ, Wilkins BW, Holowatz LA, Minson CT. Nitric oxide synthase inhibition does not alter the reactive hyperemic response in the cutaneous circulation. *J Appl Physiol* 95: 504–510, 2003.
37. Zeldin DC. Epoxygenase pathways of arachidonic acid metabolism. *J Biol Chem* 276: 36059–36062, 2001.
38. Zhao JL, Pergola PE, Roman LJ, Kellogg DL Jr. Bioactive nitric oxide concentration does not increase during reactive hyperemia in human skin. *J Appl Physiol* 96: 628–632, 2004.

Troisième étude : Rôle des cyclo-oxygénases (COX) dans l'hyperhémie post-occlusive (titre court : EETY, étude ancillaire)

Dans la continuité de l'étude des facteurs impliqués dans la fonction endothéliale microvasculaire, nous avons voulu évaluer l'implication des cyclo-oxygénases (COX) dans l'hyperhémie post-occlusive (PORH) au niveau de la microcirculation cutanée chez l'homme.

Six volontaires sains ont été inclus dans une expérience contrôlée contre placebo. Nous avons étudié l'effet du kétoprofène à 4 mM versus placebo (du NaCl à 0,9%), administré à l'aide de fibres de microdialyse, suivant une PORH après 5 minutes d'occlusion artérielle. Le flux sanguin cutané a été exprimé en conductance vasculaire cutanée maximale (CVCmax), obtenue après l'administration de nitroprussiate de sodium (SNP) à 29 mM.

Comparativement au site placebo, nous n'avons pas mis en évidence de différence sur la PORH tant au niveau du pic initial qu'au niveau de la phase d'hyperhémie prolongée.

En conclusion, les inhibiteurs des cyclo-oxygénases n'altèrent pas la PORH chez l'homme, suggérant l'absence d'implication des COX au sein des médiateurs connus pour contribuer à cette PORH.

Article publié: *Prostanoids are not involved in postocclusive reactive hyperaemia in human skin.* Hellmann M, Gaillard-Bigot F, Roustit M, Cracowski JL. *Fundam Clin Pharmacol.* 2015 Oct;29(5):510-6.

ORIGINAL
ARTICLEProstanoids are not involved in
postocclusive reactive hyperaemia in
human skinMarcin Hellmann^{a,b}, Florence Gaillard-Bigot^a, Matthieu Roustit^{a,c,d},
Jean-Luc Cracowski^{a,c,d*}^aClinical Pharmacology Department, Inserm CIC3, University Hospital, Grenoble, France^bNoninvasive Cardiac Diagnostics Department, Medical University, Gdansk, Poland^cInserm U1042, Grenoble, France^dUniversity Grenoble-Alpes, Grenoble, France**Keywords**cyclo-oxygenase,
endothelium,
ketoprofen,
laser speckle contrast
imaging,
microcirculation,
postocclusive reactive
hyperaemia,
skin microdialysis**ABSTRACT**

Several mediators contribute to postocclusive reactive hyperaemia (PORH) in the skin, including sensory nerves and endothelium-derived hyperpolarizing factors. The main objective of this study was to investigate the specific involvement of prostanoids in human skin PORH. We tested the effect of the inhibition of cyclo-oxygenases (COX) by 4 mM ketoprofen, infused through microdialysis fibers inserted into the healthy volunteers forearm skin, following 5 min brachial artery occlusion. Skin microvascular blood flux was recorded using two-dimensional Laser Speckle Contrast Imaging. Maximal cutaneous vascular conductance (CVC_{max}) was obtained following the perfusion of 29 mM sodium nitroprusside. A systematic review of the effects of COX inhibitors on skin peak PORH was also performed. We observed no significant difference between ketoprofen and placebo for the PORH peak (78 ± 8 and $71 \pm 19\%$ CVC_{max} , respectively) and area under the curve (2951 ± 721 and $2490 \pm 936\%$ $CVC_{max.s}$). A meta-analysis showed a substantial heterogeneity between studies, with overall a neutral effect of COX inhibition on peak PORH. Cyclo-oxygenase inhibition does not alter skin PORH, suggesting no involvement of prostanoids in cutaneous postocclusive vasodilatation in healthy humans.

Received 12 February 2015;
revised 2 July 2015;
accepted 15 July 2015*Correspondence and reprints:
jean-luc.cracowski@
ujf-grenoble.fr**INTRODUCTION**

Endothelium plays a crucial role in the regulation of vascular tone by releasing vasoactive substances, including nitric oxide, prostacyclin, and endothelium-derived hyperpolarizing factors [1]. Microvascular function in the skin can be studied routinely in humans using the recent laser speckle contrast imaging (LSCI). When studying microcirculation, a conventional approach is to study postocclusive reactive hyperaemia (PORH), commonly used as a marker of microvascular endothelial function [2].

Postocclusive reactive hyperaemia is the sudden increase in cutaneous or muscle blood flow after the release of an arterial occlusion [3]. Postischemic

vasodilatation has been observed in most vascular beds, but the precise vasodilatory mechanism differs between tissues [4]. Flow-mediated dilatation of the brachial or radial arteries is mainly nitric oxide (NO) dependent [5]. Recently, it has been shown that cytochrome-related endothelium-derived hyperpolarizing factors (EDHFs) are involved in this response [6]. While skeletal muscle PORH similarly depends on NO, prostaglandins appear to be the important determinants of peak flow [7].

In the skin, in contrast to other vascular beds, the inhibition of NO production does not alter PORH on the forearm [8]. The involvement of sensory nerves via local axon reflex has been described as a major contributor to both the peak and the time course [9–11].

Apart from sensory nerves, the second important endothelium-dependent dilation mechanism involves the endothelium-derived hyperpolarizing factors produced through the cytochrome epoxygenase pathway [4]. Besides the cytochrome epoxygenase pathway, endothelial cells metabolize arachidonic acid via two additional enzymes: the lipoxygenases and the cyclooxygenases (COX). Many researchers tested the implication of COX in cutaneous PORH, with conflicting results [10,11,11–15,15–18].

Given the heterogeneity of the previous studies, we investigated the specific contribution of prostanoids in human skin PORH and performed a meta-analysis of the available studies.

MATERIALS AND METHODS

Study population

We enrolled six healthy subjects recruited through the Clinical Research Center Volunteer database. Inclusion criteria were age 18 years or older and no significant medical history. For women of child-bearing age, the possibility of pregnancy was excluded by urine tests at the beginning of each study visit. For all subjects, non-inclusion criteria included any allergies to local anesthetics, cigarette smoking, and any dermatological pathology affecting the arms.

The investigation conforms to the principles outlined in the Declaration of Helsinki. Grenoble Institutional Review Board (IRB no. 6705) approval was obtained, and each volunteer gave written informed consent before participation.

Experimental set-up

Subjects attended an initial enrollment visit where inclusion and noninclusion criteria were checked by a physician, and full information given. Seven \pm three days later, they returned for the experimental visit. For women, experimental visits were performed during the menstrual phase.

On arrival at the laboratory, subjects were placed supine in a temperature-controlled room (24 ± 1 °C). After checking for visible veins, lidocaine/prilocaine cream (10 g) was applied to the ventral face of the right forearm for 40 min, with an occlusive transparent dressing placed over the cream [9]. Microdialysis fiber insertion was performed as previously described [19]. After removal of the lidocaine/prilocaine cream, we randomly chose two skin sites, 2–3 cm apart, on the ventral side of the right upper forearm, avoiding



Figure 1 Microdialysis fibers were inserted in the ventral face of the forearm and randomly perfused with 4 mm ketoprofen or 0.9% NaCl.

veins. Local asepsia was performed. Then, sterile 21 G, 50-mm needles were inserted into the skin over a length of 1.5–2 cm, and a CMA 66[®] linear microdialysis catheter with a 1 cm long, 500 μ m diameter, 20 000 Dalton cut-off membrane (CMA Microdialysis, Solna, Sweden), previously rinsed with sterile 0.9% NaCl, was immediately inserted through the needle (Figure 1). The fiber was immediately connected to a portable battery driven syringe pump (CMA 107 Microdialysis Pump[®]). Once closed, the pump started a 5 min flush sequence at 15 μ L/min and then automatically decreased to the preset flow rate of 2 μ L/min, as used previously [20].

Fiber sites were randomized to receive either 4 mm ketoprofen (a nonspecific COX inhibitor used to block prostanoid production) or placebo (0.9% NaCl), perfused for 100 min. All drugs and syringes were prepared and blinded by an independent pharmacist.

The arm was then placed on a vacuum cushion to decrease artifacts associated with arm movements, and cutaneous blood flow was measured with LSCI (PeriCam PSI System, Perimed, Järfälla, Sweden; Laser wavelength 785 nm). The laser speckle measurements were taken on the ventral side of the right upper forearm, and the laser head was placed 15 cm above the skin (with a resolution of approximately 6944 pixels/cm²).

Two hours after lidocaine/prilocaine removal, blood flow was occluded for 5 min by inflating a cuff placed on the right upper arm to 50 mmHg above the volunteer's systolic blood pressure. At the end of all experiments, 29 mM sodium nitroprusside (SNP) was perfused at both sites simultaneously for 15 min to

obtain maximal cutaneous vascular conductance (CVC_{max}) [19]. Blood pressure was recorded continuously throughout the experiment (Nexfin monitor; Bmeye B.V., Amsterdam, The Netherlands) on the contralateral hand.

Drugs

Ketoprofen 100 mg was purchased from Sanofi-Aventis (Paris, France) and diluted in 100 mL of 0.9% NaCl solution (Aguettant, Lyon, France) to obtain 4 mM ketoprofen. Sodium nitroprusside (Nitriate[®]) was purchased from Serb (Paris, France). Fifty milligrams of SNP were diluted in 8 mL of 0.9% NaCl solution (Aguettant) to obtain 29 mM SNP. All solutions were prepared extemporaneously and discarded the same day. Lidocaine/prilocaine cream (5 g tubes containing 125 mg lidocaine and 125 mg prilocaine) was purchased from Aguettant.

Data analysis

Skin blood flux was averaged over two regions of interest area of 60 mm². For each region of interest, an additional region of interest was used as a quality control, but not used for data analysis. Data were digitized, stored, and analyzed off-line with signal processing software (PimSoft 1.1.1; Perimed). The biological zero, recorded during the 5 min occlusion, was subtracted from all raw values, and data were subsequently expressed as CVC (PU/mmHg), which is the flux in perfusion units (PU) divided by the mean arterial pressure (MAP) in mmHg and as a percentage of CVC_{max} (% CVC_{max}). CVC values were averaged over 4 min periods for the baseline and SNP and over 20 s for the peak PORH. The PORH area under the curve (AUC) was given by: raw PORH AUC over 6 min – (baseline CVC × 360 s) and expressed as PU.s per mmHg.

Statistical analysis

Quantitative data are expressed as mean and standard deviation and were analyzed by paired *t*-tests, with each subject serving as his/her own control. *P* values less than 0.05 were considered statistically significant. Statistical analysis was performed using IBM SPSS Statistics for Windows, v21, Armonk, NY: IBM Corp.

Meta-analysis

A systematic review of the effects of COX inhibitors on skin peak PORH, tested in clinical trials, was performed according to the Cochrane Handbook for Systematic Reviews of Interventions Version 5.1.0 [21]. Data were

analyzed using Review Manager (RevMan) v5.2.7, Copenhagen: The Nordic Cochrane Centre, The Cochrane Collaboration, 2014. The Medline database was consulted (1950–2014). The search terms were skin, reactive hyperaemia, and COX. From these articles and from a previous review, we further found additional articles. The last search was run on January 15, 2015. We found eight published controlled trials evaluating the effect of a COX inhibitor on skin PORH, and we added the results of the present study (Hellmann 2015). In all articles, the PORH peak response was reported and introduced in the meta-analysis. One of the old studies reported median and extremes, and mean and standard deviation were calculated according to Hozo *et al.* [22]. We used a standardized mean difference approach to standardize the mean differences to a single scale. Given the substantial heterogeneity, a random-effects model was used to weight the studies relatively more equally than a fixed-effect analysis.

RESULTS

Effect of ketoprofen on skin PORH

Three males and three females, all Caucasian, were enrolled in the study. Their mean age was 24 ± 1 years, their body mass index was 21 ± 1 kg/m², and their systolic/diastolic arterial pressure was $128 \pm 11/72 \pm 5$ mmHg. The mean pain scores on insertion of the microdialysis fibers assessed on a 10 point visual analogic scale were 1.6 ± 1.1 . No adverse effects occurred.

There was no significant difference between treatment sites in absolute CVC_{max} values obtained following 29 mM SNP infusion at the end of the experiment (placebo: 2.2 ± 0.4 PU/mmHg; ketoprofen: 2.3 ± 0.4 PU/mmHg). Similarly, we observed no differences between baseline flux values at the ketoprofen site ($16 \pm 3\%$ CVC_{max}) vs. placebo site ($19 \pm 6\%$ CVC_{max}).

We observed no significant difference between ketoprofen and placebo for the PORH peak and AUC. The mean PORH peak at the placebo site was $71 \pm 19\%$ CVC_{max} vs. $78 \pm 8\%$ CVC_{max} for ketoprofen site. The PORH AUC was $2490 \pm 936\%$ $CVC_{max}\cdot s$ at the placebo site vs. ($2951 \pm 721\%$ $CVC_{max}\cdot s$) at the ketoprofen site.

Meta-analysis

The systematic review showed a substantial heterogeneity between studies, with overall a neutral effect of COX inhibition on peak PORH (Figure 2). When funnel

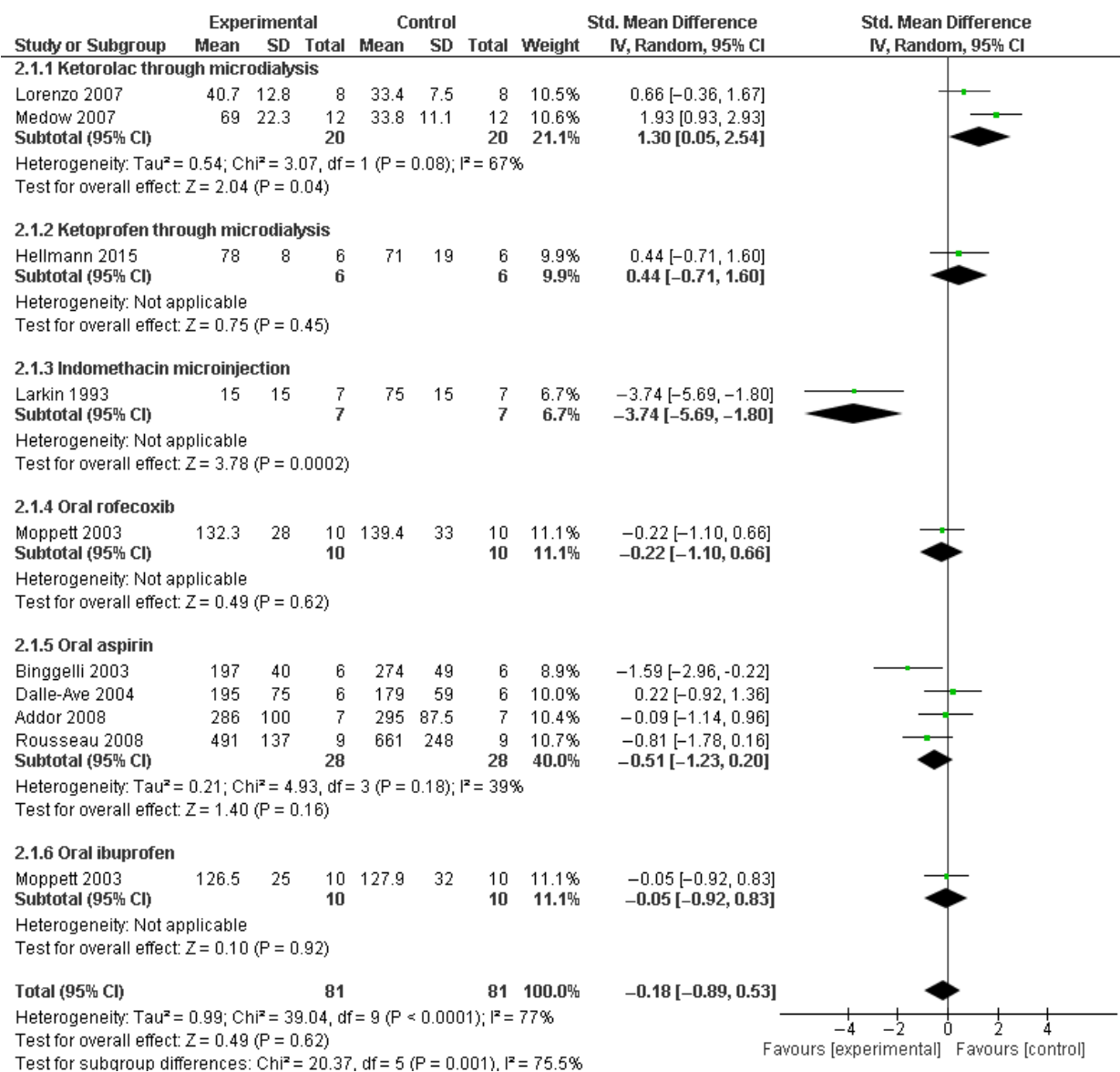


Figure 2 Meta-analysis of the effect of different cyclo-oxygenase inhibitors on skin peak postocclusive hyperaemia, stratified by drugs.

plots were constructed, we observed symmetry suggesting no publication bias. Sensitivity analysis was performed, removing Larkin or Medow’s reports [10,15], and did not affect the final outcome.

DISCUSSION

Using two-dimensional LSCI, we showed that COX inhibition does not alter skin PORH, suggesting no involvement of prostanoids in postischemic vasodilatation and a meta-analysis showed an overall neutral effect of COX inhibition on peak PORH.

The recently developed laser speckle contrast imaging (LSCI) is a technique based on speckle contrast analysis that provides an index of blood flow with excellent spatial and temporal resolution and very good reproducibility [23]. It has been shown that subdermal placement of fibers coupled with LSCI is reproducible and provides two-dimensional information, enabling mechanistic studies of skin microcirculation [19].

The major prostanoid secreted by endothelial cells is PGI₂, as the prostacyclin synthase enzyme is enriched in this cell type, but the rate limiting enzymes in prostanoid synthesis are COX. Normal endothelial cells and

vascular smooth muscle cells mostly express COX-1 [24–26]. Immunolocalization showed that COX-2 is visible, but hardly, in normal human skin, with little seen in the basal layer of the epidermis and in the dermis [27]. COX-2 was identified as a shear stress-inducible gene in vascular endothelial cell cultures, and it was shown that COX-2 is the main enzyme contributing to the body biosynthesis of prostacyclin [24]. To assess the role of COX in skin PORH, we used ketoprofen as an inhibitor of COX, as the commonly used inhibitor, ketorolac, is not commercially available in France. The choice of drug concentration was determined according to the manufacturer's specifications for intravenous use, that is, 100 mg diluted in 100 mL 0.9% NaCl. This provides a concentration of 4 mM ketoprofen, in the same order of magnitude as the 10 mM ketorolac, injected commonly by microdialysis fibers for COX pathway inhibition [20]. Ketoprofen is commonly used for its antipyretic, analgesic, and anti-inflammatory properties by inhibiting COX-1 and COX-2 enzymes reversibly, which decreases production of prostanoids. Ketoprofen is a nonselective COX inhibitor. In human whole blood, the IC_{50} values for COX-1 and COX-2 are 0.33 μ M and 0.69 μ M, respectively [28]. Using a microdialysis fiber, and a very long time of equilibration (100 min), ketoprofen concentration equilibrates across the fiber and local tissue concentrations may be in the same order of magnitude as within the fiber. Therefore, the concentration of 4 mM ketoprofen is far higher than the IC_{50} , meaning that our results are not likely to be due to a lack of effect of the drug. A limitation was the low number of subjects enrolled. This was due to the high cost of the whole procedure, and given that no effect could be seen on blinded images during each procedure, the study was stopped early for futility.

In the present study, we showed that nonspecific COX-1 and COX-2 inhibition by 4 mM ketoprofen, when delivered directly into the intradermal space, did not alter either baseline flux or PORH peak and AUC. Using a nonspecific COX inhibitor, ketorolac (10 mM) and a cutaneous microdialysis fiber system similarly inserted in the forearm, Lorenzo and Minson [11] previously found similar results. In contrast, Medow *et al.* [15] found a higher baseline flux and PORH peak following COX blockade by 10 mM ketorolac infused through microdialysis fibers, but this study differs in that they were placed in the calf skin, and we cannot rule out differences of skin reactivity between locations. Results following aspirin administration are also

conflicting: one group showed that 1 g of acetylsalicylic acid, taken orally, decreased the PORH peak on the forearm in six healthy subjects [13], while another study showed no effect of a 900 mg lysine acetylsalicylate injected intravenously on PORH [14] and no effect on the peak response following the ingestion of 1 g acetylsalicylic acid [12]. When aspirin was used at platelet anti-aggregation dose, that is, 75 mg orally, it had no effect on PORH in nine healthy subjects [18]. In contrast, intradermal microinjection of indomethacin was found to be effective in suppressing forearm PORH in one study [10]. Lastly, 800 mg ibuprofen or 25 mg rofecoxib, a specific COX-2 inhibitor, taken orally, did not alter skin PORH in 10 healthy subjects [16]. The results of the meta-analysis, while showing substantial heterogeneity, further suggests that COX blockade does not alter skin peak PORH. Given the lack of data, we were unable to perform it on other items such as PORH AUC or kinetics.

Besides systemic administration of drugs (e.g., iv or oral routes), intradermal delivery has been proposed due to the accessibility of the skin and the possibility of using elevated concentrations with limited systemic exposure. Although skin microinjection and iontophoresis have been proposed as pharmacological tools, they remain tricky to use due to nonspecific axon reflex vasodilatation and nonspecific current induced vasodilatation, respectively. While skin microdialysis is invasive, it offers the advantage of a controlled drug infusion rate and given that vascular assessments are performed 60–120 min after fiber insertion, the fiber itself does not significantly alter microvascular function. Indeed, microdialysis as well as the oral route have advantages and drawbacks, but using a local route has the major advantage of being more physiological, that is, it does not have a systemic effect that may affect the response.

In our meta-analysis, we observed a trend toward an increased peak PORH when studies were performed using microdialysis fibers. The question raised is whether this could be due to the release of vasoconstrictor prostanoids agonists of the thromboxane prostanoid receptor, such as thromboxane A_2 . Pasche *et al.* tested the effect of oral terutroban, a selective antagonist of thromboxane prostanoid receptor, on skin PORH. Terutroban altered neither peak nor AUC, suggesting no implication of thromboxane A_2 in the modulation of postischemic vasodilatation [17]. However, the latter study was performed using the oral route, and an ideal study that remains to be performed would

be to inject a thromboxane prostanoid receptor antagonist through microdialysis fibers.

Another reason for such discrepancies is that the oral administration of COX inhibitors, even at high doses, may not produce the same inhibition that skin infusion through microdialysis [29]. A possible explanation could be that systemic administration exerts potential generalized effects, indirectly affecting peripheral microcirculation [15].

In conclusion, our data and a systematic review show that prostanoids do not contribute to cutaneous postischemic vasodilatation in healthy humans.

ACKNOWLEDGEMENTS

We thank Dr. Alison Foote for critically reading and editing the manuscript and Dr. Adeline Paris for performing the blinded randomization.

FUNDING

This study was funded by grants from the French Ministry of Health. Marcin Hellmann received a French government scholarship delivered by the French embassy in Poland.

CONFLICTS OF INTEREST

The authors declare no conflict of interests.

REFERENCES

- Turner J., Belch J.J., Khan F. Current concepts in assessment of microvascular endothelial function using laser Doppler imaging and iontophoresis. *Trends Cardiovasc. Med.* (2008) **18** 109–116.
- Roustit M., Cracowski J.-L. Assessment of endothelial and neurovascular function in human skin microcirculation. *Trends Pharmacol. Sci.* (2013) **34** 373–384.
- Flammer A.J., Anderson T., Celermajer D.S., Creager M.A., Deanfield J., Ganz P. The assessment of endothelial function: from research into clinical practice. *Circulation* (2012) **126** 753–767.
- Cracowski J.-L., Gaillard-Bigot F., Cracowski C., Sors C., Roustit M., Millet C. Involvement of cytochrome epoxygenase metabolites in cutaneous postocclusive hyperemia in humans. *J. Appl. Physiol.* (2013) **114** 245–251.
- Mullen M.J., Kharbanda R.K., Cross J., Donald A.E., Taylor M., Vallance P. Heterogenous nature of flow-mediated dilatation in human conduit arteries in vivo: relevance to endothelial dysfunction in hypercholesterolemia. *Circ. Res.* (2001) **88** 145–151.
- Bellien J., Iacob M., Gutierrez L., Isabelle M., Lahary A., Thuillez C. Crucial role of NO and endothelium-derived hyperpolarizing factor in human sustained conduit artery flow-mediated dilatation. *Hypertension* (2006) **48** 1088–1094.
- Engelke K.A., Halliwill J.R., Proctor D.N., Dietz N.M., Joyner M.J. Contribution of nitric oxide and prostaglandins to reactive hyperemia in human forearm. *J. Appl. Physiol.* (1996) **81** 1807–1814.
- Wong B.J., Wilkins B.W., Holowatz L.A., Minson C.T. Nitric oxide synthase inhibition does not alter the reactive hyperemic response in the cutaneous circulation. *J. Appl. Physiol.* (2003) **95** 504–510.
- Cracowski J.-L., Lorenzo S., Minson C.T. Effects of local anaesthesia on subdermal needle insertion pain and subsequent tests of microvascular function in human. *Eur. J. Pharmacol.* (2007) **559** 150–154.
- Larkin S.W., Williams T.J. Evidence for sensory nerve involvement in cutaneous reactive hyperemia in humans. *Circ. Res.* (1993) **73** 147–154.
- Lorenzo S., Minson C.T. Human cutaneous reactive hyperaemia: role of BKCa channels and sensory nerves. *J. Physiol.* (2007) **585**(Pt 1) 295–303.
- Addor G., Delachaux A., Dischl B., Hayoz D., Liaudet L., Waeber B. A comparative study of reactive hyperemia in human forearm skin and muscle. *Physiol. Res.* (2008) **57** 685–692.
- Binggeli C., Spieker L.E., Corti R., Sudano I., Stojanovic V., Hayoz D. Statins enhance postischemic hyperemia in the skin circulation of hypercholesterolemic patients: a monitoring test of endothelial dysfunction for clinical practice? *J. Am. Coll. Cardiol.* (2003) **42** 71–77.
- Dalle-Ave A., Kubli S., Golay S., Delachaux A., Liaudet L., Waeber B. Acetylcholine-induced vasodilation and reactive hyperemia are not affected by acute cyclo-oxygenase inhibition in human skin. *Microcirculation* (2004) **11** 327–336.
- Medow M.S., Taneja I., Stewart J.M. Cyclooxygenase and nitric oxide synthase dependence of cutaneous reactive hyperemia in humans. *Am. J. Physiol. Heart Circ. Physiol.* (2007) **293** H425–H432.
- Moppett I.K., Davies J.A., Mahajan R.P. Non-selective and cyclo-oxygenase-2-specific non-steroidal anti-inflammatory drugs impair the hyperaemic response of skin to brief axillary artery occlusion. *Br. J. Anaesth.* (2003) **91** 353–356.
- Pasche A., Heim A., Liaudet L., Waeber B., Feihl F. No implication of thromboxane prostanoid receptors in reactive hyperemia of skin and skeletal muscle in human forearm. *J. Cardiovasc. Pharmacol.* (2013) **61** 127–132.
- Rousseau P., Tartas M., Fromy B., Godon A., Custaud M.-A., Saumet J.L. Platelet inhibition by low-dose aspirin but not by clopidogrel reduces the axon-reflex current-induced vasodilation in humans. *Am. J. Physiol. Regul. Integr. Comp. Physiol.* (2008) **294** R1420–R1426.
- Cracowski J.-L., Gaillard-Bigot F., Cracowski C., Roustit M., Millet C. Skin microdialysis coupled with laser speckle

- contrast imaging to assess microvascular reactivity. *Microvasc. Res.* (2011) **82** 333–338.
- 20 McCord G.R., Cracowski J.-L., Minson C.T. Prostanoids contribute to cutaneous active vasodilation in humans. *Am. J. Physiol. Regul. Integr. Comp. Physiol.* (2006) **291** R596–R602.
- 21 Higgins J.P., Greene S. *Cochrane Handbook for Systematic Reviews of Interventions Version 5.1.0* [updated March 2011] [Internet]. The Cochrane Collaboration, 2011. 2011 [cytowane 30 lipiec 2014]. Pobrano z: <http://handbook.cochrane.org/>
- 22 Hozo S.P., Djulbegovic B., Hozo I. Estimating the mean and variance from the median, range, and the size of a sample. *BMC Med. Res. Methodol.* (2005) **5** 13.
- 23 Roustit M., Millet C., Blaise S., Dufournet B., Cracowski J.-L. Excellent reproducibility of laser speckle contrast imaging to assess skin microvascular reactivity. *Microvasc. Res.* (2010) **80** 505–511.
- 24 Simmons D.L., Botting R.M., Hla T. Cyclooxygenase isozymes: the biology of prostaglandin synthesis and inhibition. *Pharmacol. Rev.* (2004) **56** 387–437.
- 25 Félétou M., Huang Y., Vanhoutte P.M. Endothelium-mediated control of vascular tone: COX-1 and COX-2 products. *Br. J. Pharmacol.* (2011) **164** 894–912.
- 26 Barau C., Ghaleh B., Berdeaux A., Morin D. Cytochrome P450 and myocardial ischemia: potential pharmacological implication for cardioprotection. *Fundam. Clin. Pharmacol.* (2015) **29** 1–9.
- 27 Abd-El-Aleem S.A., Ferguson M.W., Appleton I., Bhowmick A., McCollum C.N., Ireland G.W. Expression of cyclooxygenase isoforms in normal human skin and chronic venous ulcers. *J. Pathol.* (2001) **195** 616–623.
- 28 Bézière N., Goossens L., Pommery J., Vezin H., Touati N., Hénichart J.-P. New NSAIDs-NO hybrid molecules with antiproliferative properties on human prostatic cancer cell lines. *Bioorg. Med. Chem. Lett.* (2008) **18** 4655–4657.
- 29 Shastry S., Minson C.T., Wilson S.A., Dietz N.M., Joyner M.J. Effects of atropine and L-NAME on cutaneous blood flow during body heating in humans. *J. Appl. Physiol.* (2000) **88** 467–472.

Partie II. Approche de la pathologie de la microcirculation cutanée : exemple de la sclérodermie systémique

La sclérodémie systémique (SSc), comme mentionné en introduction, est une maladie dysimmunitaire rare, dont la prévalence est de 50 à 300 patients par million d'habitants, et à prédominance féminine avec 3 à 14 femmes pour un homme (62). Cette maladie particulièrement invalidante est caractérisée par une fibrose cutanée et viscérale, une atteinte microvasculaire diffuse et la présence d'auto-anticorps dirigés contre des antigènes cellulaires (63), témoignant d'une participation auto-immune.

En fonction du degré d'extension de l'atteinte cutanée, la sclérodémie est classée en deux grands sous-groupes (64):

- La sclérodémie cutanée diffuse, qui représente environ 40% des patients et qui se caractérise par une progression rapide des lésions de sclérose, remontant au-dessus des coudes et/ou des genoux, voire atteignant le tronc, et qui affecte une grande partie des organes internes. Il existe des anticorps anti-topoisomérase chez 30 % de ces patients.
- La sclérodémie cutanée limitée, dans laquelle la fibrose se limite principalement aux mains, aux pieds et au visage, sans remonter au-dessus des coudes et des genoux. Le phénomène de Raynaud en est la première manifestation clinique, survenant plusieurs années avant que la fibrose n'apparaisse. Une hypertension artérielle pulmonaire est fréquente et il existe des anticorps anti-centromère chez 50 à 90% des patients.

Il existe également des formes sans atteinte cutanée (sclérodémie limitée) et des formes frontières avec d'autres connectivites. Le Roy et Medsger ont plus récemment proposé des critères pour les formes débutantes de SSc, permettant de faire la distinction entre les SSc cutanées limitées, où l'épaississement cutané reste distal – en aval des coudes et des genoux – et les SSc limitées, qui n'ont aucune atteinte cutanée mais un phénomène de Raynaud, des anomalies à la capillaroscopie péri-unguéale (dilatations capillaires et/ou zones avasculaires) et/ou des autoanticorps spécifiques de la SSc (65). Les SSc limitées pourraient constituer des formes très précoces de la maladie. Cependant, certains patients répondant aux critères de Le Roy et Medsger ne développeront jamais de lésions cutanées de sclérose, même après plusieurs années d'évolution, répondant alors aux critères de SSc dite *sine scleroderma* (66).

Ces patients ne sont cependant pas indemnes de risque d'ulcération digitale ou de complications cardiopulmonaires.

La dysfonction vasculaire est un élément clé dans la pathogénie de cette maladie, précédant la fibrose (67). Elle concerne principalement la microcirculation mais les artères de conductance sont également atteintes. La microcirculation présente des anomalies de structure et de fonction, qui sont interdépendantes. Cette micro-angiopathie est caractérisée sur un plan structural par une raréfaction capillaire, le développement de mégacapillaires, et une oblitération vasculaire (14). Sur un plan fonctionnel, la dysfonction microvasculaire se manifeste par un phénomène de Raynaud pouvant s'associer à des troubles trophiques cutanés (Figure 8), ainsi qu'à une hypertension artérielle pulmonaire.



Figure 8. Sclérodermie systémique avec sclérodactylie sévère (cliché personnel).

Le phénomène de Raynaud (PR) est un syndrome correspondant à une vasoconstriction exagérée des microvaisseaux des doigts et/ou des orteils et/ou des oreilles en réponse à un stress environnemental (le froid, ou plus rarement, l'humidité) ou émotionnel (14). Il peut être primaire ou secondaire. Le phénomène de Raynaud primaire affecte 4 à 6% de la population générale avec des variations géographiques importantes.

Pour la plupart des patients présentant un PR primaire (Figure 9A), il s'agit d'une affection saisonnière exigeant des mesures conservatrices comme l'éviction de l'exposition au froid et le port des vêtements de protection. La plupart des phénomènes de Raynaud secondaires sont liés à une sclérodémie systémique. Le phénomène de Raynaud rencontré dans la sclérodémie se différencie du phénomène de Raynaud primaire par des crises plus sévères, plus fréquentes (Figure 9B), et touchant plus fréquemment d'autres territoires que les mains (nez, langue, oreilles, orteils).



Figure 9. Phénomène de Raynaud.

A : Phénomène de Raynaud primaire bilatéral (à gauche : cliché transmis par E. Hachulla ; à droite : cliché personnel). B : Phénomène de Raynaud secondaire bilatéral dans le cadre d'une sclérodémie systémique (à gauche : cliché personnel ; à droite : d'après Goundry, BMJ 2012)

Quatrième étude : Intérêt du laser SPEckle Contrast Imaging dans la détection de la dysfonction microvasculaire cutanée de la Sclérodermie systémique (titre court : SPECIES)

La dysfonction vasculaire est un élément clé dans la pathogénie de la sclérodermie systémique (SSc), et concerne à la fois la microcirculation et les artères de conductance. On considère à ce jour que les anomalies de la vasodilatation endothélium-dépendante sont principalement liées à une diminution de la libération de NO, conséquence d'une réduction de l'expression de la NO synthase endothéliale. Dans la sclérodermie, la réponse hyperhémique post-occlusive (PORH) secondaire à une occlusion artérielle est altérée.

L'étude de cette PORH peut se faire soit à l'aide de la technique de fluxmétrie laser Doppler qui présente une mauvaise résolution spatiale, soit à l'aide de la technique d'imagerie laser Doppler qui présente une mauvaise résolution temporelle, soit plus récemment, à l'aide de l'imagerie laser par analyse de la granularité du faisceau (*Laser Speckle Contrast Imaging* ou LSCI), qui présente l'avantage de combiner une excellente résolution spatiale et temporelle (12). Compte tenu d'une mise sur le marché récente de cette technologie, une seule étude a pour l'instant été réalisée dans le domaine de la sclérodermie.

L'objectif principal de cette étude était de comparer, à l'aide de cette nouvelle imagerie, la PORH obtenue sur la face dorsale de la main entre trois groupes : un groupe de volontaires sains (VS), un groupe de sujets présentant un phénomène de Raynaud primaire (RP) et un groupe de sujets atteints de SSc.

Quinze patients atteints de SSc ont été inclus et appariés sur l'âge et le sexe de 15 patients présentant un phénomène de RP et 15 VS. Nous avons étudié la PORH suivant une occlusion artérielle de 5 minutes dans les trois groupes. Le flux sanguin cutané a été exprimé en pourcentage de valeur de base et en valeur absolue de conductance vasculaire cutanée (CVC) ; les valeurs obtenues dans les trois groupes ont été comparées.

La PORH était anormale en termes de pic et d'aire sous la courbe (AUC) sur tous les doigts excepté le pouce chez les patients atteints de SSc et les patients présentant un RP par rapport aux VS. La cinétique de reperfusion était allongée uniquement chez les patients atteints de SSc, avec la présence d'un gradient de reperfusion proximo-distal.

En conclusion, le LSCI pourrait être un outil discriminant dans l'étude des anomalies de la microcirculation vasculaire cutanée chez des patients atteints de SSc par rapport à des patients présentant un phénomène de RP.

Article publié : *Abnormal amplitude and kinetics of digital postocclusive reactive hyperemia in systemic sclerosis.* Gaillard-Bigot F, Roustit M, Blaise S, Gabin M, Cracowski C, Seinturier C, Imbert B, Carpentier P, Cracowski JL. *Microvasc Res.* 2014 Jul;94:90-5.



Contents lists available at ScienceDirect

Microvascular Research

journal homepage: www.elsevier.com/locate/ymvre

Abnormal amplitude and kinetics of digital postocclusive reactive hyperemia in systemic sclerosis[☆]



F. Gaillard-Bigot^{a,b}, M. Roustit^{a,b}, S. Blaise^{a,c}, M. Gabin^a, C. Cracowski^{a,b}, C. Seinturier^c, B. Imbert^c, P. Carpentier^c, J.L. Cracowski^{a,b,*}

^a Univ. Grenoble Alpes, HP2, 38000, France

^b Clinical Pharmacology Unit, Inserm CIC003, Grenoble University Hospital, 38043, France

^c Vascular Medicine Department, Grenoble University Hospital, 38043, France

ARTICLE INFO

Article history:

Accepted 26 May 2014

Available online 2 June 2014

Keywords:

Post-occlusive reactive hyperemia

Systemic sclerosis

Raynaud's phenomenon

Microcirculation

Laser speckle contrast imaging

Skin

Primary Raynaud's Phenomenon

Vasodilatation

Endothelium

Microcirculation imaging

ABSTRACT

Objectives: Postocclusive reactive hyperemia is mediated by two major mediators: sensory nerves and endothelium-derived hyperpolarizing factors. We hypothesized that the skin microvascular response to 5 min ischemia would differ depending upon the hand location in patients with systemic sclerosis (SSc), primary Raynaud's phenomenon (PRP) and healthy controls.

Methods: Fifteen patients with SSc, 15 sex- and age-matched patients with PRP and healthy controls were enrolled. Their right hands were subjected to 5 min ischemia followed by a postocclusive hyperemia test, with local microcirculation monitoring by laser speckle contrast imaging on the dorsal face of the hand.

Results: Postocclusive reactive hyperemia was abnormal in terms of peak and area under the curve (AUC) on all fingers except the thumb in patients with SSc and PRP compared with controls. In contrast, the kinetics of the response was longer only in SSc patients, with mean (SD) time to peak on the index, middle and ring finger were respectively 72 (58), 73 (51) and 67 (47) s for SSc; 40 (20), 40 (20) and 36 (19) s for PRP; and 34 (30), 34 (30) and 29 (24) s for controls ($P = 0.009$ for interaction).

Conclusions: We observed decreased distal digital microvascular perfusion following 5 min of ischemia in patients presenting with PRP or SSc, while the kinetics was prolonged only in SSc. A dynamic assessment of digital skin blood flow using laser speckle contrast imaging following 5 min ischemia could be used as a tool to assess microvascular abnormalities in patients with Raynaud's phenomenon secondary to SSc.

© 2014 Elsevier Inc. All rights reserved.

Introduction

Raynaud's phenomenon is characterized by an acute and transient cessation of blood-flow to the digits of the hands or feet. A vasospastic attack of Raynaud's phenomenon classically exhibits triphasic color changes in the digits: a white phase, due to excessive vasoconstriction, a cyanotic phase following ischemia and a red phase, due to hyperemia following the restoration of blood flow (Cooke and Marshall, 2005; Herrick, 2005). Primary Raynaud's phenomenon (PRP) is a benign condition caused by functional changes in digital blood flow without irreversible tissue damage. The mechanisms of PRP include a central response characterized by increased activation of the sympathetic nerves and a peripheral response, called 'a local fault' by Lewis (Lewis, 1929). This response is probably multifactorial, including increased

sensitivity to cold of the adrenergic receptors of the digital arterioles, and abnormal endothelium dependent dilatation.

In contrast, secondary forms of Raynaud's phenomenon occur less frequently, mainly in patients with connective tissue disease among whom systemic sclerosis (SSc) is the most common (Cutolo et al., 2010; Gabrielli et al., 2009). SSc is characterized by a vasculopathy of small vessels, activation of the immune system, and tissue fibrosis (Trojanowska, 2010). Microvascular structural damage and dysfunction of the microvasculature represent the initial morphological and functional markers of SSc.

Morphological and functional assessment of the cutaneous microvasculature has crucial implications for diagnosis, prognosis and therapy in SSc and secondary Raynaud's phenomenon. Whereas nailfold videocapillaroscopy measures capillary morphology (Cutolo et al., 2003), the recently developed laser speckle contrast imaging (LSCI) technique can be used to quantify cutaneous blood flow with a high spatial and temporal resolution (Roustit and Cracowski, 2013). Postocclusive reactive hyperemia (PORH), i.e. the acute rise in skin blood flow following a short period of ischemia, is characterized by an initial transient peak that occurs within a few seconds, followed by

[☆] Trial registration: ClinicalTrials.gov NCT01743612.

* Corresponding author at: Unité de Pharmacologie Clinique, Centre d'Investigation Clinique de Grenoble, Inserm CIC1406, CHU de Grenoble, 38043 Grenoble Cedex 09, France. Fax: +33 4 76 76 92 62.

E-mail address: Jean-Luc.Cracowski@ujf-grenoble.fr (J.L. Cracowski).

sustained hyperemia that lasts several minutes. Two major mediators contribute to PORH: firstly, sensory nerves are major contributors to both the peak and sustained hyperemia, through a local axon reflex (Cracowski et al., 2007; Lorenzo and Minson, 2007). Secondly, there is recent evidence that endothelium-derived hyperpolarizing factors (EDHFs) play an important role, and we recently showed that the most plausible mediators were epoxyeicosatrienoic acids (EETs) (Cracowski et al., 2013). In contrast, there is no evidence that nitric oxide or prostanoids participate in PORH (Roustit and Cracowski, 2013). Therefore, skin PORH can be used as a test for axon reflex and EDHF response. We and others have previously shown an altered PORH response on the hands of patients with SSc (Della Rossa et al., 2013; Roustit et al., 2008). However, no data are available concerning regional differences in response between the different fingers, thumb and dorsum of the hand, the latter two being less frequently affected by Raynaud's syndrome.

We hypothesized that the abnormal skin microvascular response to 5 min ischemia would differ in terms of kinetics and amplitude depending upon the hand location in patients with SSc, PRP and healthy controls. The primary objective of this study was therefore to compare the amplitude, kinetics and heterogeneity of the PORH on the dorsal face of the hand in patients with SSc, sex- and age-matched patients with PRP and matched healthy controls, using laser speckle contrast imaging.

Methods

Study population

We enrolled 15 patients with SSc recruited from patients attending the Vascular Medicine Department of our hospital. For every patient with SSc, one patient with PRP and one healthy control were recruited from the general population through newspaper advertisements or through the Clinical Research Center Volunteer database, and matched according to sex and age (± 5 years). All the participants were over 18 years of age and were included between March 2013 and July 2013. Patients with PRP were diagnosed according to the criteria of LeRoy and Medsger (LeRoy and Medsger, 1992), and all 15 SSc patients fulfilled the new ACR/EULAR criteria for diagnosis of SSc (Hoogen et al., 2013). SSc was classified as limited SSc (lSSc), limited cutaneous (lcSSc) or diffuse cutaneous SSc (dcSSc) using the criteria of LeRoy et al. (LeRoy and Medsger, 2001). Subjects taking calcium-channel blockers were instructed to stop medication 1 week before enrollment in the study. Non-inclusion criteria included smoking, active digital ulcers, history of axillary trauma or surgery, history of thromboembolic disease or thrombophilia, diabetes mellitus, or any associated severe chronic disease. Additional non-inclusion criteria for PRP included an abnormal capillaroscopic pattern as described by Cutolo et al. (2003). The presence of antinuclear autoantibodies was assessed for all participants. Grenoble Institutional Review Board approval was obtained in December 2011 and each subject gave written informed consent before participation.

Study design

All subjects were fasted and all experiments were performed in a temperature-controlled room (23 ± 1 °C). After clinical examination, the participants remained supine for the whole duration of the experiments. Before recording started, the right arm and hand were immobilized with a vacuum cushion to ensure stable positioning.

Skin post-occlusive reactive hyperemia and skin blood flow measurements

Cutaneous blood flow on the dorsal face of the hand was assessed by LSCI (PeriCam PSI System; Perimed, Järfälla, Sweden). The LSCI wavelength was 785 nm, and the laser head was placed 20 to 25 cm above the skin (with a resolution of ≈ 6.9 pixels/cm²).

The image size was 9×9 cm and the acquisition rate was 3 s^{-1} during the whole procedure. Skin blood flow was occluded for 5 min by inflating a cuff placed on the right upper arm to 50 mm Hg above the subject's systolic blood pressure. Baseline blood flow was recorded over the 10 min before starting ischemia.

Blood pressure was recorded continuously throughout the experiment (Nexfin monitor; Bmeye, Amsterdam, The Netherlands) on the contralateral hand. Using a Perimed PF 5050 Pressure Unit, we measured the digital systolic blood pressure in patients with SSc on the index, middle and ring fingers of the right hand. Briefly, finger pressure measurements were performed by placing the cuff on the base of the finger and fixing the laser Doppler probe above the finger pad. The cuff was first inflated to 50 mm Hg above the humeral systolic blood pressure. The cuff pressure was then steadily deflated until the laser Doppler probe detected the return of blood perfusion, indicating finger systolic blood pressure. The digital systolic pressure index was defined as the ratio of the digital systolic pressure over the humeral systolic blood pressure.

Data analysis

Data were digitized and analyzed off-line with signal processing software (PeriSoft 2.5.5, Perimed, Järfälla, Sweden). Skin blood flow was averaged over the eleven regions of interest (ROI): first, a 500 mm² area on the dorsum of the hand, 3 areas of 60–100 mm² on the dorsal face of the proximal, medial and distal phalanxes of the index, middle and ring fingers, and one area of 60–100 mm² on the distal thumb phalanx (Fig. 1). Skin blood flow was expressed in Laser Speckle perfusion units (LSPU).

Biological zero was defined as the flux recorded during the “no-flux” period (5 min ischemia).

PORH area under the curve, expressed as LSPU.s was calculated over 6 min following the cuff release as previously performed (Cracowski et al., 2013). Time to peak (sec) was measured as the time required following the cuff release to reach the peak of the hyperemic response. A within finger heterogeneity index was calculated as the coefficient of variation within each region of interest, i.e. $SD \times 100$ divided by the mean flux, and expressed as a percentage. The distal–dorsum difference was calculated as the mean flux in the distal region of interest minus the mean flux in the dorsum, expressed in LSPU.

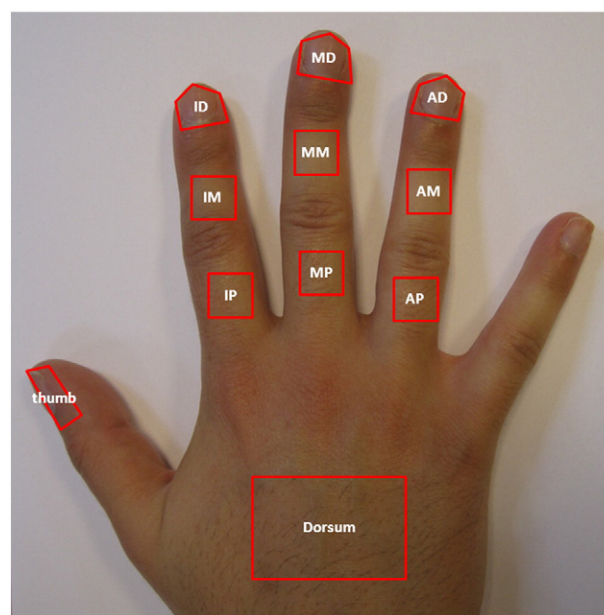


Fig. 1. Location of the 11 regions of interest on the dorsal face of the right hand.

Statistical analysis

Quantitative data are expressed as the mean and standard deviation in parenthesis. Qualitative data are expressed as numerical values and percentage in parenthesis.

Repeated-measures ANOVA were used to compare the quantitative data between the three groups. Mauchly's test of sphericity was used to assess the equality of variance. When significant (i.e. inequality of variance could not be excluded), a Greenhouse–Geisser adjustment was used. We tested the effect of the site on the hand, of the group (SSc, PRP or controls), as well as the interaction between site and group. To compare differences between groups, we performed Tukey post hoc tests (Vickers and Altman, 2001). Two-sided significance tests were used throughout. *P*-values less than 0.05 were considered statistically significant. Statistical analyses were performed using IBM SPSS Statistics v21.

Results

Population characteristics

The demographic and clinical characteristics of the 45 subjects enrolled in the study are listed in Table 1. Among the 15 patients with SSc, 10 had been on calcium channel blockers (stopped 7 days before measurements), 6 were on proton pump inhibitors, 2 on corticosteroids, one had received i.v. iloprost a year before and one was currently taking methotrexate. Among the 15 patients with PRP, one had been on calcium channel blockers (stopped before measurements), and one was on proton pump inhibitors. All SSc patients were positive for anti-nuclear antibodies. Five were positive for anti-topoisomerase I antibodies (anti-Scl70), and 6 exhibited anti-centromere antibodies.

Postocclusive reactive hyperemia

Representative images are shown in Fig. 2. We observed no difference in terms of biological zero between the three groups. At baseline, we observed a decreased flux in the distal phalanx of the index, middle and ring fingers in patients with SSc and PRP (Table 2). We also observed a decreased baseline flux in the thumbs of patients with SSc.

In terms of amplitude, peak PORH was lower in the distal phalanx of the index, middle and ring fingers in patients with SSc, while in patients

with PRP peak PORH was lower, but to a lesser extent (Table 2). Likewise, the PORH area under the curve was more reduced in patients with SSc than with PRP (Table 2).

In terms of PORH kinetics, the time to peak was longer in patients with SSc compared to patients with PRP and healthy controls (Table 2), except on the thumb. We observed no correlation between the finger systolic pressure index and PORH peak height or time to peak.

At baseline, we observed a higher within finger heterogeneity in patients with SSc and PRP compared to healthy controls, which disappeared at the peak of PORH (Table 2). Distal–dorsum differences of baseline and peak were less in patients with SSc and PRP compared to healthy controls on the index, middle and ring fingers (Table 2).

When data from the first and second phalanges of each finger were analyzed, no significant difference was observed except for the time to peak (data not shown for clarity). Time to peak exponentially increased from the dorsum to the most distal part of the fingers.

Discussion

In subjects presenting with Raynaud's phenomenon, whether primary or secondary, the amplitude of distal digital microvascular perfusion was reduced, both at baseline and following 5 min ischemia. In contrast, the kinetics of the postocclusive hyperemic response was altered only in patients with SSc. In addition, the response in thumb of SSc patients to 5 min ischemia was normal despite a lower baseline.

In a recent study using LSCI, Ruaro et al. similarly observed a lower basal flux in 61 SSc patients compared to 61 healthy subjects (Ruaro et al., 2013), consistent with our previous study using laser Doppler flowmetry (Roustit et al., 2008), and Rosato's study using LDPI (Rosato et al., 2011a, 2011b). In contrast, using LSCI, Della Rossa et al. observed an unexpected high baseline flux in patients with SSc (Della Rossa et al., 2013). This probably explains why, when PORH was expressed as a percentage of baseline, they found a decrease in amplitude compared with PRP.

At baseline, we observed on the index, middle and ring fingers, a within finger heterogeneity of skin blood flux in PRP and SSc patients compared with healthy controls, suggesting heterogenous perfusion within each region of interest. Heterogeneity disappeared for the peak of PORH, suggesting capillary recruitment. In our study, heterogeneity was assessed quantitatively as the coefficient of variation within each region of interest. Using a different way to assess flux heterogeneity,

Table 1
Epidemiological and clinical data.

	Healthy controls (n = 15)	Primary Raynaud's phenomenon (n = 15)	SSc (n = 15)
Age (years)	62 (8)	58 (2)	60 (11)
Female	15 (100)	15 (100)	15 (100)
Body mass index	26.5 (6.2)	22.3 (3.3)	25.4 (3.8)
Blood pressure (systolic/diastolic, mm Hg)	139 (20)/75 (11)	123 (16)/70 (12)	135 (24)/71 (12)
Digital systolic pressure index			
Index			0.78 (0.2)
Middle			0.82 (0.15)
Ring			0.83 (0.15)
RP	0 (0)	15 (100)	15 (100)
RP: duration (years)	NA	27.2 (11.2)	16.9 (13.1)
RP: number of fingers involved	NA	8 (3)	8 (2)
RP: thumb involved (%)	NA	7 (47)	7 (47)
RP: feet involved (%)	NA	6 (40)	9 (60)
Disease duration (years)	NA	NA	9 (7)
Digital pitting scars	0 (0)	0 (0)	2 (13)
Sclerodactyly	0 (0)	0 (0)	15 (100)
Rodnan-modified skin score	NA	NA	9 (6)
Pulmonary fibrosis/pulmonary hypertension	0 (0)/0 (0)	0 (0)/0 (0)	5 (31)/0 (0)
Oesophageal involvement	0 (0)	0 (0)	7 (47)
Capillaroscopy pattern: n (%) early/active/late	NA	NA	5 (33)/4 (27)/6 (40)

Quantitative data were expressed as mean (SD). Qualitative data were expressed as number (percentage). RP: Raynaud's phenomenon. NA: not applicable.

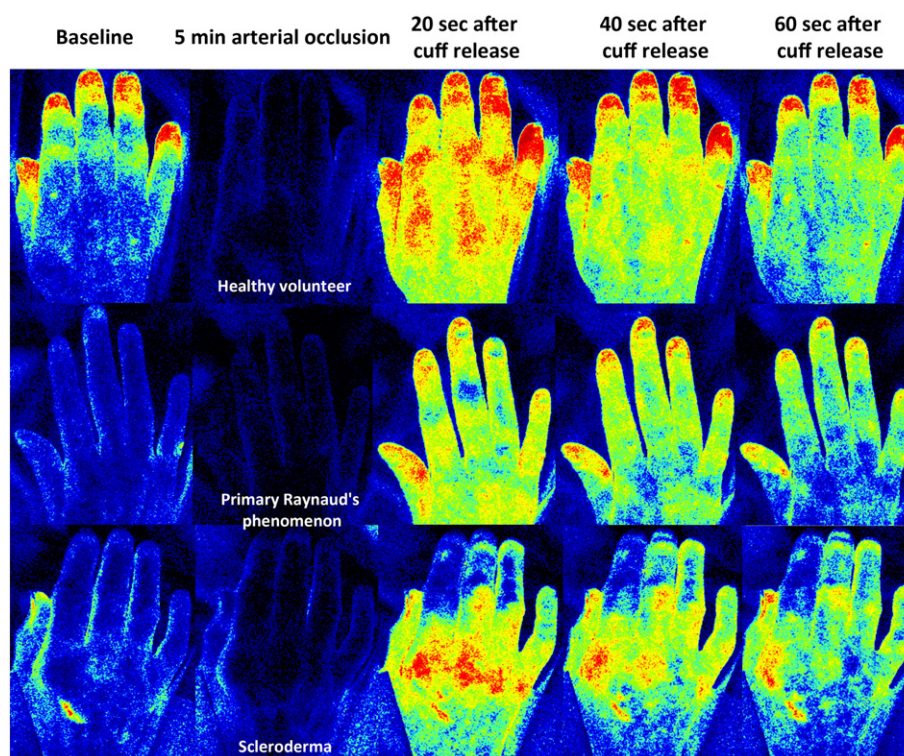


Fig. 2. Typical postocclusive reactive hyperemia obtained using Laser speckle Contrast Imaging of the dorsal face of the right hand.

i.e. classifying a dyshomogenous pattern as a very small variously distributed hypoperfused and hyperperfused area, another group found that flux heterogeneity, when assessed qualitatively, was increased in SSc only (Della Rossa et al., 2013).

Whether the altered PORH response results from structural abnormalities in the digital arteries or from a specific microvascular dysfunction, remains unclear. We found no correlation between PORH and baseline digital systolic pressure, but we were unable to monitor digital blood pressure during the postocclusive hyperemia. Conflicting results were found concerning the response of large conductance arteries in SSc patients to a short period of occlusion, with either no alteration (Andersen et al., 2002; Rajagopalan et al., 2003; Roustit et al., 2008) or lower brachial flow mediated dilatation in patients with SSc compared with healthy subjects (Bartoli et al., 2007; D'Andrea et al., 2007; Szűcs et al., 2007).

In patients with Raynaud's phenomenon, whether primary or secondary, the distal–dorsum difference observed using LSCI, was reduced both at baseline and following ischemia, similarly to a recent study (Della Rossa et al., 2013). In contrast, when looking at the thumb, patients with PRP had a distal–dorsum difference similar to healthy controls. Using thermography, Anderson et al. previously observed an altered distal–dorsum difference in patients with SSc and PRP following a cold test, with a distal–dorsum difference greater than one degree in any finger at 30°C having a positive predictive value of 70% in identifying patients with Raynaud's phenomenon secondary to SSc (Anderson et al., 2007). However, it seems that at baseline or during PORH, the distal–dorsum difference measured by LSCI does not help in classifying patients.

More recently, the reproducibility of laser speckle contrast imaging has been extensively compared with other methods such as laser Doppler flowmetry (LDF), laser Doppler perfusion imaging (LDPI) and infrared thermography (IRT) (Millet et al., 2011; Murray et al., 2009; Pauling et al., 2012; Puissant et al., 2013; Roustit et al., 2010). Interestingly, Ruaro et al. recently used LSCI to study a group of 61 SSc patients, and, for the first time detected a correlation between cutaneous blood

flow and the progressive severity of the nailfold pattern in microangiopathy (Ruaro et al., 2013). Compared to LDF, LSCI exhibited lower intra-operator variability, was less time consuming and patients showed better tolerance. Our study further supports the possibility that LSCI, when combined with a dynamic assessment of skin flux, may be an interesting tool to study regional microvascular abnormalities in skin scleroderma.

Clinical and biological evidence suggests that the primary target for scleroderma is the blood vessels (Matucci-Cerinic et al., 2013), with a relationship between finger microangiopathy and dermal thickness (Sulli et al., 2014). Vascular injury is characterized by a dysfunction of the endothelium (Herrick, 2012), and dysregulation of sensory nerves (Kahaleh and Matucci-Cerinic, 1995). Skin microvascular response to a short period of ischemia is a way to challenge the skin's microcirculation to stimulate these two pathways (Roustit and Cracowski, 2013). Lorenzo et al. showed the major role of sensory nerves and $BKCa^{2+}$ channels in PORH. Furthermore, using skin microdialysis, we recently showed that in addition to sensory nerves, epoxyeicosatrienoic acids, play a major role in skin PORH (Cracowski et al., 2013). As epoxyeicosatrienoic acids are one of the most plausible candidate endothelium derived hyperpolarizing factors (EDHF) (Cracowski et al., 2013), this suggests that skin PORH could be used as a test for neurovascular and EDHF function. Given that skin microdialysis is not readily feasible in the fingers, and that it is traumatic and may impair healing in SSc patients, we could not demonstrate which of these two pathways was altered.

Our study has several limitations, including the relatively small sample size and the enrollment of females only. However, systemic sclerosis occurs more frequently in women than in men and an excess of female patients is a consistent feature of all studies, the average ratio being 3/1. Another limitation is that we did not block the mediators contributing to PORH. Therefore, we could not determine specifically whether the release of endothelium-derived hyperpolarizing factors (EDHF) was abnormal or not.

In conclusion, we observed decreased distal digital microvascular perfusion at baseline and following 5 min of ischemia in subjects

Table 2
Postocclusive reactive hyperemia on the dorsal face of the right hand.

		Healthy controls	PRP	SSc	Site	Group	Interaction
Baseline flux (LSPU)	Dorsum	64 (15)	53 (10)	60 (18)	<0.001	<0.001	0.001
	Thumb	159 (78)	158 (80)	93 (68) ‡			
	Index	169.0 (42.2)	93.0 (47.0) ***	94.2 (46.4) ***			
	Middle	163.6 (55.3)	91.6 (50.0) **	100.1 (75.1) **			
	Ring	163.2 (55.3)	88.8 (54.3) **	98.5 (59.2) **			
Peak flux (LSPU)	Dorsum	150.4 (34.4)	162.3 (42.0)	152.4 (46.5)	<0.001	NS	<0.001
	Thumb	208.7 (59.4)	263.2 (57.4) †	213.1 (67.7)			
	Index	223.6 (37.4)	184.4 (39.9) *	170.3 (51.0) **			
	Middle	227.3 (49.2)	182.5 (46.3) †	168.9 (57.6) **			
	Ring	226.3 (47.3)	189.1 (45.6)	179.0 (60.9) *			
AUC (LSPU.s)	Dorsum	28,554 (7493)	23,245 (5432)	27,180 (7742)	<0.001	0.01	0.04
	Thumb	63,926 (21,553)	46,899 (20,614)	60,815 (32,520)			
	Index	64,035 (16,558)	45,186 (22,729) *	43,856 (17,171) *			
	Middle	61,283 (20,409)	41,538 (20,154) *	44,426 (20,470) *			
	Ring	59,977 (21,286)	40,233 (20,537) *	44,621 (21,292)			
Time to peak (s)	Dorsum	14 (12)	18 (6)	20 (17)	<0.001	0.04	0.009
	Thumb	19 (13)	32 (36)	37 (37)			
	Index	34 (30)	40 (20)	72 (58) ††			
	Middle	34 (30)	40 (20)	73 (51) ††			
	Ring	29 (24)	36 (19)	67 (47) ††			
BL Heterogeneity index (%)	Dorsum	96 (14)	104 (15)	100 (15)	0.01	0.04	NS
	Thumb	77 (27)	89 (84)	87 (20)			
	Index	64 (5)	85 (18) **	89 (24) **			
	Middle	67 (9)	87 (18) **	90 (26) *			
	Ring	67 (9)	91 (25) *	88 (24) **			
Peak Heterogeneity index (%)	Dorsum	68 (10)	63 (11)	66 (16)	NS	NS	NS
	Thumb	68 (22)	62 (6)	64 (14)			
	Index	62 (7)	66 (13)	67 (12)			
	Middle	63 (8)	68 (16)	68 (17)			
	Ring	64 (11)	64 (11)	64 (11)			
BL distal–dorsum difference (LSPU)	Thumb	95.1 (70.9)	104.9 (79.9)	32.9 (73.1) ‡	NS	0.001	0.01
	Index	105.3 (40.2)	39.9 (42.4) ***	34.1 (37.6) ***			
	Middle	99.9 (51.8)	38.5 (44.8) **	40.0 (48.6) **			
	Ring	99.5 (50.2)	35.7 (49.5) **	38.3 (51.6) **			
	Peak distal–dorsum difference (LSPU)	Thumb	58.3 (67.6)	100.9 (70.7)			
Index	73.2 (39.3)	22.1 (47.1) **	17.9 (44.2) **				
Middle	76.9 (38.9)	20.2 (49.4) **	16.5 (38.9) **				
Ring	75.9 (38.6)	26.8 (47.3) **	26.6 (36.3) **				

Data are expressed as mean (SD). AUC: area under the curve; LSPU: perfusion units. Data were analyzed with ANOVA for repeated-measures between groups, the skin site being the repeated measure. Post hoc tests: *** $P < 0.001$ vs. controls. ** $P < 0.01$ vs. controls. * $P < 0.05$ vs. controls. † $P = 0.06$ vs. controls. ‡ $P < 0.05$ vs. controls and PRP, †† $P < 0.001$ vs. controls and PRP.

presenting with Raynaud's phenomenon, whether primary or secondary. In contrast, the kinetics of the postocclusive hyperemic response was altered only in patients with SSc. Thus a dynamic assessment of digital skin blood flow using laser speckle contrast imaging following 5 min ischemia could be used as a tool to assess microvascular abnormalities in patients with Raynaud's phenomenon secondary to systemic sclerosis.

Conflict of interest

The authors declare no conflicts of interests.

Funding

This work was supported by the patients' association 'Association des Sclérodermiques de France'.

Acknowledgments

We thank the patients' association 'Association des Sclérodermiques de France' for patient participation; the Délégation Régionale à la

Recherche Clinique of Grenoble University Hospital for sponsoring. We also thank Mrs Dominique Abry and Anne Tournier for assisting with the LSCI measurements and volunteer management; and Dr Alison Foote for critically reading and editing the manuscript.

References

- Andersen, G.N., Mincheva-Nilsson, L., Kazzam, E., Nyberg, G., Klintland, N., Petersson, A.S., Rantapaa-Dahlqvist, S., Waldenström, A., Caidahl, K., 2002. Assessment of vascular function in systemic sclerosis: indications of the development of nitrate tolerance as a result of enhanced endothelial nitric oxide production. *Arthritis Rheum.* 46, 1324–1332.
- Anderson, M.E., Moore, T.L., Lunt, M., Herrick, A.L., 2007. The "distal–dorsal difference": a thermographic parameter by which to differentiate between primary and secondary Raynaud's phenomenon. *Rheumatology* 46, 533–538.
- Bartoli, F., Blagojevic, J., Bacci, M., Fiori, G., Tempestini, A., Conforti, M.L., Guiducci, S., Miniati, I., Di Chicco, M., Del Rosso, A., Perfetto, F., Castellani, S., Pignone, A., Cerinic, M.M., 2007. Flow-mediated vasodilation and carotid intima-media thickness in systemic sclerosis. *Ann. N. Y. Acad. Sci.* 1108, 283–290.
- Cooke, J.P., Marshall, J.M., 2005. Mechanisms of Raynaud's disease. *Vasc. Med.* 10, 293–307.
- Cracowski, J.L., Lorenzo, S., Minson, C.T., 2007. Effects of local anaesthesia on subdermal needle insertion pain and subsequent tests of microvascular function in human. *Eur. J. Pharmacol.* 559, 150–154.

- Cracowski, J.L., Gaillard-Bigot, F., Cracowski, C., Sors, C., Roustit, M., Millet, C., 2013. Involvement of cytochrome epoxygenase metabolites in cutaneous postocclusive hyperemia in humans. *J. Appl. Physiol.* 114, 245–251.
- Cutolo, M., Grassi, W., Matucci Cerinic, M., 2003. Raynaud's phenomenon and the role of capillaroscopy. *Arthritis Rheum.* 48, 3023–3030.
- Cutolo, M., Sulli, A., Smith, V., 2010. Assessing microvascular changes in systemic sclerosis diagnosis and management. *Nat. Rev. Rheumatol.* 6, 578–587.
- D'Andrea, A., Stisi, S., Caso, P., di Uccio, F.S., Bellissimo, S., Salerno, G., Scarafile, R., Riegler, L., Cuomo, S., Citro, R., Scherillo, M., Calabrò, R., 2007. Associations between left ventricular myocardial involvement and endothelial dysfunction in systemic sclerosis: noninvasive assessment in asymptomatic patients. *Echocardiography* 24, 587–597.
- Della Rossa, A., Cazzato, M., d' Ascanio, A., Tavoni, A., Bencivelli, W., Pepe, P., Mosca, M., Baldini, C., Rossi, M., Bombardieri, S., 2013. Alteration of microcirculation is a hallmark of very early systemic sclerosis patients: a laser speckle contrast analysis. *Clin. Exp. Rheumatol.* 31, 109–114.
- Gabrielli, A., Avvedimento, E.V., Krieg, T., 2009. Scleroderma. *N. Engl. J. Med.* 360, 1989–2003.
- Herrick, A.L., 2005. Pathogenesis of Raynaud's phenomenon. *Rheumatol. Oxf.* 44, 587–596.
- Herrick, A.L., 2012. The pathogenesis, diagnosis and treatment of Raynaud phenomenon. *Nat. Rev. Rheumatol.* 8, 469–479.
- Hoogen, F. van den, Khanna, D., Franses, J., Johnson, S.R., Baron, M., Tyndall, A., Matucci-Cerinic, M., Naden, R.P., Medsger, T.A., Carreira, P.E., Riemekasten, G., Clements, P.J., Denton, C.P., Distler, O., Allanore, Y., Furst, D.E., Gabrielli, A., Mayes, M.D., van Laar, J.M., Seibold, J.R., Czirjak, L., Steen, V.D., Inanc, M., Kowal-Bielecka, O., Müller-Ladner, U., Valentini, G., Veale, D.J., Vonk, M.C., Walker, U.A., Chung, L., Collier, D.H., Csuka, M.E., Fessler, B.J., Guiducci, S., Herrick, A., Hsu, V.M., Jimenez, S., Kahaleh, B., Merkel, P.A., Sierakowski, S., Silver, R.M., Simms, R.W., Varga, J., Pope, J.E., 2013. 2013 classification criteria for systemic sclerosis: an American college of rheumatology/European league against rheumatism collaborative initiative. *Ann. Rheum. Dis.* 72, 1747–1755.
- Kahaleh, B., Matucci-Cerinic, M., 1995. Raynaud's phenomenon and scleroderma. Dysregulated neuroendothelial control of vascular tone. *Arthritis Rheum.* 38, 1–4.
- LeRoy, E.C., Medsger, T.A., 1992. Raynaud's phenomenon: a proposal for classification. *Clin. Exp. Rheumatol.* 10, 485–488.
- LeRoy, E.C., Medsger, T.A., 2001. Criteria for the classification of early systemic sclerosis. *J. Rheumatol.* 28, 1573–1576.
- Lewis, T., 1929. Experiments relating to the peripheral mechanism involved in spasmodic arrest of the circulation of the fingers, a variety of Raynaud's disease. *Heart* 14.
- Lorenzo, S., Minson, C.T., 2007. Human cutaneous reactive hyperaemia: role of BKCa channels and sensory nerves. *J. Physiol.* 585, 295–303.
- Matucci-Cerinic, M., Kahaleh, B., Wigley, F.M., 2013. Review: evidence that systemic sclerosis is a vascular disease. *Arthritis Rheum.* 65, 1953–1962.
- Millet, C., Roustit, M., Blaise, S., Cracowski, J.L., 2011. Comparison between laser speckle contrast imaging and laser Doppler imaging to assess skin blood flow in humans. *Microvasc. Res.* 82, 147–151.
- Murray, A.K., Moore, T.L., Manning, J.B., Taylor, C., Griffiths, C.E.M., Herrick, A.L., 2009. Noninvasive imaging techniques in the assessment of scleroderma spectrum disorders. *Arthritis Care Res.* 61, 1103–1111.
- Pauling, J.D., Shipley, J.A., Raper, S., Watson, M.L., Ward, S.G., Harris, N.D., McHugh, N.J., 2012. Comparison of infrared thermography and laser speckle contrast imaging for the dynamic assessment of digital microvascular function. *Microvasc. Res.* 83, 162–167.
- Puissant, C., Abraham, P., Durand, S., Humeau-Heurtier, A., Faure, S., Lefthériot, G., Rousseau, P., Mahé, G., 2013. Reproducibility of non-invasive assessment of skin endothelial function using laser Doppler flowmetry and laser speckle contrast imaging. *PLoS ONE* 8, e61320.
- Rajagopalan, S., Pfenninger, D., Kehrer, C., Chakrabarti, A., Somers, E., Pavlic, R., Mukherjee, D., Brook, R., D'Alecy, L.G., Kaplan, M.J., 2003. Increased asymmetric dimethylarginine and endothelin 1 levels in secondary Raynaud's phenomenon: implications for vascular dysfunction and progression of disease. *Arthritis Rheum.* 48, 1992–2000.
- Rosato, E., Gigante, A., Barbano, B., Cianci, R., Molinaro, I., Pisarri, S., Salsano, F., 2011a. In systemic sclerosis macrovascular damage of hands digital arteries correlates with microvascular damage. *Microvasc. Res.* 82, 410–415.
- Rosato, E., Rossi, C., Molinaro, I., Giovannetti, A., Pisarri, S., Salsano, F., 2011b. Laser Doppler perfusion imaging in systemic sclerosis impaired response to cold stimulation involves digits and hand dorsum. *Rheumatology* 50, 1654–1658.
- Roustit, M., Cracowski, J.-L., 2013. Assessment of endothelial and neurovascular function in human skin microcirculation. *Trends Pharmacol. Sci.* 34, 373–384.
- Roustit, M., Simmons, G.H., Baguet, J.P., Carpentier, P., Cracowski, J.L., 2008. Discrepancy between simultaneous digital skin microvascular and brachial artery macrovascular post-occlusive hyperemia in systemic sclerosis. *J. Rheumatol.* 35, 1576–1583.
- Roustit, M., Millet, C., Blaise, S., Dufournet, B., Cracowski, J.L., 2010. Excellent reproducibility of laser speckle contrast imaging to assess skin microvascular reactivity. *Microvasc. Res.* 80, 505–511.
- Ruaro, B., Sulli, A., Alessandri, E., Pizzorni, C., Ferrari, G., Cutolo, M., 2013. Laser speckle contrast analysis: a new method to evaluate peripheral blood perfusion in systemic sclerosis patients. *Ann. Rheum. Dis.* 203514.
- Sulli, A., Ruaro, B., Alessandri, E., Pizzorni, C., Cimmino, M.A., Zampogna, G., Gallo, M., Cutolo, M., 2014. Correlations between nailfold microangiopathy severity, finger dermal thickness and fingertip blood perfusion in systemic sclerosis patients. *Ann. Rheum. Dis.* 73, 247–251.
- Szűcs, G., Tímár, O., Szekanez, Z., Dér, H., Kerekes, G., Szamosi, S., Shoenfeld, Y., Szegedi, G., Soltész, P., 2007. Endothelial dysfunction precedes atherosclerosis in systemic sclerosis—relevance for prevention of vascular complications. *Rheumatology* 46, 759–762.
- Trojanowska, M., 2010. Cellular and molecular aspects of vascular dysfunction in systemic sclerosis. *Nat. Rev. Rheumatol.* 6, 453–460.
- Vickers, A.J., Altman, D.G., 2001. Statistics notes: analysing controlled trials with baseline and follow up measurements. *BMJ* 323, 1123–1124.

Partie III. Approches pharmacologiques et thérapeutiques de l'iontophorèse de tréprostinil appliquée à la microcirculation cutanée

1. La thérapeutique de la sclérodermie systémique

La sclérodermie systémique (SSc) est une maladie qui peut engager le pronostic fonctionnel et/ou vital des malades et ce, de façon rapide. La thérapeutique est limitée car aucun traitement étiologique n'existe et la prise en charge est donc axée sur les traitements symptomatiques des différentes atteintes.

Nous avons axé notre travail, dans cette troisième partie, sur l'étude pharmacologique et thérapeutique de l'atteinte de la dysfonction vasculaire de la SSc qui implique une microangiopathie. Le signe fonctionnel le plus évident de cette dysfonction microvasculaire est le phénomène de Raynaud. Ce phénomène, ici secondaire, peut être très invalidant lorsqu'il survient de façon fréquente, ou bien en cas de complications – la principale complication de cette vasoconstriction digitale étant la survenue d'ulcérations pulpaire. L'évolution aboutit habituellement à une guérison sous forme de cicatrices pulpaire, mais avec des récives, notamment lors des saisons hivernales.

Les manifestations cutanées périphériques de la sclérodermie systémique et leur prise en charge thérapeutique : le phénomène de Raynaud

Comme nous l'avons vu, le phénomène de Raynaud rencontré dans la SSc se distingue du phénomène de Raynaud primaire par des crises plus sévères, plus fréquentes et touchant plus fréquemment d'autres territoires que les mains (nez, langue, oreilles, orteils). Peu de classes thérapeutiques sont efficaces dans la prise en charge thérapeutique du phénomène de Raynaud lié à une SSc. Comparativement au placebo, la nifédipine diminue significativement le nombre et la sévérité des crises. Néanmoins, le bénéfice des inhibiteurs calciques dans le phénomène de Raynaud de la SSc apparaît modeste compte tenu de la sévérité de la maladie (moyenne de 4,1 crises de moins par semaine et réduction de 33% de leur gravité) (68). Les inhibiteurs de PDE-5 peuvent également être utilisés. La fluoxétine n'est recommandée par le consensus de *L'European League Against Rheumatism* (EULAR) que suite à un avis d'expert (recommandation de bas grade en l'absence de données solides) (69). L'iloprost (un analogue stable de la prostacycline) par voie orale (non disponible en Europe), à la dose de 50 µg ou 100 µg, versus placebo permet à 12 semaines une diminution de la durée et de la sévérité des crises, mais pas leur fréquence (70).

L'iloprost utilisé par voie intraveineuse de manière séquentielle a montré, dans une étude prospective randomisée sur 12 mois, qu'il avait un effet supérieur à la nifédipine à la dose 40 mg/j per os (71), au prix d'effets indésirables fréquents.

Les manifestations cutanées périphériques de la sclérodermie systémique et leur prise en charge thérapeutique : les ulcérations digitales

Les ulcères digitaux sont la complication cutanée la plus sévère et la plus invalidante (Figure 10). Leur fréquence est estimée à 43% dans les formes cutanées limitées et 51% dans les formes cutanées diffuses (72). La physiopathologie fait intervenir une ischémie vasculaire et des facteurs mécaniques liés à une peau scléreuse sous tension. Le traitement des ulcérations digitales de la sclérodermie systémique est d'abord préventif dans le cadre d'une bonne hygiène cutanée et unguéale.



Figure 10. *Ulcération digitale pulpaire active (gauche) et en cours de cicatrisation (droite, clichés personnels).*

Sur un plan curatif, l'iloprost par voie intraveineuse est recommandé en cure de cinq jours dans le phénomène de Raynaud sévère associé à des ulcérations digitales (16, 69). Il a montré sa supériorité aux traitements conventionnels en cas d'ischémie digitale sévère ou de gangrène digitale. Dans une étude randomisée versus placebo, l'iloprost apportait un bénéfice en termes de fréquence de crises de Raynaud et de délai de cicatrisation des ulcérations (73).

Utilisé dans une étude ouverte sous la forme d'une perfusion par semaine toutes les six semaines sur une période de 12 mois, l'iloprost par voie intraveineuse apporte un bénéfice sur le phénomène de Raynaud et pourrait avoir un effet sur l'évolution de la maladie comme en témoigne l'amélioration des scores cutanés (71), mais l'effet sur la sclérodactylie reste controversé. Les inhibiteurs de la PDE-5 sont également indiqués dans le traitement des ulcères digitaux. En effet, une méta-analyse récente indique que les inhibiteurs de la PDE-5 améliorent la guérison des ulcères digitaux (69). En outre, les résultats d'un petit essai clinique indiquent qu'ils empêchent le développement de nouveaux ulcères digitaux (69). Le bosentan, antagoniste non sélectif des récepteurs de l'endothéline ETA et ETB, a également démontré dans le cadre de l'étude RAPIDS-2 qu'il réduisait significativement le risque de développement de nouveaux ulcères (74), avec un nombre de nouveaux ulcères de 1,9 dans le groupe traité versus 2,7 dans le groupe placebo, pour un traitement de 24 semaines. Cependant, le bosentan n'a montré aucun bénéfice sur la cicatrisation des ulcères préexistants et ne dispose par conséquent d'une AMM en Europe que dans la prévention des ulcérations digitales chez des patients atteints de SSc ayant des ulcères digitaux actifs récidivants. Il est à noter que le bosentan n'améliore pas le phénomène de Raynaud (75).

Depuis 2008 et l'extension de l'indication du Tracleer® (bosentan) à la prise en charge prophylactique des ulcères digitaux des patient atteint de SSc, aucun nouveau traitement n'a obtenu d'autorisation de mise sur le marché ni en France, ni en Europe et ni aux États-Unis.

En conclusion, le phénomène de Raynaud de la sclérodermie est une source de gêne fonctionnelle sévère tandis que les ulcérations digitales de la sclérodermie sont un phénomène fréquent et extrêmement invalidant, pouvant aller jusqu'à l'amputation d'un ou de plusieurs doigts et représentant la première source de handicap fonctionnel chez ces patients. La prise en charge thérapeutique des manifestations vasculaires périphériques est actuellement limitée et seulement partiellement efficace : inhibiteurs calciques pour la prise en charge du phénomène de Raynaud, antagonistes de l'endothéline par voie orale (bosentan) indiqués en prévention de l'apparition d'ulcérations digitales, analogues de la prostacycline par voie intraveineuse (iloprost) en curatif – mais au prix d'effets indésirables très fréquents (céphalées, bouffées vasomotrices, nausées, vomissements, douleurs maxillaires, myalgies) – et inhibiteurs de la PDE-5.

Discussion et perspectives

Le paradoxe, sur le plan pharmacologique, de la prise en charge du phénomène de Raynaud et des ulcérations digitales de la sclérodermie est que la diffusion tissulaire des rares médicaments administrés par voie systémique ciblant la microangiopathie est limitée par la raréfaction capillaire des tissus atteints. Cette limitation de la diffusion est difficilement compensable par une augmentation des doses administrées compte tenu des effets indésirables systémiques fréquents (exemple de l'iloprost).

Parmi les méthodes d'administration locale d'un médicament, l'iontophorèse consiste à appliquer sur la peau un courant de faible intensité (20 à 100 μ A le plus souvent) à travers une capsule ou éponge contenant un médicament ionisé, afin de provoquer une migration transcutanée de ce médicament (76). En fonction des caractéristiques de la molécule, du tissu cible et des concentrations utilisées, l'effet pharmacodynamique pourra être limité au derme, alors que dans d'autres cas la molécule diffusera dans l'organisme avec ou sans action systémique, en fonction des concentrations atteintes.

Dans la sclérodermie, l'administration ciblée de traitements vasodilatateurs par voie locale pourrait augmenter le flux sanguin cutané digital, et améliorer la cicatrisation ou prévenir l'apparition des ulcérations, tout en réduisant considérablement le risque d'effets indésirables systémiques, assurant à ce traitement des ulcérations digitales de la SSc un profil efficacité/tolérance favorable.

2. Principes de l'iontophorèse

Breve histoire de l'iontophorèse

L'iontophorèse est un processus qui entraîne une pénétration accrue de substances ionisées (ions et/ou molécules chargées) dans ou à travers un tissu lorsqu'un gradient de potentiel électrique est appliqué (77). Dans la littérature médicale scientifique, le terme d'iontophorèse désigne une technique non invasive d'administration transcutanée d'un médicament à travers une capsule ou éponge sous l'influence d'un courant de faible intensité (20 à 100 μ A le plus souvent) permettant le transfert des molécules ionisées (76).

Historiquement, cette technique aurait été décrite pour la première fois en 1747 par Veratti (78). Cette idée s'inscrit dans l'esprit italien du XVIII^e siècle, où Galvani fit ses célèbres expériences sur les effets de l'électricité sur la contraction musculaire de pattes de grenouilles, et où Volta construisit la première cellule électrique (précurseur de la pile électrique). À la suite de ces inventions, au début du XIX^e siècle, le galvanisme devenait très populaire et fut utilisé pour le traitement de troubles neurologiques, gynécologiques et/ou génito-urinaires, ainsi que pour la destruction électrochimique (79).

Cette technique perdit temporairement sa popularité vers la fin du XIX^e siècle, lorsque des inventions plus sophistiquées dans le domaine de l'électricité virent le jour, et ce n'est qu'au début du XX^e siècle que l'iontophorèse fut redécouverte par Leduc, qui introduisit le terme de ionothérapie et formula les lois qui régissent ce processus (80,81).

Il démontra que les «médicaments» ioniques pénétraient dans la peau et pouvaient exercer des effets locaux et systémiques. Dans son expérience, il utilisa deux lapins connectés en série à une machine iontophorétique. Le premier lapin avait du sulfate de strychnine sur l'électrode positive, le deuxième avait du cyanure de potassium sur l'électrode analogue négative. Lorsque Leduc activa l'iontophorèse en délivrant un courant de 40 à 50 mA, le premier lapin fut saisi de convulsions tétaniques en raison de l'introduction de l'ion strychnine, tandis que le deuxième lapin mourut rapidement avec des signes d'intoxication au cyanure. Dans une deuxième expérience, deux nouveaux lapins subirent la même expérience mais cette fois, Leduc inversa le courant.

Dans ces conditions, les animaux restèrent indemnes. Cette expérience saisissante fournit des preuves convaincantes sur le fait que l'iontophorèse était une technique puissante pour l'introduction de médicaments dans et à travers les tissus.

Cette découverte stimula une nouvelle vague d'enthousiasme concernant l'iontophorèse et conduisit à de nombreuses applications au début du XX siècle.

L'intérêt pour l'iontophorèse diminua au cours du XX siècle mais nous assistons depuis le début du XIX siècle à une phase de « redécouverte » spectaculaire de l'iontophorèse dans des domaines variés tels que l'odontologie, la dermatologie, l'otorhinolaryngologie ou encore l'ophtalmologie (82), bien que les mécanismes de succès ou d'échec restent encore bien souvent incompris.

Description de l'iontophorèse

Le principe de base est simple : par l'application d'un courant de faible intensité entre deux électrodes disposées à la surface de la peau, il est possible de transporter de manière active des molécules dans le derme sans induire de lésion (Figure 11).

Deux mécanismes différents sont à l'œuvre dans le procédé iontophorétique : l'*électroré pulsion* d'une part et l'*électro-osmose* d'autre part. L'électroré pulsion est un phénomène électrophysique basé sur la répulsion des charges de même polarité. Toute molécule chargée positivement et positionnée au contact d'une anode est systématiquement repoussée par cette-dernière. Il en va de même pour toute molécule chargée négativement et positionnée au contact d'une cathode. Lorsqu'une solution d'une molécule chargée est positionnée entre la peau et une électrode de même charge, l'électroré pulsion provoque une migration de ces molécules vers le derme. La force d'électroré pulsion est alors suffisamment forte pour que la molécule traverse l'épiderme – donc notamment sa couche cornée – puis pénètre dans le derme. Ce mécanisme s'applique évidemment à toutes les molécules et tous les atomes ionisés présents dans la solution.

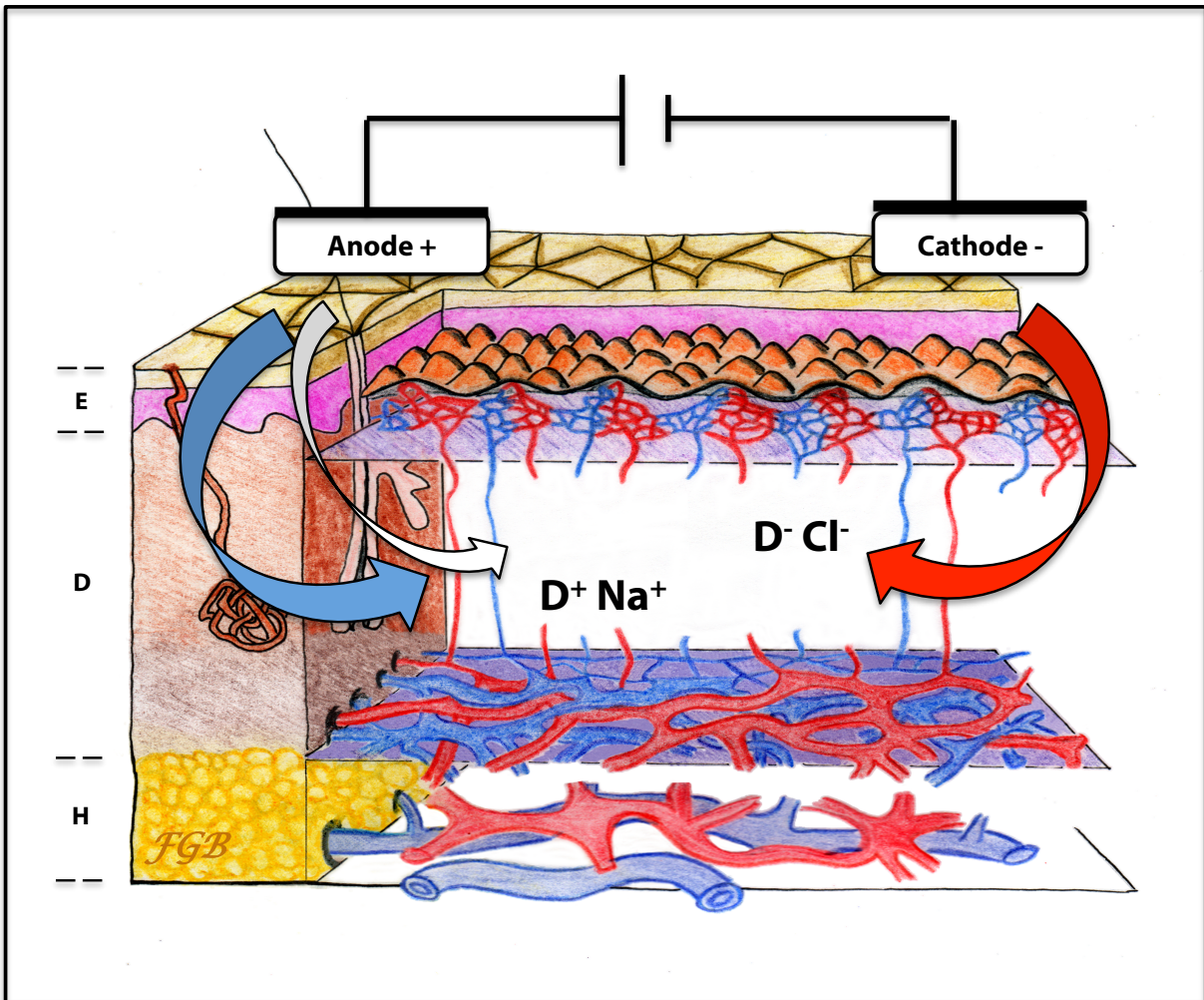


Figure 11. Représentation schématique du transfert iontophorétique de molécules ionisées. Les molécules chargées positivement (D^+) se déplacent depuis l'anode vers le derme (flèche bleue) tandis que les molécules chargées négativement (D^-) se déplacent depuis la cathode vers le derme (flèche rouge). Le flux électro-osmotique est représenté par la flèche blanche. E : épiderme. D : derme. H : hypoderme.

L'électro-osmose est un mécanisme peut-être moins intuitif. Il peut être défini comme la création d'un flux de solvant dans le sens de l'anode vers la cathode sous l'effet du gradient de potentiel électrique. L'application d'un courant entre les deux électrodes conduit à un déséquilibre électrochimique de part et d'autre de la peau, au niveau des électrodes. L'électroneutralité dans chaque électrode est maintenue grâce à une augmentation de la perméabilité cutanée aux ions de charges opposées et d'origine endogène (contre-ion) qui traversent la peau dans le sens du derme vers l'électrode. On observe ainsi un passage accru de cations Na^+ au niveau de la cathode et d'anions Cl^- au niveau de l'anode.

Toutefois en raison de la polarité réputée négative de la peau à pH neutre, les anions seraient partiellement bloqués dans leur remonté vers l'anode par une barrière de charge négative. Le flux des anions vers l'anode serait donc moins important que celui des cations vers la cathode. Cette différence d'intensité entre les deux flux produirait un gradient en faveur du flux cationique Na^+ , capable d'entraîner les molécules d'eau de l'anode vers la cathode. Ce flux, appelé flux électro-osmotique, est suffisamment important pour attirer des molécules chargées positivement mais aussi des molécules neutres présentes au niveau de l'anode à travers le derme. Il serait donc théoriquement possible de faire migrer des molécules neutres par iontophorèse.

Facteurs influençant le transport iontophorétique

Si le principe même de l'iontophorèse est simple, sa maîtrise demeure d'une extrême complexité, comme en témoignent le peu d'applications thérapeutiques actuelles.

En fonction des caractéristiques de la molécule, du tissu cible et des concentrations utilisées, l'effet pharmacodynamique pourra être limité au derme, alors que dans d'autres cas la molécule diffusera dans l'organisme avec ou sans action systémique en fonction des concentrations atteintes. Plusieurs facteurs concourent au passage iontophorétique d'une molécule dans le derme : les propriétés physico-chimiques de la molécule utilisée, les paramètres électriques du dispositif et les facteurs dépendant des caractéristiques de la peau.

Concernant les propriétés physico-chimiques, outre la charge de la molécule qui utilise le principe même de l'iontophorèse, son ionisation – variable dépendant du pKa de chacune de ses fonctions acides et basiques – joue également un rôle important (83). Des logiciels permettent de simuler la charge globale d'une molécule en fonction du pH. Il est alors possible d'estimer le point isoélectrique d'une molécule (pI) – c'est à dire la valeur du pH pour laquelle la somme globale de ses charges est nulle – pour définir le sens de l'iontophorèse en fonction du pH de la solution. En effet, le phénomène d'électrorépulsion dépend de la polarité de la molécule et conditionne, en théorie, le choix du sens de l'iontophorèse (76). On parle de *sens cathodal* lorsque la molécule, généralement chargée négativement, est déposée au niveau de la cathode et de *sens anodal* lorsque la molécule, généralement chargée positivement, est déposée au niveau de l'anode.

Outre le degré d'ionisation, il est admis que pour être facilement transportée par voie iontophorétique, une molécule doit être assez concentrée, de faible poids moléculaire et n'être ni trop hydrophile ni trop lipophile (75, 76, 79-82). Dans la pratique, il est très difficile de prévoir qu'elle sera le profil iontophorétique d'une molécule avant de l'avoir testée.

Concernant les paramètres électriques du dispositif, la polarité de l'électrode active – celle qui reçoit la molécule d'intérêt – et la quantité de courant sont les deux paramètres électriques les plus importants dans le transport iontophorétique (76). La polarité doit être la même que celle de la molécule, comme mentionné plus haut. Le choix concerne celle des deux modalités, anodale ou cathodale, qui sera retenue (facteur dépendant uniquement de la molécule). Pour la quantité de courant, celle-ci est fonction à la fois de l'intensité et de la durée d'application du courant : $Q = I \times t$, exprimée en Coulomb (ou en A.s). Comme il existe une linéarité entre le flux iontophorétique et la quantité de courant, il est possible de faire varier soit l'intensité, soit la durée (ou les deux en même temps) pour augmenter la dose de la molécule d'intérêt qui pénètre dans le derme. En théorie, il n'existe pas de limite de durée d'application. En revanche il existe un seuil d'intensité, ou plus précisément un seuil de densité d'intensité, c'est-à-dire d'intensité par unité de surface de peau. Ce seuil, fixé à $500 \mu\text{A}/\text{cm}^2$, est considéré comme la limite tolérable. Au-delà, il semble exister un risque important d'irritation cutanée, voire de brûlure (83).

Concernant les propriétés de la peau, le principal facteur limitant le passage iontophorétique est le franchissement de la couche cornée encore dénommée *stratum corneum*. Mesurant de 8 à 20 μm d'épaisseur (86), cette couche qui est la plus superficielle de l'épiderme assure un rôle fondamental de barrière mécanique, chimique, microbiologique et de photoprotection. Le transport de molécules par voie iontophorétique dépend donc étroitement de cette épaisseur de cornéocytes, qui comprend des variations régionales importantes, pouvant atteindre jusqu'à dix fois l'épaisseur moyenne au niveau des paumes de mains et des plantes de pieds (86). Le transport iontophorétique dépend également de l'intégrité de la surface cutanée et de son taux d'hydratation. L'on ne peut imaginer enfin qu'il ne soit influencé par la densité des annexes présentes (la pilosité, par exemple, reflétant la densité des poils associés à leurs glandes sébacées).

En conclusion, depuis la première étude sur l'iontophorèse faite par Leduc en 1908 à des fins thérapeutiques, cette technique a été largement explorée et de nombreux modèles expérimentaux ont été générés. Pour autant, les facteurs influençant cette technique demeurent complexes et difficiles à maîtriser dans leur totalité. Cette technique simple et non-invasive a beaucoup à offrir et attend encore l'élucidation de ses subtilités.

3. L'iontophorèse thérapeutique dans la SSc : synthèse des études cliniques et précliniques menées par l'équipe depuis 2009

Depuis 2006, l'équipe du centre d'investigation clinique du CHU de Grenoble s'est spécialisée dans l'exploration microvasculaire des troubles trophiques et notamment ceux du patient atteint de SSc. Pendant une période de sept ans, l'équipe du Professeur Cracowski a publié plus d'une dizaine d'articles cliniques et précliniques sur la mise au point d'une nouvelle stratégie de prise en charge des ulcères digitaux dans la sclérodermie (Figure 12).

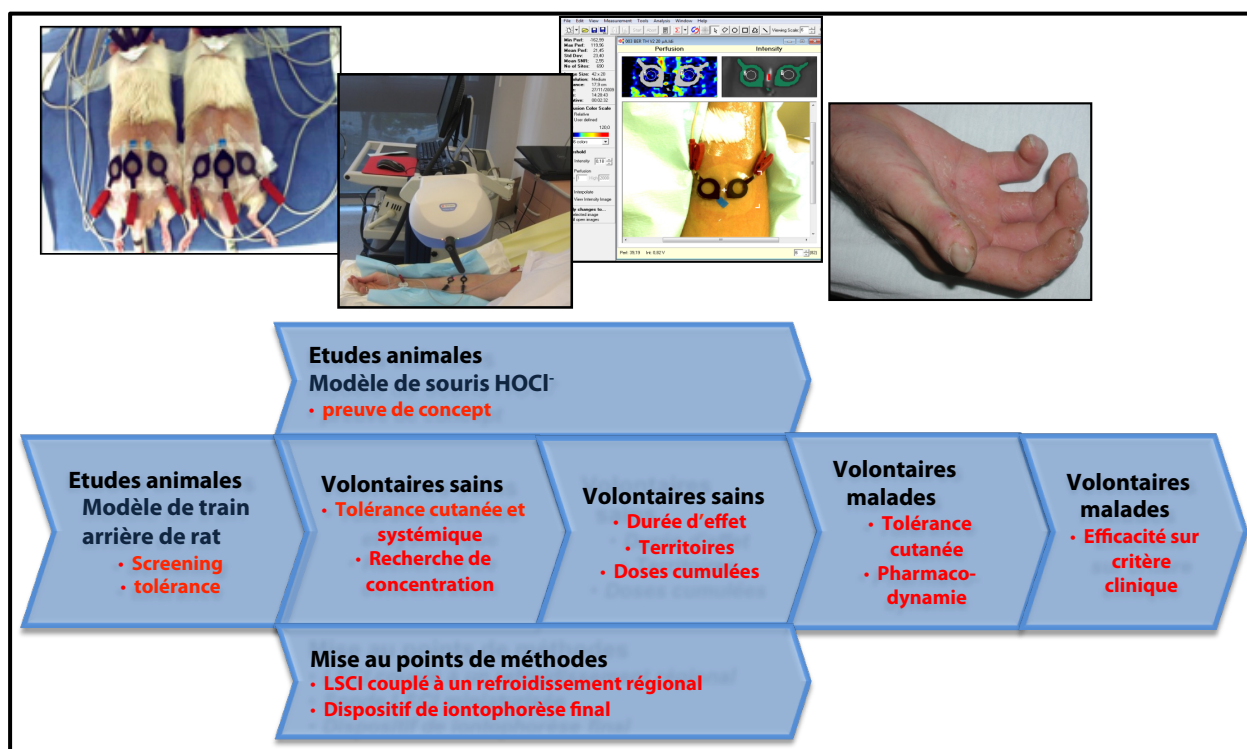


Figure 12. Programme de recherche de l'équipe dans le domaine de l'iontophorèse thérapeutique appliquée aux patients atteints de sclérodermie systémique.

En 2009, Roustit et collaborateurs ont réalisé la première étude d'évaluation de la perfusion après administration d'un vasodilatateur puissant par iontophorèse, le nitroprussiate de sodium (SNP), chez des patients atteints de SSc. Ses résultats démontrent qu'il est possible de faire varier le flux microcirculatoire au niveau de l'avant-bras des patients et que ces variations peuvent être mesurées en imagerie par Laser Doppler.

En 2010, Blaise et collaborateurs ont montré dans une étude clinique sur volontaires sains que la prise orale d'un inhibiteur de la phosphodiesterase 5 – le sildénafil – permet de potentialiser l'effet du SNP administré par iontophorèse. Cette étude a été la première de l'équipe à mettre l'accent sur la volonté de trouver des traitements efficaces dans la prise en charge des troubles trophiques.

En 2011, un modèle préclinique sur train arrière de rats a été mis au point afin d'explorer la faisabilité de l'iontophorèse thérapeutique et de disposer d'un outil de screening systématique de molécules candidates. Les résultats ont notamment permis d'identifier le tréprostinil comme étant un bon candidat pour l'iontophorèse thérapeutique.

Une fois le modèle validé, plusieurs études ont été conduites pour identifier de nouveaux candidats. C'est ainsi qu'en 2012, Roustit et collaborateurs ont testé l'iontophorèse de deux antagonistes du récepteur à l'endothéline-1 sur le modèle animal, puis chez des volontaires sains. Malheureusement, malgré un effet pharmacologique observé chez l'animal aucun résultat n'a été obtenu chez l'homme.

Les résultats obtenus avec l'iontophorèse de tréprostinil sur le modèle animal ont permis le lancement d'un premier essai clinique sur volontaires sains. En 2013, Blaise et collaborateurs ont montré dans une étude clinique sur volontaires sains que l'iontophorèse cathodale de tréprostinil sur l'avant-bras peut induire une vasodilatation importante et soutenue. Cet essai a également éliminé l'iloprost comme molécule initialement candidate à l'iontophorèse thérapeutique, du fait de la survenue d'un effet indésirable local (brûlure).

Parallèlement aux études cliniques, Kotzki et collaborateurs ont testé en 2013 deux nouvelles classes thérapeutiques dans une étude préclinique : les stimulateurs de la guanylate cyclase soluble et les agonistes du récepteurs IP non analogues de la prostacycline.

Toujours dans une étude préclinique, Kotzki et collaborateurs ont comparé trois protocoles d'iontophorèse cathodale de tréprostinil en 2015. Un protocole utilisant un courant continu classique, un protocole utilisant un courant pulsé de moyenne intensité et un protocole utilisant un courant pulsé de haute intensité.

Cinquième étude : Iontophorèse de Tréprostinil, une étude Pharmacodynamique et Pharmacocinétique, preuve de concept (titre court: TIPPS)

L'ulcère ischémique digital (UD) est une complication grave de la sclérodémie systémique (SSc). Les prostanoïdes intraveineux sont les seuls traitements approuvés pour les UD actifs, mais ils induisent des effets secondaires, limitant la dose et nécessitent une administration sous surveillance (habituellement en milieu hospitalier).

L'objectif principal de cette étude était d'évaluer l'effet d'une méthode non invasive d'administration de médicament, l'iontophorèse de tréprostinil, chez des patients atteints de SSc ne présentant pas d'ulcération pulpaire.

Trois études ont été menées : une étude pharmacocinétique chez 12 volontaires sains a montré que le pic de concentration cutanée était atteint 2 heures après l'iontophorèse de tréprostinil, alors que le dosage plasmatique n'a pas détecté le produit. Puis, une étude en double aveugle contrôlée contre placebo, avec escalade de doses a évalué l'effet du tréprostinil sur le flux sanguin de la microcirculation cutanée chez 22 volontaires sains. L'effet de la dose la plus élevée a ensuite été comparé à celui du placebo chez 12 patients atteints de SSc. Pendant toutes les procédures, le flux sanguin de la microcirculation cutanée était enregistré par LSCI et exprimé en conductance vasculaire cutanée (CVC).

L'iontophorèse de tréprostinil augmentait significativement le flux sanguin de la microcirculation cutanée chez les sujets sains et chez les patients atteints de SSc.

En conclusion, L'iontophorèse cutanée digitale de tréprostinil est une technique faisable, bien tolérée et qui augmente la perfusion cutanée digitale. Cette nouvelle approche thérapeutique pourrait être testée en tant que traitement pour les UD liés à la SSc.

Article publié: [*Cutaneous Iontophoresis of Treprostinil in Systemic Sclerosis: A Proof-of-Concept Study.*](#) M Roustit, F Gaillard-Bigot, S Blaise, F Stanke-Labesque, C Cracowski, C Seinturier, JF Jourdil, B Imbert, P Carpentier et JL Cracowski. Clin Pharmacol Ther. 2014 Apr;95(4):439-45.

Cutaneous Iontophoresis of Treprostinil in Systemic Sclerosis: A Proof-of-Concept Study

M Roustit^{1,2}, F Gaillard-Bigot¹, S Blaise^{1,3}, F Stanke-Labesque^{1,4}, C Cracowski², C Seinturier³, J-F Jourdil⁴, B Imbert³, PH Carpentier³ and J-L Cracowski^{1,2}

Ischemic digital ulcer (DU) is a serious complication of systemic sclerosis (SSc). Intravenous prostanoids are the only approved treatment for active DUs, but they induce dose-limiting side effects and require hospitalization. Our objective was to evaluate the effect of iontophoresis (a noninvasive drug delivery method) of treprostinil in SSc patients. Three studies were conducted: a pharmacokinetic study in 12 healthy volunteers showed that peak dermal concentration was reached at 2 hours, whereas plasma treprostinil was undetected. Then, a placebo-controlled, double-blind incremental dose study assessed the effect of treprostinil on digital skin blood flow in 22 healthy subjects. The effect of the highest dose was then compared with that of placebo in 12 SSc patients. Treprostinil significantly increased skin blood flow in healthy subjects ($P = 0.006$) and in SSc patients ($P = 0.023$). In conclusion, digital iontophoresis of treprostinil is feasible, is well tolerated, and increases digital skin perfusion. It could be tested as a treatment for SSc-related DUs.

Systemic sclerosis (SSc) is a rare disease characterized by extensive fibrosis and vascular alterations predominantly affecting the extremities. Microvascular dysfunction is a key feature of the pathophysiology of SSc that occurs early in the progression of the disease.¹ One of the main complications of SSc microvasculopathy is the development of digital ulcers (DUs), which are painful, cause functional impairment, and have a major negative impact on the quality of life.² Chronic ulcers can become infected, resulting in gangrene, osteomyelitis, and amputation, leading to permanent disability and self-image problems.²

Intravenous prostacyclin analogues (iloprost) are the only approved treatment for active SSc-related DUs.³ However, their therapeutic effect is counterbalanced by potentially serious vasodilation-induced, dose-limiting side effects (e.g., severe headaches, flushing, tachycardia, and hypotension). Their use usually requires hospitalization and close monitoring while infusing the drug, which are associated with increased costs. The paradox is that elevated concentrations of prostanoids are needed in the extremities (where ulcers develop), but decreased functional capillary density prevents the drug from diffusing properly to the digits. Elevated doses of drugs are therefore needed, leading to systemic adverse drug reactions. Therefore, topical administration of these

drugs may be a way of avoiding the toxicity of systemic treatments.

Iontophoresis is a noninvasive, current-driven drug delivery method. It has been suggested as an interesting alternative to systemic delivery of vasodilators in the treatment of SSc-related DUs.^{4,5} Previous studies by our group have focused on the screening of vasodilators (including prostacyclin analogues and endothelin receptor antagonists) that can be iontophoretically administered.^{6,7} The 20-minute cathodal iontophoresis of treprostinil, a prostacyclin analogue, induced sustained vasodilation and was well tolerated in a rat model⁶ and on the forearm of healthy subjects.⁸ However, key issues remain to establish the proof of concept of treprostinil iontophoresis in the treatment of DUs: systemic and dermal pharmacokinetics of iontophoretically delivered treprostinil are unknown; this procedure has never been performed on the digits where the skin is glabrous (with a high density of arteriovenous anastomoses) and therefore presents distinct characteristics from nonglabrous (i.e., hairy) skin; and finally, the safety of treprostinil iontophoresis and its effect on skin blood flow have never been tested in SSc patients, in whom sclerodactyly may affect intradermal drug delivery.

The primary objective of this work was to evaluate the effect of iontophoretically delivered treprostinil on digital skin blood

¹UMR 1042-HP2, INSERM and University Grenoble-Alpes, Grenoble, France; ²Clinical Pharmacology Unit, INSERM CIC1406, Grenoble University Hospital, Grenoble, France; ³Vascular Medicine Department, Grenoble University Hospital, Grenoble, France; ⁴Laboratory of Pharmacology, Grenoble University Hospital, Grenoble, France. Correspondence: M Roustit (MRoustit@chu-grenoble.fr)

Received 22 October 2013; accepted 17 December 2013; advance online publication 12 February 2014. doi:10.1038/clpt.2013.255

flow in patients with SSc. We also assessed the safety of the procedure. First, we performed pharmacokinetic and incremental dose studies in healthy subjects.

RESULTS

Intradermal vs. plasma concentrations of treprostinil after iontophoresis on the forearm of healthy subjects

Twelve healthy volunteers (six men and six women) were enrolled in this study. Their mean age was 20.8 ± 2 and mean body mass index was $22.2 \pm 2.6 \text{ kg/m}^2$. Systolic and diastolic arterial blood pressures were 114.6 ± 11.3 and $70.2 \pm 10.4 \text{ mm Hg}$, respectively. Four women were taking oral contraceptives.

Baseline cutaneous vascular conductances were 0.48 ± 0.1 and 0.47 ± 0.09 perfusion units/mm Hg at the placebo and the treprostinil skin sites, respectively. The insertion of microdialysis catheters induced inflammation, which increased mean cutaneous vascular conductances despite apparent return to baseline during the resting period in individual tracings (0.45 ± 0.08 and 0.53 ± 0.06 perfusion units/mm Hg, respectively; $P = 0.006$). Because the data are expressed as percentage of baseline (%BL), we used cutaneous vascular conductances after fiber insertion as the BL to avoid exaggeration of the treatment effect. Following iontophoresis, skin blood flow was significantly higher at the treprostinil site than at the placebo site (values of area under the concentration–time curve (AUC) up to 8 hours after the end of iontophoresis (AUC_{0–8h}) were $23,066.1 \pm 15,718$ and $11,187.1 \pm 10,092 \text{ %BL-minute}$, respectively; $P = 0.02$; **Figure 1**).

The intradermal concentration of treprostinil was measurable from the first to the seventh hour after the end of iontophoresis. Peak concentration was reached during the second hour and was $<1.8 \text{ pg/ml}$ in all samples at hour 8 (**Figure 1**). By contrast, the treprostinil concentration was lower than the quantification threshold in all plasma samples.

Petechiae ($n = 4$) and a small hematoma ($n = 1$) were observed after the insertion of the microdialysis fibers. They spontaneously resolved within 24–72 hours. Iontophoresis induced erythema at both sites (placebo: $n = 3$; and treprostinil: $n = 1$) without any itching. It spontaneously resolved within 30 minutes to 5 hours.

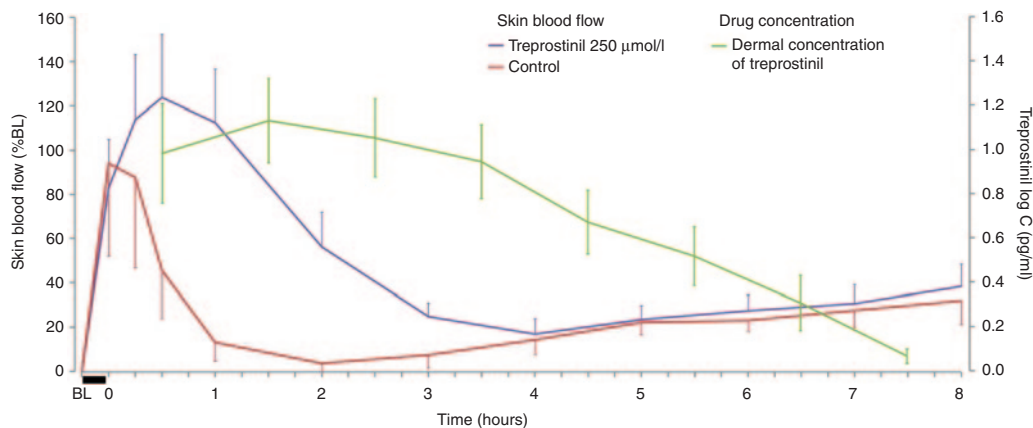


Figure 1 Skin blood flow recorded on the forearm after a 40 mC/cm^2 cathodal iontophoresis (black bar) of treprostinil and placebo, expressed as the percentage increase from baseline flow. Treprostinil was quantified in the dermis with microdialysis samples collected every hour and analyzed by liquid chromatography–tandem mass spectrometry. Treprostinil was detected in the dermis for up to 8 hours after the end of iontophoresis.

Study Highlights

WHAT IS THE CURRENT KNOWLEDGE ON THE TOPIC?

- ✓ DUs related to SSc are associated with substantial morbidity. Intravenous prostacyclin analogues comprise the only approved treatment for active DUs, but they induce dose-limiting side effects. They also require hospitalization, which is associated with increased costs.

WHAT QUESTION DID THIS STUDY ADDRESS?

- ✓ Our objective was to establish the proof of concept of the use of treprostinil (a prostacyclin analogue) through iontophoresis, a noninvasive, current-driven drug delivery method.

WHAT THIS STUDY ADDS TO OUR KNOWLEDGE

- ✓ Iontophoresis of treprostinil delivers elevated dermal concentration, although it is undetectable in the plasma. The different protocols tested showed a correlation between the quantity of current and the pharmacological effect. A single dose at 240 mC/cm^2 significantly increases digital skin perfusion in both healthy subjects and SSc patients, and the procedure is safe.

HOW THIS MIGHT CHANGE CLINICAL PHARMACOLOGY AND THERAPEUTICS

- ✓ This original approach may improve the safety of prostacyclin analogues used to treat SSc-related DUs while decreasing associated costs. The efficacy of treprostinil iontophoresis on ulcer healing should now be tested on a larger scale.

Safety and pharmacodynamic effect of incremental doses of treprostinil delivered by digital iontophoresis in healthy subjects

Twenty-two healthy subjects were included in this study. All but one subject included in Study 1 participated in Study 2 (**Supplementary Table S1** online). The mean age of subjects was 21.4 ± 2.3 and their mean body mass index was $21.5 \pm 2.2 \text{ kg/m}^2$. Systolic and diastolic arterial blood pressures were 115.3 ± 11.2 and $68.1 \pm 10.4 \text{ mm Hg}$, respectively. Ten of 13 women were taking oral contraceptives.

All three continuous iontophoresis protocols were well tolerated. Desquamation was observed on the fingertips of one hand in a young male. Because all the fingertips were concerned, the involvement of iontophoresis was excluded. Discontinuous currents were stopped after the 40 mC/cm² protocol due to uncomfortable tingling (reported by all subjects) and the absence of pharmacodynamic effect.

Skin blood flow was significantly higher at the treprostinil site than at the placebo site only for the highest dose (240 mC/cm²). Values of AUC_{0-4h} were 29,703 ± 23,460 and 18,426 ± 18,365 %BL·minute, respectively ($P = 0.006$; detailed data for all iontophoresis protocols are available in **Supplementary Table S2** online).

Treprostinil concentration was below the quantification threshold in all plasma samples for all doses. Following the intermediate analysis, in the confirmatory study a complete pharmacokinetic study was not performed as originally planned (**Supplementary Methods** online). However, one blood sample was collected from each subject 30 minutes after the end of iontophoresis (240 mC/cm², $n = 6$). The plasma concentration of treprostinil was 783 and 933 pg/ml in two volunteers and <1.8 pg/ml in the four other volunteers.

Safety and pharmacodynamic effect of treprostinil delivered by digital iontophoresis in SSc patients

Twelve SSc patients were enrolled in this study. The characteristics of the population are summarized in **Table 1**. The most commonly prescribed drugs were proton-pump inhibitors ($n = 8$), calcium channel blockers ($n = 6$; stopped 1 week prior to inclusion), statins ($n = 3$), and angiotensin-converting enzyme inhibitors ($n = 3$).

Skin blood flow was significantly higher at the treprostinil site than at the placebo site. Values of AUC_{0-4h} were 47,826 ± 43,941 and 30,000 ± 27,543 %BL·minute, respectively ($P = 0.023$; **Figure 2**). In responding patients, vasodilation did not spread beyond the application site (**Figure 3**). We ran *post hoc* analyses to identify parameters associated with nonresponse. We found that the two patients with a “late” capillaroscopy pattern were nonresponders.

Iontophoresis at 240 mC/cm² was well tolerated. We observed one episode of Raynaud’s phenomenon at the end of iontophoresis at the placebo site but not at the treprostinil site. Two patients experienced mild headaches. However, all plasma samples collected from each patient 30 minutes after the end of iontophoresis showed treprostinil concentration <1.8 pg/ml.

DISCUSSION

The treatment of active SSc-related DUs is challenging. The dose-limiting adverse effects of i.v. iloprost and the costs associated with the hospitalization required for its administration are currently limitations. Treprostinil, a related compound, has been tested in a pilot trial⁹ with encouraging results. However, s.c. treprostinil induces severe injection site pain, leading to a high rate (5 of 12 patients) of drug discontinuation.⁹ Alternative routes of administration are therefore needed. Recently, a

sustained release oral formulation of treprostinil has been shown to be effectively absorbed in SSc patients but, logically, prostanoid-related adverse drug events were observed in the vast majority of patients.¹⁰

The current work was aimed at establishing the proof-of-concept for the local, noninvasive delivery of treprostinil using iontophoresis. We show that treprostinil remains detectable in the dermis of healthy skin for up to 8 hours, although systemic concentrations are extremely low. On the finger pad, iontophoresis at 240 mC/cm² was feasible, was well tolerated, and induced vasodilation in most healthy participants and SSc patients. We also observed a transient increase in skin blood flow at the placebo site, which is attributed to a nonspecific, current-induced vasodilation.¹¹ This tends to reduce the difference in absolute values of skin blood flow between placebo and treprostinil. However, it is not possible to predict how this difference can translate into a clinical effect. Although the only drug approved in DU healing (i.e., iloprost) is a potent vasodilator, and vascular dysfunction is the hallmark of SSc, the efficacy of prostaglandin I₂ analogues is not expected to be solely due to their vascular properties. Indeed, the efficacy of i.v. therapy with iloprost is prolonged over several weeks, whereas vasodilation-induced effects are observed only during drug infusion or shortly after. This prolonged effect is attributed to other properties,

Table 1 Demographic and clinical characteristics of SSc patients (N = 12)

Age (years)	59.9 ± 11.4
Female	12 (100%)
Postmenopausal	11 (92%)
BMI (kg/m ²)	26.6 ± 3.6
Arterial blood pressure	
Systolic (mm Hg)	138 ± 19
Diastolic (mm Hg)	70 ± 13
Raynaud’s phenomenon	12 (100%)
Duration (years)	11.8 ± 7.4
Number of fingers involved	7.7 ± 1.7
Thumb involved	10 (83%)
Feet involved	2 (17%)
Scleroderma (lcSSc)	12 (100%)
Duration (years)	10 ± 6.9
Sclerodactyly	12 (100%)
Rodnan score	8.7 ± 4.9
Previous digital ulcer	1 (8%)
Capillaroscopy pattern ²²	
Early	4 (33%)
Active	6 (50%)
Late	2 (17%)

Quantitative data are expressed as mean ± SD. Qualitative data are expressed as number (percentage). BMI, body mass index; lcSSc, limited cutaneous SSc; SSc, systemic sclerosis.

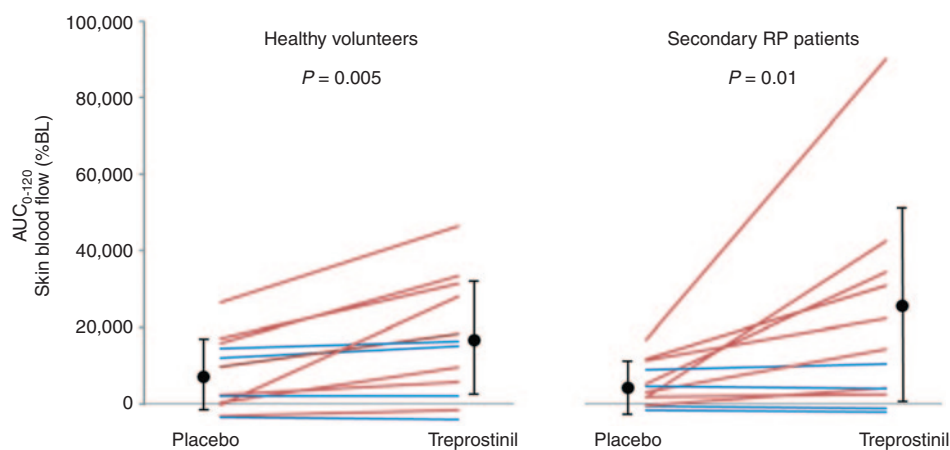


Figure 2 Skin blood flow expressed as area under the curve (AUC) of cutaneous vascular conductances after iontophoresis (240 mC/cm²) of treprostiniil and placebo in 12 healthy subjects and 12 systemic sclerosis patients. Black dots and bars represent mean (SD) area under the curve of cutaneous vascular conductances. Eight subjects (four healthy volunteers and four patients) did not respond to treatment (blue lines).

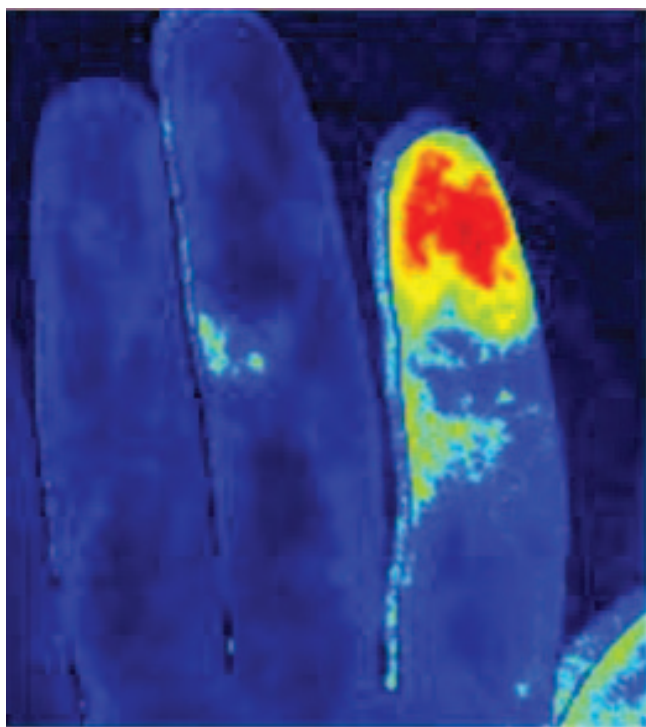


Figure 3 Skin blood flow recorded with laser speckle contrast imaging after removal of electrodes. Treprostiniil was applied on the index finger and placebo on the middle finger. Colors range from dark blue (no perfusion) to red (high perfusion).

such as downregulation of lymphocyte adhesion to endothelial cells and inhibition of the production of tumor necrosis factor- α . Furthermore, iloprost has been recently shown to exert prostaglandin I₂ receptor-dependent immunomodulatory activity in SSc patients.¹²

The sustained vasodilation that we observed on the forearm of healthy subjects is consistent with our previous results using comparable iontophoretic parameters (i.e., quantity of charge of 40 mC/cm²).⁸ The current study shows that on the finger pad, however, this quantity of current is not sufficient to increase

skin blood flow, as has been reported in studies with other vasodilators such as sodium nitroprusside, both in patients with SSc and in healthy participants.¹³ This may be due to anatomical differences in the skin's microcirculation between the forearm and the finger pad, with a higher density of vessels and arteriovenous anastomoses in the latter, leading to increased dermal clearance. Another explanation could be the greater thickness of the epidermis on the finger pad as compared with that of the forearm.

Many parameters are involved in iontophoretic transport. The parameters that can be controlled by investigators include the treated skin area, the drug concentration in the iontophoresis reservoir, the intensity of the current, and the duration of current application.¹⁴ We decided to gradually step up the dose in Study 2 by adjusting the duration of the iontophoresis protocol. Indeed, increased current intensity may be responsible for tingling and itching, in addition to discomfort from the procedure, leading in some cases to the discontinuation of iontophoresis before the complete dose had been delivered.¹⁵ On the other hand, using higher concentrations did not show any further vasodilation in previous experimental studies.⁶

Discontinuous current was also tested because iontophoretic transport might be enhanced when intermittent current sequences are used rather than a continuous sequence, with the same quantity of charge. Experimental animal studies in our laboratory had suggested a potential benefit of such a protocol, with a greater increase in skin blood flow. However, we observed no effect when discontinuous sequences at 40 mC/cm² were used in humans. Moreover, intermittent short, high-intensity sequences generated discomfort in all subjects. Thus, we maintained only continuous administration in the incremental study. We finally observed that a six-times-higher dose was required to achieve vasodilation on the finger pad as compared with the dose on the forearm.

Our preliminary pharmacokinetic study in healthy participants suggests that when delivered by cutaneous iontophoresis, treprostiniil remains in the dermis for up to 8 hours.

Simultaneous plasma monitoring shows that the systemic diffusion of the drug is below the detection threshold. Thus, the dermal vs. systemic concentration ratio in the forearm suggests that iontophoresis of treprostinil could allow sufficient doses to be delivered locally while limiting systemic exposure. However, this assumption could not be confirmed on the finger pad. A limitation of this study is that for technical and ethical reasons, the dermal pharmacokinetics of treprostinil was not explored in the finger pads of either healthy subjects or patients. Indeed, as fiber insertion in the finger pad is traumatic and leads to bleeding, we decided not to perform microdialysis to avoid any trauma to patients with possible healing impairment. Tape stripping, another technique used to assess dermal pharmacokinetics *in vivo*, could not be used in this protocol because continuous quantification over the same skin area is not possible.¹⁵ However, the pharmacodynamic effect observed in patients despite the absence of positive plasma concentration assessment suggests a favorable pharmacokinetic profile in the finger pad.

Treprostinil concentration from all blood samples in all series of the incremental dose study (Study 2) was below the quantification threshold. As planned in the protocol, the collection of complete pharmacokinetic data was stopped at the interim analysis, and only one sample was collected in the confirmatory study, 30 minutes after the end of iontophoresis (corresponding to the maximum pharmacodynamic effect). Nevertheless, although lower than that observed after i.v. or s.c. infusion, significant treprostinil concentrations were found in two healthy volunteers.¹⁶ One of these two subjects was a responder, whereas the other was not, and neither experienced adverse drug events.

On the finger pad, we observed vasodilation in two-thirds of the healthy subjects and patients. The absence of vasodilation was not related to the Rodnan skin score. When looking at the capillaroscopy pattern, the two patients with a “late” pattern did not respond, which could be explained by the reduced capillary density in these patients. Nonetheless, further investigations are needed to explore in depth the parameters that determine the response. Indeed, several properties of the skin barrier that were not explored in the current study may influence iontophoresis, e.g., transepidermal water loss, skin hydration, epidermal and dermal thickness, and skin elasticity. Future studies should also determine the optimal concentration of treprostinil needed to enhance the pharmacodynamic effect on the finger pad, as well as determine the appropriate rate of repeated administrations.

The current study did not aim at directly comparing the effect of treprostinil iontophoresis on skin blood flow between healthy subjects and SSc patients, and the two populations are not comparable. Rather, we aimed at establishing the feasibility of the local administration of treprostinil, its pharmacodynamic effect on skin blood flow, and the safety of the procedure. This establishes its proof-of-concept in patients without ulcers, suggesting that the procedure can now be tested in patients with DUs. However, our objective was not to assess efficacy in ulcer

healing, and to date, skin blood flow has not been established as a surrogate for DUs. In the current study, it was used as a marker of the pharmacodynamic effect of treprostinil to objectify the dermal delivery of the drug. Nonetheless, recent work has demonstrated that differences in skin blood flow, assessed with laser speckle contrast imaging, are correlated with the nail-fold capillaroscopy pattern of microangiopathy.¹⁷ Importantly, the capillaroscopy pattern is a predictive marker of severe peripheral vascular involvement assessed using the Medsger severity scale¹⁸ (i.e., the occurrence of fingertip ulceration). The odds ratios for the future occurrence of DU were 2.49, 6.18, and 15.35 for the early, the active, and the late pattern, respectively.¹⁹ Although the surrogacy of skin blood flow remains to be directly established, these recent data suggest a potential benefit of laser speckle contrast imaging as a surrogate for the occurrence of DU.

In conclusion, the iontophoresis of treprostinil is feasible and well tolerated. Moreover, it increases digital skin blood flow in both healthy subjects and in SSc patients. Taken together, our data suggest that the iontophoresis of treprostinil could provide an efficient, safe, noninvasive, and cost-saving treatment for SSc-related DUs. However, controlled studies are needed both to assess the efficacy of iontophoretically administered treprostinil in DU healing and to compare this strategy with the systemic administration of iloprost.

METHODS

Study population. Healthy volunteers were recruited through local newspaper advertisements, and patients were recruited through our Vascular Medicine department. All patients had limited cutaneous SSc, according to the criteria of LeRoy and Medsger,²⁰ with sclerodactyly. All subjects were included between January 2012 and January 2013.

All subjects were 18 years of age or older. Noninclusion criteria included pregnancy (urine pregnancy tests were performed at the beginning of each visit) and cigarette smoking. None of the healthy subjects had any chronic disease or ongoing treatment (other than oral contraception for women). For patients, the presence of active DUs was a noninclusion criterion. Patients taking calcium channel blockers were instructed to stop medication 1 week before inclusion. Patients taking endothelin receptor antagonists or phosphodiesterase-5 inhibitors or those who had received i.v. iloprost in the previous 15 days were not included.

The investigation conforms to the principles outlined in the Declaration of Helsinki. Grenoble Institutional Review Board CPP Sud-Est V (Institutional Review Board 6705) approval was obtained on 21 November 2011, and each subject gave written informed consent before participation.

Study design

Study 1: intradermal vs. plasma concentration of treprostinil after iontophoresis on the forearm of healthy subjects. This was an open-label pharmacokinetic study enrolling healthy subjects. On arrival at the laboratory, subjects were placed in a temperature-controlled room (23 ± 1 °C); they remained supine during all measurements. After 30-minute acclimatization, two ellipsoid skin sites (~ 12 cm²) were chosen on the ventral side of the right forearm, avoiding visible veins. One of these two sites was randomly selected as the treprostinil site, and the other one as the placebo site. Baseline skin blood flow was recorded for 10 minutes with laser speckle contrast imaging (**Supplementary Methods** online). Both sites were then treated with 5 g of lidocaine/prilocaine cream (Anesderm; Pierre Fabre, Boulogne, France). One hour later, the lidocaine/prilocaine cream was removed, and two linear microdialysis fibers were inserted at

the dermis–hypodermis junction at the treprostinil site (**Supplementary Methods** online and **Supplementary Figure S1** online) and an i.v. catheter was inserted contralaterally. Skin blood flow was continuously recorded at the two skin sites on the forearm until the vasodilation induced by the trauma returned to baseline (at least 45 minutes).

Iontophoresis at 40 mC/cm² (**Supplementary Methods** online) was then performed at both sites; treprostinil was delivered at the site equipped with the microdialysis fibers, whereas NaCl was used at the placebo site. Skin blood flow measurements, microdialysis samples, and venous blood samples were collected until 8 hours after the end of iontophoresis (**Supplementary Figure S1** online). Blood pressure was recorded continuously (Nexfin monitor, Bmeye BV, Amsterdam, The Netherlands) on the left hand during skin blood flow measurements. The design of Study 1 is schematized in **Supplementary Figure S2** online.

Study 2: safety and pharmacodynamic effect of incremental doses of treprostinil delivered by digital iontophoresis in healthy subjects. The primary objective of this double-blind study was to assess the safety of different iontophoresis protocols of treprostinil and placebo (NaCl) on the finger pads of healthy subjects. Digital skin blood flow was also assessed. Subjects enrolled in Study 1 could participate in one or two visits of Study 2. The iontophoresis sites were the finger pads of two fingers randomly chosen from the index, the middle, and the ring fingers. The operator and the volunteer were blinded as to whether the volunteer received treatment or placebo.

Four protocols were sequentially tested, with a go/no-go decision based on safety and tolerability: 40 mC/cm² (continuous current), 40 mC/cm² (discontinuous current), 120 mC/cm² (continuous current), and 240 mC/cm² (continuous current), where the dose of treprostinil delivered is considered as being proportional to the current used (**Supplementary Methods** online). Six participants were included in each iontophoresis protocol. A confirmatory study with six other participants was subsequently performed at the highest dose. Data were pooled for the 12 participants who were tested with the 240 mC/cm² protocol.

Skin blood flow and blood pressure were continuously recorded for at least 2 hours after the end of iontophoresis, until return to baseline skin blood flow. Blood samples from the contralateral arm were also collected (**Supplementary Methods** online).

Study 3: safety and pharmacodynamic effect of treprostinil delivered by digital iontophoresis in SSc patients. This double-blind study aimed at evaluating safety and comparing skin blood flow after digital iontophoresis of treprostinil or placebo (240 mC/cm²) in SSc patients. The skin sites were the finger pads of two fingers chosen as described above. The operator and the volunteer were blinded as to whether the volunteer received treatment or placebo.

At the end of iontophoresis, skin blood flow and blood pressure were measured as described in Study 1 and continuously recorded for up to 4 hours after the end of iontophoresis. Blood samples from the contralateral arm were also collected (**Supplementary Methods** online).

In all studies, photographs of all skin sites were taken before and immediately after iontophoresis, and at the end of each visit. A clinical visit to monitor safety was planned 10 ± 6 days after the final visit.

Data analysis

Data were analyzed with signal processing software (PIMSoft 1.1.1; Perimed, Järfälla, Sweden). Skin blood flow was expressed as cutaneous vascular conductance, which is the flow in arbitrary perfusion units divided by the mean arterial pressure in mm Hg.²¹ We then calculated the percentage change from baseline flow (%BL) and subsequently performed a minute-by-minute analysis to calculate AUC until return to baseline flux, with a minimum recording time of 2 hours (AUC_{0-2h}) and up to 8 hours (AUC_{0-8h}) after the end of iontophoresis.

Statistical analysis

Categorical data were reported as frequency and percentage, and continuous data were reported as mean and SD. Skin blood flow after treprostinil and placebo iontophoresis simultaneously recorded in the same subject were compared using paired *t*-tests or nonparametric tests (Wilcoxon rank test), the latter when the conditions of application of parametric tests were not respected. We considered *P* values of ≤0.05 as significant. Statistical analysis was performed with SPSS 13.0 for Windows (SPSS, Chicago, IL).

SUPPLEMENTARY MATERIAL is linked to the online version of the paper at <http://www.nature.com/cpt>

ACKNOWLEDGMENTS

We thank Dominique Abry and Anne Tournier for blood sampling; Adeline Paris, Sylvain Kotzki, and Constance Minebois for preparing the drugs and blinding; Manon Gabin and Benoît Sulpis for helping with data collection; and Alison Foote for critically reading and editing the manuscript.

AUTHOR CONTRIBUTIONS

M.R., F.G.B., S.B., F.S.-L., C.C., C.S., and J.-L.C. wrote the manuscript. M.R., S.B., F.S.-L., P.H.C., and J.-L.C. designed the research. M.R., F.G.B., S.B., C.C., C.S., B.I., P.H.C., and J.-L.C. performed the research. M.R., F.S.-L., J.-F.J., and J.-L.C. analyzed the data. F.S.-L. and J.-F.J. contributed new reagents/analytical tools.

CONFLICT OF INTEREST

This study was funded by grants from the French government (“Programme Hospitalier de Recherche Clinique Inter-régional 2011”) and from the “Association des Sclérodermiques de France.” Bioprojet Pharma supplied treprostinil. None of the sponsors had any involvement in the design and conduct of the study, nor in the preparation, review, or approval of the current article. M.R., S.B., and J.-L.C. hold a patent on treprostinil iontophoresis for the treatment of ulcers. The other authors declared no conflict of interest.

© 2014 American Society for Clinical Pharmacology and Therapeutics

- Gabrielli, A., Avvedimento, E.V. & Krieg, T. Scleroderma. *N. Engl. J. Med.* **360**, 1989–2003 (2009).
- Steen, V., Denton, C.P., Pope, J.E. & Matucci-Cerinic, M. Digital ulcers: overt vascular disease in systemic sclerosis. *Rheumatology (Oxford)* **48** (suppl. 3), iii19–iii24 (2009).
- Kowal-Bielecka, O. *et al.*; EUSTAR Co-Authors. EULAR recommendations for the treatment of systemic sclerosis: a report from the EULAR Scleroderma Trials and Research group (EUSTAR). *Ann. Rheum. Dis.* **68**, 620–628 (2009).
- Murray, A.K., Herrick, A.L., Gorodkin, R.E., Moore, T.L. & King, T.A. Possible therapeutic use of vasodilator iontophoresis. *Microvasc. Res.* **69**, 89–94 (2005).
- Murray, A.K., Moore, T.L., King, T.A. & Herrick, A.L. Vasodilator iontophoresis a possible new therapy for digital ischaemia in systemic sclerosis? *Rheumatology (Oxford)* **47**, 76–79 (2008).
- Blaise, S., Roustit, M., Millet, C., Ribuoat, C., Boutonnat, J. & Cracowski, J.L. Cathodal iontophoresis of treprostinil and iloprost induces a sustained increase in cutaneous flux in rats. *Br. J. Pharmacol.* **162**, 557–565 (2011).
- Roustit, M. *et al.* Iontophoresis of endothelin receptor antagonists in rats and men. *PLoS ONE* **7**, e40792 (2012).
- Blaise, S., Roustit, M., Hellmann, M., Millet, C. & Cracowski, J.L. Cathodal iontophoresis of treprostinil induces a sustained increase in cutaneous blood flux in healthy volunteers. *J. Clin. Pharmacol.* **53**, 58–66 (2013).
- Chung, L. & Fiorentino, D. A pilot trial of treprostinil for the treatment and prevention of digital ulcers in patients with systemic sclerosis. *J. Am. Acad. Dermatol.* **54**, 880–882 (2006).
- Shah, A.A. *et al.* Open label study of escalating doses of oral treprostinil diethanolamine in patients with systemic sclerosis and digital ischemia: pharmacokinetics and correlation with digital perfusion. *Arthritis Res. Ther.* **15**, R54 (2013).
- Roustit, M. & Cracowski, J.L. Assessment of endothelial and neurovascular function in human skin microcirculation. *Trends Pharmacol. Sci.* **34**, 373–384 (2013).

12. Truchetet, M.E., Allanore, Y., Montanari, E., Chizzolini, C. & Brembilla, N.C. Prostaglandin I(2) analogues enhance already exuberant Th17 cell responses in systemic sclerosis. *Ann. Rheum. Dis.* **71**, 2044–2050 (2012).
13. Roustit, M., Blaise, S. & Cracowski, J.L. Sodium nitroprusside iontophoresis on the finger pad does not consistently increase skin blood flow in healthy controls and patients with systemic sclerosis. *Microvasc. Res.* **77**, 260–264 (2009).
14. Kalia, Y.N., Naik, A., Garrison, J. & Guy, R.H. Iontophoretic drug delivery. *Adv. Drug Deliv. Rev.* **56**, 619–658 (2004).
15. Roustit, M., Blaise, S. & Cracowski, J.L. Trials and tribulations of skin iontophoresis in therapeutics. *Br. J. Clin. Pharmacol.* (2013); e-pub ahead of print 16 April 2013.
16. Laliberte, K., Arneson, C., Jeffs, R., Hunt, T. & Wade, M. Pharmacokinetics and steady-state bioequivalence of treprostinil sodium (Remodulin) administered by the intravenous and subcutaneous route to normal volunteers. *J. Cardiovasc. Pharmacol.* **44**, 209–214 (2004).
17. Ruaro, B., Sulli, A., Alessandri, E., Pizzorni, C., Ferrari, G. & Cutolo, M. Laser speckle contrast analysis: a new method to evaluate peripheral blood perfusion in systemic sclerosis patients. *Ann. Rheum. Dis.* (2013); e-pub ahead of print 16 August 2013.
18. Medsger, T.A. Jr *et al.* A disease severity scale for systemic sclerosis: development and testing. *J. Rheumatol.* **26**, 2159–2167 (1999).
19. Smith, V. *et al.* Do worsening scleroderma capillaroscopic patterns predict future severe organ involvement? a pilot study. *Ann. Rheum. Dis.* **71**, 1636–1639 (2012).
20. LeRoy, E.C. & Medsger, T.A. Jr. Criteria for the classification of early systemic sclerosis. *J. Rheumatol.* **28**, 1573–1576 (2001).
21. Roustit, M. & Cracowski, J.L. Assessment of endothelial and neurovascular function in human skin microcirculation. *Trends Pharmacol. Sci.* **34**, 373–384 (2013).
22. Cutolo, M. *et al.* Nailfold videocapillaroscopic patterns and serum autoantibodies in systemic sclerosis. *Rheumatology (Oxford)*. **43**, 719–726 (2004).

Sixième étude : Efficacité de l'iontophorèse de tréprostinil sur un biomarqueur intermédiaire, test de refroidissement cutané local (titre court: TIPPS, étude ancillaire)

Pour cette étude, nous avons mis au point un dispositif de refroidissement loco-régional de la main permettant l'enregistrement continu des variations de flux sanguin de la microcirculation cutanée par *laser speckle contrast imaging* (LSCI).

L'objectif principal de cette étude en double aveugle était d'évaluer si l'iontophorèse cutanée de tréprostinil sur la pulpe digitale de patients atteints de SSc sans ulcère digital améliorait le flux sanguin cutané pendant un test de refroidissement cutané locorégional.

Onze patients atteints de SSc cutanée limitée ont subi une iontophorèse cutanée de tréprostinil et de placebo (NaCl à 0,9%) en double aveugle, randomisée sur deux pulpes digitales. La main était ensuite insérée pendant 30 minutes dans une boîte de refroidissement à 8°C, et microcirculation sanguine cutanée était enregistrée en continu par LSCI. Le flux sanguin cutané était exprimé en conductance vasculaire cutanée (CVC).

Au cours du refroidissement local, la CVC était significativement plus élevée au site du tréprostinil par rapport au site placebo et restait plus élevée 30 minutes après la fin du test au froid.

En conclusion, chez les patients atteints de SSc, l'iontophorèse cutanée de tréprostinil augmente le flux sanguin de la pulpe digitale lors du refroidissement local de la main et pendant la phase de réchauffement initiale.

Article publié: *Treprostinil Iontophoresis Improves Digital Blood Flow during Local Cooling in Systemic Sclerosis*. F Gaillard-Bigot, M Roustit, S Blaise, C Cracowski, C Seinturier, B Imbert, P Carpentier et JL Cracowski. *Microcirculation*. 2016 Apr;23(3):266-70.

Treprostinil Iontophoresis Improves Digital Blood Flow during Local Cooling in Systemic Sclerosis

FLORENCE GAILLARD-BIGOT,^{*,†,‡} MATTHIEU ROUSTIT,^{*,†,‡} SOPHIE BLAISE,^{‡,§} CLAIRE CRACOWSKI,^{†,‡}
CHRISTOPHE SEINTURIER,[§] BERNARD IMBERT,[§] PATRICK CARPENTIER[§] AND JEAN-LUC CRACOWSKI^{*,†,‡}

*University Grenoble Alpes, Grenoble, France; †Clinical Pharmacology Unit, INSERM CIC1406, Grenoble University Hospital, Grenoble, France;
‡INSERM, U1042, HP2, Grenoble, France; §Vascular Medicine Department, Grenoble University Hospital, Grenoble, France

Address for correspondence: Jean-Luc Cracowski, M.D., Ph.D., Unité de Pharmacologie Clinique, Centre d'Investigation Clinique de Grenoble - Inserm CIC1406, CHU de Grenoble, 38043 Grenoble Cedex 09, France. E-mail: Jean-Luc.Cracowski@ujf-grenoble.fr

Received 21 October 2015; accepted 23 January 2016.

ABSTRACT

Introduction: Severe Raynaud's syndrome and DUs are the most prevalent manifestations of SSc peripheral microvascular disease. We tested whether treprostinil iontophoresis on the finger pad of patients with SSc would improve digital blood flow during hand cooling.

Methods: Eleven patients with limited cutaneous SSc underwent a double-blinded iontophoresis of treprostinil (2.56×10^{-4} M during two hours) and placebo (NaCl 0.9%) on two finger pads. Then, the hand was inserted for 30 minutes in a fenestrated cooling box at 8°C, and skin blood flow was recorded continuously using LSCL.

Results: During the local cooling, CVC was significantly higher at the treprostinil site than at the placebo site and remained higher 30 minutes after the test.

Conclusions: In patients with SSc, digital treprostinil iontophoresis shifts skin blood flow upward during local cooling of the hand and during the initial rewarming phase. Digital treprostinil iontophoresis should now be tested in larger scale studies.

KEY WORDS: systemic sclerosis, Raynaud's phenomenon, microcirculation, laser speckle contrast imaging, prostacyclin

Abbreviations used: AUC, areas under the curve; CVC, cutaneous vascular conductance; dcSSc, diffuse cutaneous SSc; DUs, digital ulcers; lcSSc, limited cutaneous SSc; LSCL, laser speckle contrast imaging; PU, perfusion unit; RP, Raynaud's phenomenon; SSc, systemic sclerosis.

Please cite this paper as: Gaillard-Bigot F, Roustit M, Blaise S, Cracowski C, Seinturier C, Imbert B, Carpentier P, Cracowski J-L. Treprostinil iontophoresis improves digital blood flow during local cooling in systemic sclerosis. *Microcirculation* 23: 266–270, 2016.

INTRODUCTION

SSc is a rare connective tissue disease characterized by microvascular disease associated with skin fibrosis and autoimmunity. RP and DUs are the most prevalent manifestations of the peripheral microvascular disease. The lifetime risk of developing DU is 43% and 51% for lcSSc and dcSSc, respectively [1]. DUs lead to distal digital amputation in 4.8% of cases [1], and are associated with increased cardiovascular morbidity [2]. They are painful and lead to impaired hand function that explains 75% of the overall functional disability [3].

Curative treatments of existing DUs remain limited, intravenous iloprost being the only approved therapy [4]. However, this requires hospitalization and has dose-limiting side effects. Oral sildenafil might be another option [5]. We are currently developing an alternative, non-invasive route for local delivery of prostacyclin analogs, such as treprostinil,

at skin sites of interest, using iontophoresis. We previously demonstrated that cathodal iontophoresis of treprostinil enabled the local delivery of the drug without systemic effects in murine models [6,7], healthy volunteers [8], patients with SSc, and diabetics [9,10].

We have developed a fenestrated air cooling box that enables measurement of skin blood flow using LSCL, while cooling locally. The aim of this double-blind study was to assess whether treprostinil iontophoresis on the finger pad of SSc patients would shift the skin blood flow toward higher values during hand cooling.

METHODS

We enrolled 11 patients with lcSSc (Table 1) fulfilling the ACR/EULAR criteria [11]. Patients taking calcium-channel blockers were instructed to stop medications one week before inclusion. Patients taking other vasodilator treatment for SSc

Table 1. Epidemiological and clinical data of the 11 patients with SSC

Age (years)	59.6 (9.1)
Female gender	11 (100%)
Disease duration (years)	9 (5)
RP	11 (100%)
Digital pitting scars	1 (9%)
Previous active DU	1 (9%)
Rodnan-modified skin score	8.4 (4.2)
Esophageal involvement	5 (45%)
Capillaroscopy pattern: early/active/late	3 (36%)/5 (46%)/2 (18%)
Autoantibodies	11 (100%)
Anticentromere	9 (81%)
Anti-topoisomerase I	2 (18%)
Anti-RNA polymerase III	0

Quantitative data are expressed as mean (SD). Qualitative data are expressed as number (percentage).

were not included. Grenoble Institutional Review Board approval was obtained in December 2012, and each subject gave written informed consent before participation. Inclusion and exclusion criteria can be found on the clinical-trial.gov web site (<http://clinicaltrials.gov/show/NCT01554540>).

Between November 2012 and February 2013, each patient underwent a simultaneous double-blinded iontophoresis of treprostinil (0.1 mg/mL, i.e., 2.56×10^{-4} M) and placebo (NaCl 0.9%) on two finger pads (using a computer-generated randomization allocation among the index, middle, and ring fingers of the right hand) in Grenoble University Hospital Clinical Research Center.

On arrival at the laboratory, subjects were placed in a temperature-controlled room ($23 \pm 11^\circ\text{C}$) and remained supine during all measurements. After 30-minute acclimatization, two cathodal iontophoresis were performed for 120 minutes using 7.2 cm^2 electrodes (Iogel; IomedInc., SaltLakeCity, UT, USA) as previously described [9]. All solutions were prepared extemporaneously by a pharmacist independent from the study. After the end of the iontophoresis, skin blood flow was continuously recorded with LSCI (PeriCam PSI System, Perimed, Järfälla, Sweden) for five minutes. Then, the right hand was inserted in a fenestrated cooling box (Perimed) at 8°C , for 30 minutes (Figure 1). Skin blood flow of the palm of the hand was recorded continuously during the cooling test, and 30 minutes after removal of the hand from the box. We also recorded skin blood flow for five minutes at 120, 180, and 240 minutes after the cooling test. The LSCI wavelength was 785 nm, and the laser head was placed 20–25 cm above the skin (with a resolution of $\sim 6.9 \text{ pixels/cm}^2$). The image size was $9 \times 9 \text{ cm}$ and the acquisition rate was 3 per second during the whole procedure. Within subject reproducibility

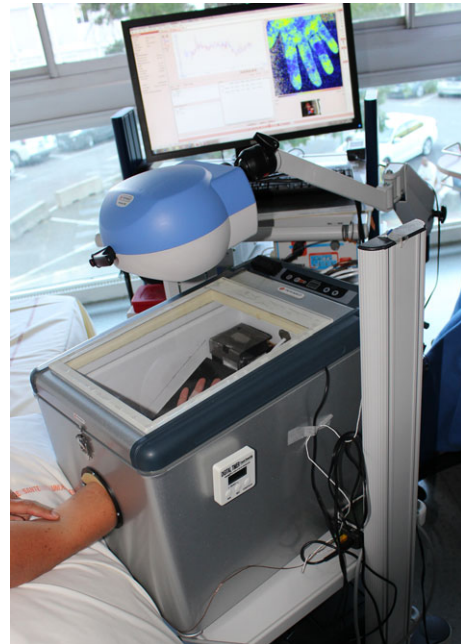


Figure 1. Protocol setup: representative experiment. After the end of the iontophoresis, the right hand was inserted in the fenestrated cooling box at 8°C , for 30 minutes. Skin blood flow was continuously recorded with LSCI through the window.

of LSCI was very good [12]. Skin blood flow was averaged at each iontophoretic site and expressed as CVC, that is, PU divided by mean arterial pressure. AUC were calculated over 30 minutes during the local cooling period (AUC_{0-30} expressed as PU/mmHg min) and over 30 minutes following local cooling (AUC_{30-60}). Data were analyzed using a two-way repeated measure ANOVA. The main assessment criterion was CVC expressed as AUC during 30 minutes (expressed as PU/mmHg min). Two-sided p values <0.05 were considered significant. Statistical analyses were performed using IBM SPSS software (Statistics for Windows, v21; IBM Corp, Amonk, NY, USA).

RESULTS

Patients' characteristics are given in Table 1. Before iontophoresis, skin blood flow was comparable between the treprostinil site and the placebo site (2.8 ± 1.7 and $2.8 \pm 1.6 \text{ PU/mmHg}$, respectively, NS). Among the 11 patients, two were taking angiotensin-converting enzyme inhibitors, seven were taking proton pump inhibitors, one was under methotrexate, and two under corticosteroids. Five patients were taking calcium-channel blockers that were stopped at the time of experimentation. No patient was under prostacyclin analog during the experimentation. Raynaud's phenomenon affected all fingers, except the thumb, in all patients, and the frequency in winter time was higher than one attack by day in all but one patient.

The two-hour iontophoresis procedure was well tolerated by all patients. After treprostnil iontophoresis, CVC was higher at the treprostnil site compared to the placebo site (1.9 ± 1.1 and 1.2 ± 0.9 PU/mmHg, respectively, $p = 0.002$). During the 30-minute local cooling, CVC was significantly higher at the treprostnil site than at the placebo site and remained higher 30 minutes after the test (Figure 2). AUC_{0-30} were 36 ± 28 and 25 ± 22 PU/mmHg min, respectively, and AUC_{30-60} were 30 ± 21 and 22 ± 15 PU/mmHg min, respectively, (ANOVA for repeated measures: $p = 0.025$ for treatment, NS for time, with no significant interaction between treatment and time). During the late part of the rewarming phase, CVC at 120, 180, and 240 minutes were not significantly different (NS for treatment, time, and their interaction). When compared to an adjacent control site (third finger), NaCl iontophoresis did not influence skin blood flow response to cold. We observed one clinical episode of RP on one finger at the end of iontophoresis at the placebo site but not at the treprostnil site.

DISCUSSION

We demonstrated that a single two-hour iontophoresis of treprostnil on the finger pad increased skin blood flow before, during, and up to 30 minutes after a local cooling test in patients with SSc.

It has been previously suggested that the delivery of vasodilators such as sodium nitroprusside through iontophoresis could be tested in peripheral microvascular manifestations of scleroderma [13]. The major issue was to find a polarized amphiphilic drug that would neither undergo skin metabolism nor rapid skin clearance, and

treprostnil seemed to be a better candidate than sodium nitroprusside. We previously showed that treprostnil was detectable in the forearm dermis up to approximately eight hours after the end of the iontophoresis while skin blood flow remained high up to four to six hours [9]. Here, using a new local cooling box enabling us to quantify skin blood flow while cooling, we demonstrated that treprostnil iontophoresis was able to shift skin blood flow upward during 30-minute local cooling and during the initial rewarming phase.

One limitation is that we used the local cooling test as a surrogate marker for peripheral vascular disease, that is, RP and DUs. In secondary RP, excessive vasoconstriction of digital arteriovenous anastomosis and digital arteries follows local finger cooling, through an amplification of α_{2C} adrenoceptor-mediated sympathetic vasoconstriction [14]. Indeed, local cooling tests have been used for early drug development in severe RP; for example, the development of ORM-12741, an α_{2C} -adrenoceptor antagonist and fasudil, a rho-kinase inhibitor, were stopped following the demonstration of the lack of effect on cold challenges [15,16]. Cold challenges were also used to test the effects of sildenafil and tadalafil in patients with RP [17,18] as well as MQX-503, a formulation of nitroglycerin, [19,20]. The advantage of our cooling box is that it allows simultaneous skin cooling and monitoring of skin blood flow using LSCI, a reliable two-dimensional imaging technique recently tested in patients with scleroderma [21]. LSCI had previously been used to evaluate the effects of therapies on skin blood flow in scleroderma [22,23].

This study remains preliminary, as for safety reasons we tested a single iontophoresis administration, and only one of the enrolled patients had recurrent digital ulcerations and another one had digital pitting scars. We plan to test repeated

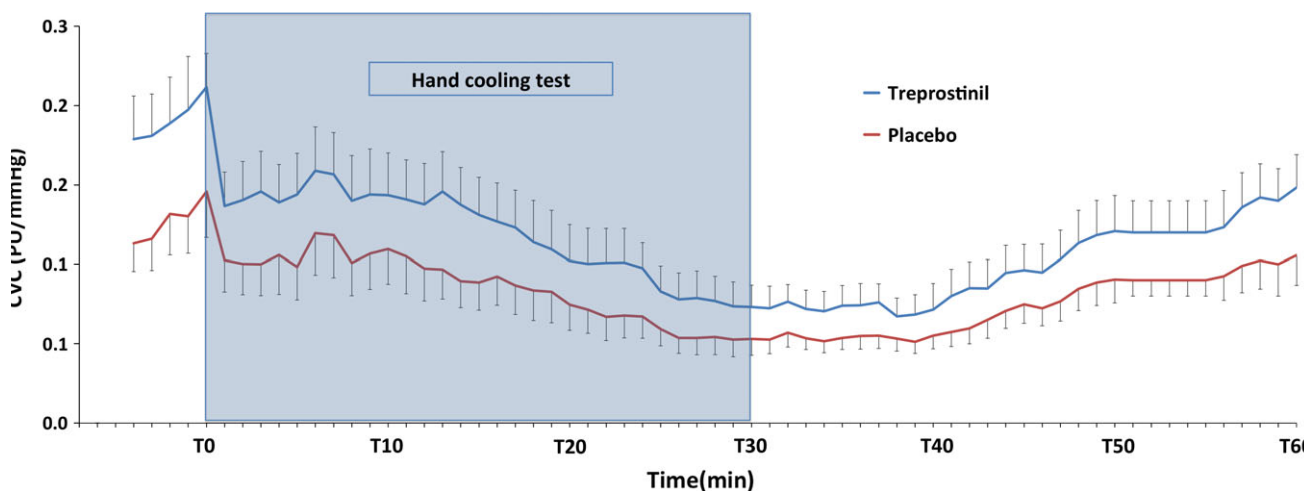


Figure 2. Effect of the iontophoresis of treprostnil and placebo on the microvascular response to hand cooling in patients with SSc. Data are expressed as CVC, recorded on finger pads.

iontophoresis in a group of patients with severe RP or active digital ulcerations.

CONCLUSIONS AND PERSPECTIVE

This study showed that digital treprostinil iontophoresis shifts skin blood flow upward during local cooling of the hand and during the initial rewarming phase in patients with SSc. Digital treprostinil iontophoresis should now be tested in larger scale studies with clinical endpoints.

ACKNOWLEDGMENTS

We warmly thank the patients' association 'Association des Sclérodermiques de France' for patient participation; and the "Délégation Régionale à la Recherche Clinique" of Grenoble

University Hospital for sponsoring. We also thank Mrs Dominique Abry and Anne Tournier for assisting with the LSCI measurements and volunteer management; and Dr Alison Foote for critically reading and editing the manuscript. This work was financially supported by the patients' association "Association des Sclérodermiques de France," the French Health Ministry, and Bioprojet.

CONFLICTS OF INTEREST

M Roustit, S Blaise and J-L Cracowski hold a patent on treprostinil iontophoresis for the treatment of skin ulcers. J-L Cracowski received an investigator driven grant from Bioprojet for this study. M Roustit and J-L Cracowski have collaborations with Bioprojet and United Therapeutics. The other authors declare no conflicts of interest.

REFERENCES

- Hachulla E, Clerson P, Launay D, Lambert M, Morell-Dubois S, Queyrel V, Hatron PY. Natural history of ischemic digital ulcers in systemic sclerosis: single-center retrospective longitudinal study. *J Rheumatol* 34: 2423–2430, 2007.
- Mihai C, Landewé R, van der Heijde D, Walker UA, Constantin PI, Gherghe AM, Ionescu R, Rednic S, Allanore Y, Avouac J, Czirják L, Hachulla E, Riemekasten G, Cozzi F, Airò P, Cutolo M, Mueller-Ladner U, Matucci-Cerinic M. Digital ulcers predict a worse disease course in patients with systemic sclerosis. *Ann Rheum Dis* 2015. pii: annrheumdis-2014-205897. [Epub ahead of print].
- Mouthon L, Mestre-Stanislas C, Bérezné A, Rannou F, Guilpain P, Revel M, Pagnoux C, Guillemin L, Fermanian J, Poiraudou S. Impact of digital ulcers on disability and health-related quality of life in systemic sclerosis. *Ann Rheum Dis* 69: 214–217, 2010.
- Kowal-Bielecka O, Landewe R, Avouac J, Chwiesko S, Miniati I, Czirjak L, Clements P, Denton C, Farge D, Fligelstone K, Földvari I, Furst DE, Müller-Ladner U, Seibold J, Silver RM, Takehara K, Toth BG, Tyndall A, Valentini G, van den Hoogen F, Wigley F, Zulian F, Matucci-Cerinic M. EULAR recommendations for the treatment of systemic sclerosis: a report from the EULAR Scleroderma Trials and Research group (EUSTAR). *Ann Rheum Dis* 68: 620–628, 2009.
- Hachulla E, Hatron P-Y, Carpentier P, Agard C, Chatelus E, Jégo P, Mouthon L, Queyrel V, Fauchais AL, Michon-Pasturel U, Jaussaud R, Mathian A, Granel B, Diot E, Farge-Bancel D, Mekinian A, Avouac J, Desmurs-Clavel H, Clerson P. Efficacy of sildenafil on ischaemic digital ulcer healing in systemic sclerosis: the placebo-controlled SEDUCE study. *Ann Rheum Dis* 2015. pii: annrheumdis-2014-207001. [Epub ahead of print].
- Blaise S, Roustit M, Millet C, Ribuot C, Boutonnat J, Cracowski JL. Cathodal iontophoresis of treprostinil and iloprost induces a sustained increase in cutaneous flux in rats. *Br J Pharmacol* 162: 557–565, 2011.
- Kotzki S, Roustit M, Arnaud C, Godin-Ribuot D, Cracowski J-L. Effect of continuous vs pulsed iontophoresis of treprostinil on skin blood flow. *Eur J Pharm Sci* 72: 21–26, 2015.
- Blaise S, Roustit M, Hellmann M, Millet C, Cracowski JL. Cathodal iontophoresis of treprostinil induces a sustained increase in cutaneous blood flux in healthy volunteers. *J Clin Pharmacol* 53: 58–66, 2013.
- Roustit M, Gaillard-Bigot F, Blaise S, Stanke-Labesque F, Cracowski C, Seinturier C, Jourdil JF, Imbert B, Carpentier PH, Cracowski JL. Cutaneous iontophoresis of treprostinil in systemic sclerosis: a proof-of-concept study. *Clin Pharmacol Ther* 95: 439–445, 2014.
- Hellmann M, Roustit M, Gaillard-Bigot F, Cracowski J-L. Cutaneous iontophoresis of treprostinil, a prostacyclin analog, increases microvascular blood flux in diabetic malleolus area. *Eur J Pharmacol* 758: 123–128, 2015.
- van den Hoogen F, Khanna D, Fransen J, Johnson SR, Baron M, Tyndall A, Matucci-Cerinic M, Naden RP, Medsger TAJr, Carreira PE, Riemekasten G, Clements PJ, Denton CP, Distler O, Allanore Y, Furst DE, Gabrielli A, Mayes MD, vanLaar JM, Seibold JR, Czirjak L, Steen VD, Inanc M, Kowal-Bielecka O, Müller-Ladner U, Valentini G, Veale DJ, Vonk MC, Walker UA, Chung L, Collier DH, Csuka ME, Fessler BJ, Guiducci S, Herrick A, Hsu VM, Jimenez S, Kahaleh B, Merkel PA, Sierakowski S, Silver RM, Simms RW, Varga J, Pope JE. 2013 classification criteria for systemic sclerosis: an American college of rheumatology/European league against rheumatism collaborative initiative. *Ann Rheum Dis* 72: 1747–1755, 2013.
- Roustit M, Millet C, Blaise S, Dufournet B, Cracowski JL. Excellent reproducibility of laser speckle contrast imaging to assess skin microvascular reactivity. *Microvasc Res* 80: 505–511, 2010.
- Little J, Murray A, Dinsdale G, Wilkinson J, Moore T, Herrick AL. Whole finger iontophoresis of sodium nitroprusside to increase blood flow in patients with systemic sclerosis: influence of concentration. *Int J Pharm* 490: 446–449, 2015.
- Flavahan NA. A vascular mechanistic approach to understanding Raynaud phenomenon. *Nat Rev Rheumatol* 11: 146–158, 2015.
- Fava A, Wung PK, Wigley FM, Hummers LK, Daya NR, Ghazarian SR, Boin F. Efficacy of rho-kinase inhibitor fasudil in secondary Raynaud's phenomenon. *Arthritis Care Res* 64: 925–929, 2012.
- Herrick A, Murray A, Ruck A, Rouru J, Moore T, Whiteside J, Hakulinen P, Wigley F, Snapir A. A double-blind placebo-controlled crossover trial of the alpha-2C adrenoceptor antagonist ORM-12741 for prevention of cold-induced vasospasm in patients with systemic sclerosis. *Arthritis Rheum* 64: S636, 2012.
- Roustit M, Hellmann M, Cracowski C, Blaise S, Cracowski JL. Sildenafil increases digital skin blood flow during all phases of

- local cooling in primary Raynaud's phenomenon. *Clin Pharmacol Ther* 91: 813–819, 2012.
18. Friedman EA, Harris PA, Wood AJ, Stein CM, Kurnik D. The effects of tadalafil on cold-induced vasoconstriction in patients with Raynaud's phenomenon. *Clin Pharmacol Ther* 81: 503–509, 2007.
19. Chung L, Shapiro L, Fiorentino D, Baron M, Shanahan J, Sule S, Hsu V, Rothfield N, Steen V, Martin RW, Smith E, Mayes M, Simms R, Pope J, Kahaleh B, Csuka ME, Gruber B, Collier D, Sweiss N, Gilbert A, Dechow FJ, Gregory J, Wigley FM. MQX-503, a novel formulation of nitroglycerin, improves the severity of Raynaud's phenomenon: a randomized, controlled trial. *Arthritis Rheum* 60: 870–877, 2009.
20. Hummers LK, Dugowson CE, Dechow FJ, Wise RA, Gregory J, Michalek J, Yenokyan G, McGready J, Wigley FM. A multi-centre, blinded, randomised, placebo-controlled, laboratory-based study of MQX-503, a novel topical gel formulation of nitroglycerine, in patients with Raynaud phenomenon. *Ann Rheum Dis* 72: 1962–1967, 2013.
21. Ruaro B, Sulli A, Alessandri E, Pizzorni C, Ferrari G, Cutolo M. Laser speckle contrast analysis: a new method to evaluate peripheral blood perfusion in systemic sclerosis patients. *Ann Rheum Dis* 73: 1181–1185, 2014.
22. Ruaro B, Sulli A, Smith V, Paolino S, Pizzorni C, Cutolo M. Short-term follow-up of digital ulcers by laser speckle contrast analysis in systemic sclerosis patients. *Microvasc Res* 101: 82–85, 2015.
23. Domsic RT, Dezfulian C, Shoushtari A, Ivanko D, Kenny E, Kwok CK, Medsger TA Jr, Champion HC. Endothelial dysfunction is present only in the microvasculature and microcirculation of early diffuse systemic sclerosis patients. *Clin Exp Rheumatol* 32: S-154–S-160, 2014.

Septième étude : Effets vasculaires de l'iontophorèse cutanée de tréprostinil sur la jambe, le doigt et le pied : escalade de doses (titre court : TIPPS, étude ancillaire)

En tant que système transdermique d'administration de médicaments, l'iontophorèse de tréprostinil fournit une voie alternative à la voie orale. Dans nos précédentes expériences, nous avons montré que le tréprostinil augmente le flux sanguin de la microcirculation cutanée, mais avec une variabilité importante.

L'objectif principal de cette étude était d'évaluer et de comparer l'effet du tréprostinil utilisé à la concentration de 1 mg/ml (2,5 mM) administré par iontophorèse cutanée sur 3 sites cutanés différents de volontaires sains : la jambe, la plante du pied et la pulpe du doigt. Notre hypothèse était qu'une concentration plus élevée conduirait à une vasodilatation plus cohérente et plus importante par rapport aux études précédemment menées et ce, sans effet secondaire grave.

Douze volontaires sains ont subi une iontophorèse cutanée de tréprostinil (2,5 mM) et de placebo (NaCl 0,9%) en double aveugle sur les 3 sites : la jambe (20 minutes à 240 μ A), la plante du pied et la pulpe du doigt (120 minutes à 240 μ A pour chacun). Le flux sanguin cutané était enregistré par *laser speckle contrast imaging* (LSCI) et exprimé en conductance vasculaire cutanée (CVC).

L'iontophorèse de tréprostinil a augmenté le flux sanguin de la microcirculation cutanée sur la jambe, le doigt et la plante du pied. Ceci a été associé à un passage systémique modéré, sans effet secondaire. En outre, nous avons observé un effet dépendant de la concentration.

En conclusion, l'iontophorèse de tréprostinil à 2,5 mM provoque une vasodilatation soutenue, sans effet secondaire et prolongée du flux sanguin de la microcirculation cutanée tant au niveau de la jambe que de la face plantaire et la pulpe digitale chez le volontaire sains. Il est possible d'envisager ce nouvel outil thérapeutique sous forme de cures intermittentes et répétées dans le traitement préventif ou curatif des ulcérations digitales chez les patients atteints de SSc ou de diabète de type 2.

Article publié : [*Vascular Effects of Treprostinil Cutaneous Iontophoresis on the Leg, Finger, and Foot*](#). F Gaillard-Bigot, M Roustit, JF Jourdil, F Stanke-Labesque, JL Cracowski. J Clin Pharmacol. 2017 Apr 7.

Vascular Effects of Treprostinil Cutaneous Iontophoresis on the Leg, Finger, and Foot

The Journal of Clinical Pharmacology
2017, 00(0) 1–6
© 2017, The American College of
Clinical Pharmacology
DOI: 10.1002/jcph.898

**Florence Gaillard-Bigot, MSc¹, Matthieu Roustit, PharmD, PhD^{1,2,3},
Jean-François Jourdil, MSc⁴, Françoise Stanke-Labesque, PharmD, PhD^{2,4},
and Jean-Luc Cracowski, MD, PhD^{1,2,3}**

Keywords

iontophoresis, prostacyclin, treprostinil, microcirculation, laser speckle contrast imaging

Transdermal drug delivery offers significant potential for noninvasive administration of therapeutic agents, but the stratum corneum is a major barrier limiting the passive transepidermal diffusion of most drugs.¹ Iontophoresis is a simple noninvasive method for transdermal drug delivery based on the transfer of charged molecules using a low-intensity electric current.^{2,3} It is capable of expanding the range of compounds that can be delivered transdermally and enhances skin delivery of drugs exhibiting a poor skin absorption profile, such as hydrophilic, charged, or high-molecular-weight molecules.^{2,4} Furthermore, this technique enables control of the amount of drug delivered without producing severe skin irritation and can be customized for a given patient.^{2,5} Skin iontophoresis of vasodilators is an alternative to oral drug administration and may decrease systemic adverse effects in diseases such as systemic sclerosis (SSc) or diabetes.^{6–8} In addition, the topical administration of vasodilators by iontophoresis has been suggested as a suitable treatment strategy for digital ulcers, as it allows elevated concentrations to be reached in the target tissue while limiting systemic toxicity.^{6,7}

Treprostinil is a prostacyclin analogue injected subcutaneously as a treatment for pulmonary hypertension. In recent experiments in animals and in humans, we have demonstrated that treprostinil could be safely administered and significantly increased skin microvascular blood flux on the finger pads of patients with SSc and in the legs of patients with diabetes.^{9–11} However, we observed high variability in the response in fingers and no response when applied to the sole of the foot. Among the parameters involved in iontophoretic transport, we previously showed that the observed pharmacological effect differed depending on the current intensity, current duration, and current

pattern.^{11–13} Another major parameter that influences iontophoretic transport is the drug concentration at the electrode.^{2,3} The first demonstration by our group of the ability of treprostinil to increase skin microvascular blood flux in healthy subjects was performed on the forearm with treprostinil at 250 μM ¹⁰; treprostinil-induced hyperemia was observed in all 20 subjects. Because of the potential risk of side effects with high concentrations, as has been observed with 2.5 mM treprostinil administered subcutaneously (severe injection-site pain, headaches, flushing, tachycardia, and hypotension),^{14–16} we had never tested undiluted treprostinil solution in cutaneous iontophoresis. Nevertheless, in all studies, cutaneous iontophoresis of treprostinil was well tolerated, with no side effects either in healthy subjects or in patients with chronic disease, in addition to low systemic exposure.^{10,11,13}

The main objective of the present study was to evaluate and compare the effect of treprostinil solution at 1 mg/mL (2.5 mM) delivered by cutaneous

¹Inserm CIC1406, Clinical Pharmacology Department, Grenoble Alps University Hospital, Grenoble, France

²Inserm HP2, Grenoble, France

³Univ. Grenoble-Alpes, Grenoble, France

⁴Laboratory of Pharmacology, Grenoble Alps University Hospital, Grenoble, France

Submitted for publication 11 December 2016; accepted 27 February 2017.

Corresponding Author:

Florence Gaillard-Bigot, MSc, Inserm CIC1406, Centre d'Investigation Clinique de Grenoble, CHU de Grenoble 38043 Grenoble Cedex 09, France

Email: florencegaillardbigot@gmail.com

Study registration: Clinicaltrials.gov (NCT01554540)

Chemical compounds studied in this article: Treprostinil (PubChem CID: 6918140) Sodium chloride (PubChem CID: 5234)

iontophoresis at 3 skin sites: on the leg, the sole of the foot, and the finger pad of healthy subjects. Our hypothesis was that the high concentration tested would lead to a more consistent and potent vasodilatation compared with previous reports, without serious side effects. The end point was skin hyperemia quantified using laser speckle contrast imaging.

Materials and Methods

Study Population

The investigation conformed to the principles outlined in the Declaration of Helsinki. The study protocol was approved by Grenoble Institutional Review Board (IRB 6705), and each subject gave written informed consent before participation. The study was registered at clinicaltrials.gov (NCT01554540).

This study enrolled 12 healthy subjects recruited from the general population through the Clinical Research Center Volunteer database. All participants were older than 18 years of age and were treated between June and August 2015.

For all subjects, noninclusion criteria included pregnancy (urine pregnancy tests were performed for women at the beginning of each visit), cigarette smoking or any allergy, or dermatological disease. None had any chronic disease or ongoing treatment except for oral contraception and acetaminophen.

Drugs

Treprostinil 1 mg/mL solution (2.5 mM, Remodulin) was supplied by Bioprojet Pharma (Paris, France). An NaCl solution was chosen as the placebo and diluent, as it has been shown to induce less nonspecific axon reflex vasodilatation than deionized water.¹⁷ All solutions were prepared extemporaneously by an independent unblinded pharmacist. The investigators and subjects were blinded to treatment.

Study Design

This was a double-blind, randomized, clinical pharmacology study. Each subject attended 3 visits, with a minimal period of 48 hours between each visit.

On arrival at the laboratory, subjects were placed in a temperature-controlled room ($23^{\circ}\text{C} \pm 1^{\circ}\text{C}$) and remained supine for the whole experiment. Blood pressure was recorded on the contralateral arm (Agilent M3, M3046A Monitor, Philips, Boeblingen, Germany) during skin blood flux measurements. Photographs of the skin were taken before starting and immediately after iontophoresis.

Treprostinil Iontophoresis Protocol

At each visit, after 30-minute acclimatization, 2 ellipsoidal skin sites (approximately 12 cm^2) were chosen and marked using a surgical pencil. Baseline skin blood

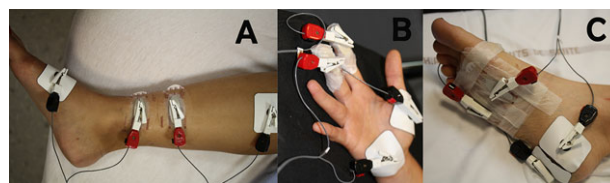


Figure 1. Experimental protocol. Iontophoresis at 40 mC/cm^2 (20 minutes at $240\ \mu\text{A}$, ie, $33\ \mu\text{A/cm}^2$) was performed on leg (A). Iontophoresis at 240 mC/cm^2 (120 minutes at $240\ \mu\text{A}$, ie, $33\ \mu\text{A/cm}^2$) was performed on finger pads (B) and on sole of foot (C).

flux was recorded during 5 minutes by laser speckle contrast imaging. Then, 2 ellipsoidal 7.2 cm^2 Ag–AgCl electrodes (Iogel, Iomed Inc., Salt Lake City, Utah) were soaked with either 1.5 mL of treprostinil or NaCl solution and blinded by an independent pharmacist (marked as “proximal” or “distal” for the leg and “medial” or “lateral” for the finger and foot). Drug-containing electrodes were connected to the cathode, whereas the anode was connected to dispersive electrodes placed 10 cm apart (Figure 1). Low-voltage, computer-driven generators were used (PF 751 Peri-Iont USB Power Supply, Perimed, Järfälla, Sweden). Voltage was continuously recorded to estimate skin resistance.

For the first visit, iontophoresis was performed on the medial and caudal side of the leg (avoiding visible veins; Figure 1A). One of the 2 sites was randomly selected as the treprostinil site and the other one as the placebo site. Iontophoresis at 40 mC/cm^2 (20 minutes at $240\ \mu\text{A}$, ie, $33\ \mu\text{A/cm}^2$) was then performed simultaneously at both sites, as previously tested on the leg.¹³

At the second visit, iontophoresis was performed on the finger pads of 2 fingers randomly chosen between the index and the middle (Figure 1B). Iontophoresis at 240 mC/cm^2 (120 minutes at $240\ \mu\text{A}$, ie, $33\ \mu\text{A/cm}^2$) was then performed simultaneously at both sites, as previously described.¹¹ At the third visit the procedure was repeated, but on the sole of one foot (Figure 1C).

Skin Microvascular Blood Flux Measurements

Before recording, the site of interest was immobilized with a vacuum cushion to avoid movement artifacts. Cutaneous blood flux was measured by laser speckle contrast imaging (LSCI; PeriCam PSI System, Perimed, Järfälla, Sweden).¹⁸ The LSCI wavelength was 785 nm, and the laser head was placed 20 to 25 cm above the skin (with a resolution of ≈ 6.9 pixels/cm). The image size was approximately $12 \times 12\text{ cm}$, and the acquisition rate was 1 s^{-1} . For the leg, microvascular blood flux was measured for 5 minutes before, immediately after the end of iontophoresis, and 15 minutes, 30 minutes, 1 hour, 2 hours, 3 hours, and 4 hours after the end of iontophoresis. For the finger pad and the sole of the foot, microvascular blood flux was measured

for 5 minutes before, immediately after the end of iontophoresis, and 15 minutes, 30 minutes, 1 hour, 1 hour, 30 minutes, 2 hours, 2 hours, 30 minutes, and 3 hours after the end of iontophoresis. The protocol differed given that the response was expected to last less time compared with the leg.

Plasma Concentration of Treprostinil Following Iontophoresis

Venous blood samples were collected from a catheter inserted in the forearm. For the leg, samples were collected immediately after the end of iontophoresis and 15 minutes, 30 minutes, 1 hour, 2 hours, 3 hours, and 4 hours after the end of iontophoresis. For the finger pad and the sole of the foot, samples were collected 1 hour before the end of iontophoresis, immediately after the end of iontophoresis, and 30 minutes, 1 hours, 1 hours, 30 minutes, 2 hours, 2 hours, 30 minutes, and 3 hours after the end of iontophoresis. The protocol was chosen to match the pharmacodynamic pattern. Treprostinil concentrations were measured by liquid chromatography–tandem mass spectrometry as previously described.¹¹

Data Analysis

Data were analyzed with signal processing software (PIMSoft 1.1.1; Perimed, Järfälla, Sweden). Skin blood flux was expressed as cutaneous vascular conductance (CVC), which is the flux in arbitrary perfusion units divided by the mean arterial pressure in mm Hg.¹⁹ We then calculated the percentage change from baseline flux (%BL) and the area under the curve for 4 hours (AUC_{0-4h} , expressed as %BL·min) for the leg site, and the area under the curve for 3 hours (AUC_{0-3h} , expressed as %BL·min) after the end of iontophoresis for both the finger and foot sites. The 2-dimensional treprostinil diffusion was calculated at the peak of the hyperemia on LSCI and expressed as square millimeters. Each image was transferred to ImageJ 1.44 (NIH software, in the public domain), and the mean value of the control area was used as a cutoff.

Statistical Analysis

A sample size of 12 in each group was estimated to have 80% power to detect a probability of 0.85 that an observation in the treprostinil site was superior to placebo using a Wilcoxon signed-rank test with a 2-sided significance level of .05 (nQuery Advisor 7.0; Statistical Solutions Ltd., Cork, Ireland).

Continuous data are reported as mean and standard deviation and categorical data as number and percentage. Skin blood flux after treprostinil and placebo iontophoresis, simultaneously recorded in the same subject, were compared using a Wilcoxon signed-rank test. We considered $P \leq .05$ as significant. The AUC of

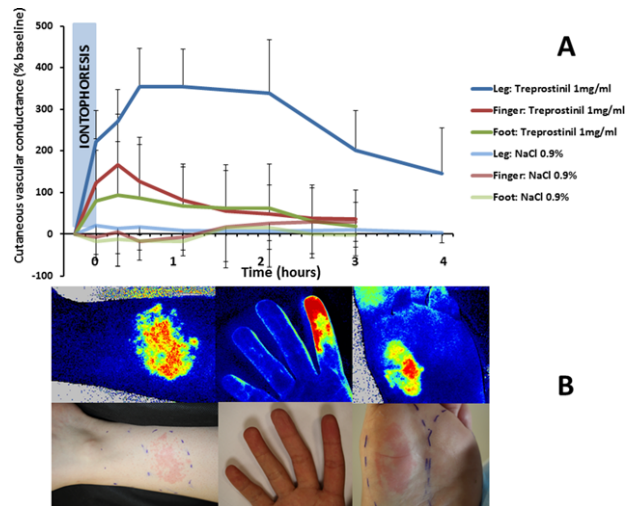


Figure 2. Effect of 2.5 mM treprostinil iontophoresis in the leg, finger, and sole of the foot, on cutaneous vascular conductance (CVC) expressed as a percentage of baseline, mean and SD (A), and on cutaneous perfusion (B). Pictures recorded with LSCI and photos taken at the same time, 1 hour after the end of iontophoresis for the leg and 15 minutes after the end for the finger pads and the sole of the foot (B). For cutaneous perfusion, colors range from dark blue (no perfusion) to red (high perfusion).

treprostinil at each site was compared using Friedman's analysis of variance (ANOVA). Response to treatment was as previously defined: a 25% increase or more in skin blood flow between treprostinil and placebo.¹¹ Statistical analyses were performed using IBM SPSS Statistics version 21.

Results

Study Population

Twelve healthy volunteers (4 men and 8 women) were enrolled in this study. Their mean age was 23.5 ± 1.8 years, and their BMI was 21.0 ± 1.1 kg/m². Systolic and diastolic arterial blood pressure was 107 ± 10 and 69 ± 9 mm Hg, respectively. Heart rate was 64 ± 8 bpm. Four women were on oral contraception.

Effect of Cathodal Iontophoresis of Treprostinil on Skin Blood Flux in the Leg, Sole of the Foot, and Finger Pad

On the leg, 2.5 mM treprostinil induced a significant increase in CVC compared with NaCl (AUC_{0-4h} was $48\,097 \pm 17\,446$ vs 1583 ± 3132 %BL·min, respectively; $P = .002$). The peak flux was obtained 1 hour after the end of treprostinil iontophoresis, and flux remained above baseline up to 4 hours after the end of iontophoresis (Figure 2). Treprostinil induced hyperemia over an area of 1214 ± 231 mm². Skin resistance did not differ between the 2 skin sites.

On the sole of the foot and finger pad, 2.5 mM treprostinil induced a similar significant increase in CVC compared with NaCl (AUC_{0-3h} was

10 882 ± 13 805 vs -404 ± 9023 %BL·min, for the foot, $P = .0006$, whereas AUC_{0-3h} was 13 442 ± 14 193 vs 1994 ± 9377 %BL·min, for the finger, $P = .002$). For both sites, the peak flux was obtained approximately 15 minutes after the end of treprostiniol iontophoresis, and the flux remained higher than baseline up to 2 hours after the end of iontophoresis (Figure 2). Treprostiniol induced hyperemia over an area of 482 ± 383 mm² for the sole of the foot and 1029 ± 467 mm² for the finger pad. Skin resistance did not differ between the 2 skin sites.

When we compared the effect across sites, the hyperemia was more pronounced on the leg compared with the foot and finger despite a shorter iontophoresis protocol (Friedman's ANOVA, $P = .001$). Whereas treprostiniol-induced hyperemia was observed in all subjects on the leg and the finger, the hyperemia was less consistent on the foot (Figure 3).

Plasma Concentration of Treprostiniol

The treprostiniol plasma concentration was below the quantification threshold of 3.6 pg/mL in 9 of 12 volunteers. We observed low systemic diffusion in 3 samples from 3 different subjects, with a maximal peak of 23.8 pg/mL measured immediately after the end of 2 hours of iontophoresis to the foot; the other peaks were 15 minutes after the end of iontophoresis to the leg and 120 minutes after the end of 2 hours of iontophoresis to the sole.

Concentration Response: Comparison With Previous Studies

To determine whether the effect of 2.5 mM treprostiniol iontophoresis was superior to the 250 μM solution used in previous studies, we compared the AUC of treprostiniol minus placebo between studies.

For the leg, we observed a greater effect with 2.5 mM (Table 1) compared with 250 μM with similar kinetics, with the peak flux obtained approximately 1 hour after the end of the iontophoresis. However, in terms of the area effected, the effect did not reach statistical significance. For the sole of the foot, we observed a greater effect with 2.5 mM compared with 250 μM (Table 1). For the finger, we observed a similar effect in terms of amplitude with 2.5 mM and 250 μM treprostiniol, with similar kinetics, the peak flux being obtained approximately 15 minutes after the end of iontophoresis. However, vasodilation was observed in all our subjects compared with only 8 of 12 in the study by Roustit et al¹¹ and was more diffuse in terms of area.

Skin and Systemic Tolerance of the Iontophoresis of Treprostiniol

No serious side effect occurred. We observed no significant change in mean arterial pressure after the

iontophoresis of treprostiniol. As expected, skin erythema localized to the probe area was observed after removal of the heating probe (Figure 2B), exhibiting a patchy pattern on the leg and a uniform pattern on the finger and foot (Figure 2B), which disappeared in a few hours.

Discussion

In this study, cathodal iontophoresis of 2.5 mM treprostiniol increased skin blood flow in the leg, finger, and sole of the foot. This was associated with a mild systemic diffusion in a few subjects without side effects.

On the leg, the peak flux was obtained 1 hour after the end of treprostiniol iontophoresis, and flux remained above baseline up to 4 hours after the end of iontophoresis. The duration of the effect was shorter on the fingers and feet, the peak flux being obtained 15 minutes after the end of treprostiniol iontophoresis, with the flux remaining above baseline for up to 2 hours. The time course of the pharmacodynamic effect was consistent with our previous studies.^{11,13}

Since the first investigation for therapeutic purposes by Leduc in 1908, iontophoresis has been widely explored as a means to deliver drugs, and many experimental models have been generated.^{2,4,20-22} Iontophoresis enhances drug delivery through the skin by electrorepulsion and electroosmosis and, in a minor way, by passive flux.²²⁻²⁶ Given that treprostiniol is negatively charged at cutaneous pH, a cathode-to-anode current direction was used for iontophoresis, and therefore electroosmosis did not participate in treprostiniol transport through the skin. Therefore, factors influencing treprostiniol transcutaneous iontophoresis can be divided into 3 separate categories: electric current properties, physicochemical properties of the compound, and the structure of the skin barrier. When the current intensity is stronger, more ions penetrate at one time.²⁷ In addition, the use of high voltage during iontophoresis facilitates the transport of drugs by a mechanism of pore formation, which decreases the skin's resistance.²⁸⁻³⁰ However, elevated currents cause irritation and skin damage,^{3,4} which is the reason why we chose low-intensity currents that are nearly undetectable and painless.

Among the physicochemical properties, drug concentration is the most important parameter. Increased uptake by the skin during iontophoresis is theoretically expected to be associated with high drug concentrations.³¹ When comparing our data with previous results by our group, we observed a concentration-response effect in the form of a higher maximal effect on the leg and foot. On the digits, the efficacy was similar, but the effect was more diffuse and more consistent, that is, all subjects exhibited vasodilatation

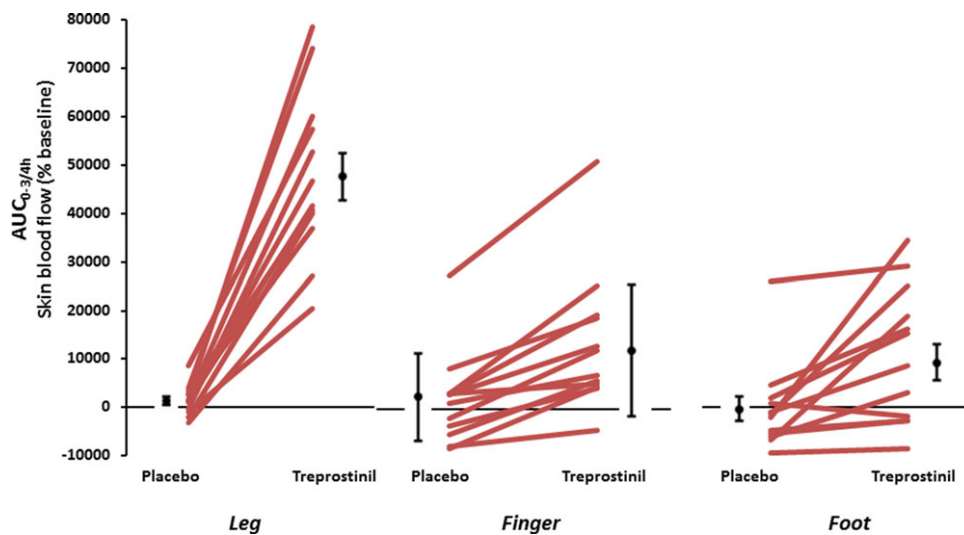


Figure 3. Skin blood flow expressed as area under the curve (AUC) of cutaneous vascular conductance after iontophoresis of treprostinil and placebo in 12 healthy subjects. Black dots and bars represent mean (SD) area under the curve of CVC.

Table I. Comparison of the Concentration Response in Different Skin Areas of the Body

	Iontophoresis Protocol	Amplitude of Increase in Skin Blood Flow (%BL·min)		Hyperemia Area (mm ²)	
Treprostinil concentration		250 μ M	2.5 mM	250 μ M	2.5 mM
Leg	20 minutes at 240 μ A	AUC _{0-4h} 31 161 \pm 20 346 %BL·min	AUC _{0-4h} 46 514 \pm 15 949 ^a %BL·min	1033 \pm 407	1214 \pm 231
Sole of the foot	120 minutes at 240 μ A	No effect	AUC _{0-3h} 11 286 \pm 9136 ^b %BL·min	No effect	482 \pm 383
Finger pad	120 minutes at 240 μ A	AUC _{0-3h} 10 333 \pm 11 198 %BL·min	AUC _{0-3h} 11 448 \pm 6604 %BL·min	215 \pm 164	1029 \pm 467 ^b

The amplitude of the increase in skin blood flow was calculated as treprostinil AUC minus placebo AUC.

^a $P < .001$ and ^b $P < .001$ versus 250 μ M. Data for treprostinil 250 μ M were calculated from references 11 and 13.

with 2.5 mM treprostinil compared with only 66% with 250 μ M.

A greater and more consistent effect was obviously observed on the leg compared with that in the digits and feet that was related to regional differences in skin structure and thickness. Indeed, the thickness of the stratum corneum was approximately 10 to 50 μ m in most areas of the body, whereas it could reach several hundred micrometers (300–400 μ m) on the palms and the soles.^{32–34} In addition, transfollicular and transappendageal (skin pores) routes constituted the major pathways for ionized molecules. Therefore, treprostinil which is an anion, is likely to be transported through hair follicles and sweat ducts. The presence of hair follicles on the leg but not on the palms of the hands and the soles of the feet may be a factor explaining the weaker effect.^{35–37} Finally, the density of microvessels in the dermis, which is higher in the digits and the soles of the feet than on the legs, might explain

an increased skin clearance of treprostinil at these sites.

In conclusion, cathodal iontophoresis of 2.5 mM treprostinil induced a sustained, safe and consistent increase in skin blood flow in the leg, finger, and sole of the foot. Repeated intermittent treprostinil iontophoresis should now be tested as a preventive or curative treatment in patients with scleroderma or diabetes exhibiting digital, leg, or foot skin ulcerations.

Acknowledgments

Pharma supplied treprostinil. We thank Alison Foote for critically reading and editing the manuscript and Lucie Ulmer and Cecile Girard for help with technical measurements.

Funding

This study was funded by grants from the SATT Linksum Grenoble Alpes and the French Ministry of Health.

References

1. Tyle P. Iontophoretic devices for drug delivery. *Pharm Res.* 1986;3(6):318–326.
2. Kalia YN, Naik A, Garrison J, Guy RH. Iontophoretic drug delivery. *Adv Drug Deliv Rev.* 2004;56(5):619–658.
3. Roustit M, Blaise S, Cracowski J-L. Trials and tribulations of skin iontophoresis in therapeutics. *Br J Clin Pharmacol.* 2014;77(1):63–71.
4. Dixit N, Bali V, Baboota S, Ahuja A, Ali J. Iontophoresis — an approach for controlled drug delivery: a review. *Curr Drug Deliv.* 2007;4(1):1–10.
5. Wang Y, Thakur R, Fan Q, Michniak B. Transdermal iontophoresis: combination strategies to improve transdermal iontophoretic drug delivery. *Eur J Pharm Biopharm.* 2005;60(2):179–191.
6. Murray AK, Moore TL, King TA, Herrick AL. Vasodilator iontophoresis—a possible new therapy for digital ischaemia in systemic sclerosis? *Rheumatology.* 2008;47(1):76–79.
7. Murray AK, Herrick AL, Gorodkin RE, Moore TL, King TA. Possible therapeutic use of vasodilator iontophoresis. *Microvasc Res.* 2005;69(1–2):89–94.
8. Henricson J, Nilsson A, Tesselaar E, Nilsson G, Sjöberg F. Tissue viability imaging: Microvascular response to vasoactive drugs induced by iontophoresis. *Microvasc Res.* 2009;78(2):199–205.
9. Blaise S, Roustit M, Millet C, Ribuot C, Boutonnat J, Cracowski JL. Cathodal iontophoresis of treprostinil and iloprost induces a sustained increase in cutaneous flux in rats. *Br J Pharmacol.* 2011;162(3):557–565.
10. Blaise S, Roustit M, Hellmann M, Millet C, Cracowski J-L. Cathodal iontophoresis of treprostinil induces a sustained increase in cutaneous blood flux in healthy volunteers. *J Clin Pharmacol.* 2013;53(1):58–66.
11. Roustit M, Gaillard-Bigot F, Blaise S, et al. Cutaneous iontophoresis of treprostinil in systemic sclerosis: a proof-of-concept study. *Clin Pharmacol Ther.* 2014;95(4):439–445.
12. Kotzki S, Roustit M, Arnaud C, Godin-Ribuot D, Cracowski J-L. Effect of continuous vs pulsed iontophoresis of treprostinil on skin blood flow. *Eur J Pharm Sci.* 2015;72:21–26.
13. Hellmann M, Roustit M, Gaillard-Bigot F, Cracowski J-L. Cutaneous iontophoresis of treprostinil, a prostacyclin analog, increases microvascular blood flux in diabetic malleolus area. *Eur J Pharmacol.* 2015;758:123–128.
14. Chung L, Fiorentino D. A pilot trial of treprostinil for the treatment and prevention of digital ulcers in patients with systemic sclerosis. *J Am Acad Dermatol.* 2006;54(5):880–882.
15. Shah AA, Schiopu E, Hummers LK, et al. Open label study of escalating doses of oral treprostinil diethanolamine in patients with systemic sclerosis and digital ischemia: pharmacokinetics and correlation with digital perfusion. *Arthritis Res Ther.* 2013;15(2):R54.
16. Benza RL, Tapson VF, Gomberg-Maitland M, Poms A, Barst RJ, McLaughlin VV. One-year experience with intravenous treprostinil for pulmonary arterial hypertension. *J Heart Lung Transplant.* 2013;32(9):889–896.
17. Roustit M, Cracowski JL. Non-invasive assessment of skin microvascular function in humans: an insight into methods. *Microcirculation.* 2012;19(1):47–64.
18. Roustit M, Millet C, Blaise S, Dufournet B, Cracowski JL. Excellent reproducibility of laser speckle contrast imaging to assess skin microvascular reactivity. *Microvasc Res.* 2010;80(3):505–511.
19. Roustit M, Cracowski J-L. Assessment of endothelial and neurovascular function in human skin microcirculation. *Trends Pharmacol Sci.* 2013;34(7):373–384.
20. Kanikkannan N. Iontophoresis-based transdermal delivery systems. *Biodrugs Clin Immunother Biopharm Gene Ther.* 2002;16(5):339–347.
21. Curdy C, Kalia YN, Guy RH. Non-invasive assessment of the effects of iontophoresis on human skin in-vivo. *J Pharm Pharmacol.* 2001;53(6):769–777.
22. Guy RH, Kalia YN, Delgado-Charro MB, Merino V, López A, Marro D. Iontophoresis: electrorepulsion and electroosmosis. *J Control Release.* 2000;64(1-3):129–132.
23. Gratieri T, Kalia YN. Mathematical models to describe iontophoretic transport in vitro and in vivo and the effect of current application on the skin barrier. *Adv Drug Deliv Rev.* 2013;65(2):315–329.
24. Kim A, Green PG, Rao G, Guy RH. Convective solvent flow across the skin during iontophoresis. *Pharm Res.* 1993;10(9):1315–1320.
25. Burnette RR, Ongpipattanakul B. Characterization of the pore transport properties and tissue alteration of excised human skin during iontophoresis. *J Pharm Sci.* 1988;77(2):132–137.
26. Burnette RR, Ongpipattanakul B. Characterization of the permselective properties of excised human skin during iontophoresis. *J Pharm Sci.* 1987;76(10):765–773.
27. Rapperport AS, Larson DL, Henges DF, Lynch JB, Blocker TG, Lewis RS. Iontophoresis. A method of antibiotic administration in the burn patient. *Plast Reconstr Surg.* 1965;36(5):547–552.
28. Inada H, Ghanem AH, Higuchi WI. Studies on the effects of applied voltage and duration on human epidermal membrane alteration/recovery and the resultant effects upon iontophoresis. *Pharm Res.* 1994;11(5):687–697.
29. Sims SM, Higuchi WI, Srinivasan V. Skin alteration and convective solvent flow effects during iontophoresis. II. Monovalent anion and cation transport across human skin. *Pharm Res.* 1992;9(11):1402–1409.
30. Glaser RW, Leikin SL, Chernomordik LV, Pastushenko VF, Sokirko AI. Reversible electrical breakdown of lipid bilayers: formation and evolution of pores. *Biochim Biophys Acta.* 1988;940(2):275–287.
31. O'malley EP, Oester YT. Influence of some physical chemical factors on iontophoresis using radio-isotopes. *Arch Phys Med Rehabil.* 1955;36(5):310–316.
32. Singh S, Singh J. Transdermal drug delivery by passive diffusion and iontophoresis: a review. *Med Res Rev.* 1993;13(5):569–621.
33. Holbrook KA, Odland GF. Regional differences in the thickness (cell layers) of the human stratum corneum: an ultrastructural analysis. *J Invest Dermatol.* 1974;62(4):415–422.
34. Fernandez-Flores A. Regional variations in the histology of the skin. *Am J Dermatopathol.* 2015;37(10):737–754.
35. Singh P, Anliker M, Maibach HI. Facilitated drug delivery during transdermal iontophoresis. *Curr Probl Dermatol.* 1995;22:184–188.
36. Turner NG, Guy RH. Iontophoretic transport pathways: dependence on penetrant physicochemical properties. *J Pharm Sci.* 1997;86(12):1385–1389.
37. Turner NG, Guy RH. Visualization and quantitation of iontophoretic pathways using confocal microscopy. *J Invest Dermatol Symp Proc.* 1998;3(2):136–142.

Huitième étude : Effet vasculaires de l'iontophorèse cutanée de tréprostinil chez le diabétique (titre court : TIPPS, étude ancillaire)

Les ulcères de pied sont l'une des complications les plus fréquentes et graves du diabète de type 2. Peu de médicaments sont efficaces pour améliorer la cicatrisation des ulcères de la microcirculation cutanée.

L'objectif principal de cette étude était de déterminer si l'iontophorèse de tréprostinil augmentait le flux sanguin microvasculaire cutané dans la région supra-malléolaire de volontaires sains et de patients diabétiques.

Douze sujets sains et 12 patients atteints de diabète de type 2 ont subi une iontophorèse de tréprostinil à 250 mM et de placebo (NaCl 0,9%) sur la face antérieure de jambe. Le flux sanguin cutané était enregistré par *laser speckle contrast imaging* (LSCI) et exprimé en conductance vasculaire cutanée (CVC).

Chez les volontaires sains et les patients diabétiques, l'iontophorèse de tréprostinil à 250 mM a induit une augmentation significative du flux sanguin de la microcirculation cutanée par rapport au placebo. Dans les deux groupes, le flux maximal était obtenu entre 30 minutes et 1 heure après la fin de l'iontophorèse et le flux est resté plus élevé par rapport au contrôle jusqu'à 6 heures après la fin de l'iontophorèse. Aucun effet secondaire important n'est survenu.

En conclusion, l'iontophorèse de tréprostinil à 250 mM augmente le flux sanguin de la microcirculation cutanée dans la zone supra-malléolaire de volontaires sains et de patients diabétiques, sans induire d'effet secondaire systémique ou local.

Article publié: [*Cutaneous iontophoresis of treprostinil, a prostacyclin analog, increases microvascular blood flux in diabetic malleolus area.*](#) M Hellmann, M Roustit, F Gaillard-Bigot et JL Cracowski.

Eur J Pharmacol. 2015 Jul 5;758:123-8.



Endocrine pharmacology

Cutaneous iontophoresis of treprostinil, a prostacyclin analog, increases microvascular blood flux in diabetic malleolus area



Marcin Hellmann^{a,b}, Matthieu Roustit^{a,c,d}, Florence Gaillard-Bigot^a,
Jean-Luc Cracowski^{a,c,d,*}

^a Inserm CIC1406, Clinical Pharmacology Department, University Hospital, Grenoble, France

^b Noninvasive Cardiac Diagnostics Department, Medical University, Gdansk, Poland

^c Inserm HP2, Grenoble, France

^d Univ. Grenoble-Alpes, HP2, Grenoble, France

ARTICLE INFO

Article history:

Received 11 December 2014

Received in revised form

19 March 2015

Accepted 25 March 2015

Available online 3 April 2015

Keywords:

Iontophoresis

Prostacyclin

Treprostinil

Microcirculation

Laser speckle contrast imaging

Diabetic foot ulcers

Chemical compounds studied in this article:

Treprostinil (PubChem CID: 6918140)

Sodium chloride (PubChem CID: 5234)

ABSTRACT

Diabetic foot ulcers are one of the most common and serious complications of diabetes mellitus. Few drugs are effective in enhancing the healing of microvascular skin ulcers. The main objective of the present study was to determine whether iontophoresis of treprostinil, a prostacyclin analog, increases skin microvascular blood flux in the malleolus area of healthy subjects and diabetic patients. We recruited 12 healthy subjects and 12 type 2 diabetic patients. Cathodal iontophoresis (40 mC/cm²) of treprostinil 250 μM and NaCl 0.9% was performed in the malleolus area. Skin hyperemia was quantified using non-invasive laser speckle contrast imaging, and expressed as the area under the curve (AUC) of cutaneous vascular conductance (CVC). In healthy controls and diabetic patients, treprostinil 250 μM induced a significant increase in CVC compared with NaCl (for diabetic patients, AUC_{0–6 h} was 19970 ± 8697; versus 2893 ± 5481%BL.min, respectively; *P* = 0.002). In both groups, the peak flux was obtained between 30 min and 1 h after the end of treprostinil iontophoresis and flux remained higher than baseline up to 6 h after ending of iontophoresis. No significant side-effect occurred. Cutaneous iontophoresis of 250 μM treprostinil increases microvascular blood flux in the malleolus area in healthy volunteers and diabetic patients, without inducing systemic or local side-effects. Treprostinil cathodal iontophoresis should be further investigated as a new local therapy for diabetic ulcers.

© 2015 Elsevier B.V. All rights reserved.

1. Introduction

Diabetes mellitus is a worldwide public health problem with serious complications, such as impaired wound healing. In addition, diabetic foot ulcers are associated with pain and functional disability and can become infected resulting in gangrene, osteomyelitis and amputation. Tissue ischemia is the major cause for non-healing ulcers. Indeed, the microcirculation, by providing tissue perfusion and delivery of oxygen and nutrients, plays a pivotal role in wound healing (Baltzis et al., 2014). Microvascular dysfunction is characteristic of the pathophysiology of diabetes mellitus, with specific features such as decreased endothelium-dependent vasodilation (Veves et al., 1998) and abnormal neurovascular microcirculatory response (Caselli et al., 2003).

Besides etiologic treatment, the local therapy of skin ulcers mainly relies on debridement of the wound and dressings. Esse-

ntial complementary measures in diabetic patients include pressure off-loading and infection control. Despite these treatments, complications are frequent and stress the need for new treatments (Baltzis et al., 2014). Few drugs are effective in enhancing the healing of microvascular skin ulcers. Intravenous prostacyclin analogs have been tested, among which iloprost is indicated in critical ischemia. It has been also tested as a treatment of diabetic foot ulcers, but data are still too scarce to conclude about its potential efficacy (O'Meara et al., 2001). However, the systemic administration of prostacyclin analogs has frequent serious vasodilatation-induced side effects (e.g. severe headaches, flushing, tachycardia and hypotension). In addition, the paradox is that impaired microvasculature may prevent a systematically administered drug from reaching the wound area. In order to get around these disadvantages, another prostacyclin analog, pimilprost, has been topically applied and promotes wound healing in diabetic mice (Yamamoto et al., 1996).

Treprostinil is a prostacyclin analog, developed for subcutaneous administration in treating pulmonary hypertension. It has high affinity for the prostanoid DP₁, EP₂ and IP receptors (Whittle et al., 2012). Activation of prostanoid IP, DP₁ and EP₂ receptors can

* Corresponding author at : Inserm CIC1406, Centre d'Investigation Clinique de Grenoble, CHU de Grenoble, 38043 Grenoble Cedex 09, France.
Tel.: +33 4 76 76 92 60; fax: +33 4 76 76 92 62.

E-mail address: Jean-Luc.Cracowski@ujf-grenoble.fr (J.-L. Cracowski).

all result in vasodilatation. In contrast, iloprost has high binding affinity for prostanoid EP₁ and IP receptors, and to a lesser extent EP₃ agonism (Woodward et al., 2011; Whittle et al., 2012). It should be noted that activation of EP₁ receptors can provoke vasoconstriction, and hence may offset the IP-receptor mediated vasodilator effects of iloprost. Treprostinil may therefore differ from iloprost in its overall beneficial vasodilatation profile (Whittle et al., 2012).

Iontophoresis is a non-invasive method for transdermal drug delivery based on the transfer of charged molecules using a low-intensity electric current (Roustit et al., 2014a). It presents several advantages compared to usual passive transdermal administration, such as a faster release of the drug into the skin, the capacity to deliver macromolecules and a better control of the delivered dose (Kalia et al., 2004).

We previously showed that 20 min cathodal iontophoresis of treprostinil induced a sustained vasodilation and was well tolerated in rats (Blaise et al., 2011) and on the forearm of healthy subjects (Blaise et al., 2013). Moreover, we have recently demonstrated that on the forearm treprostinil iontophoresis provides elevated concentration into the dermis, while it was not detectable in the plasma (Roustit et al., 2014b). However, iontophoresis of treprostinil has never been performed on the leg. As diabetic foot ulcers are the primary cause of microvascular ulcers, there is crucial need for data on the lower limb, especially in diabetic patients.

The main objective of the present study was to determine whether treprostinil iontophoresis increases skin microvascular blood flux in the malleolus area of healthy subjects and diabetic patients. Treprostinil skin hyperemia was quantified using non-invasive laser speckle contrast imaging. We also assessed the safety of the procedure.

2. Materials and methods

2.1. Study population

This study enrolled healthy subjects and patients with type 2 diabetes recruited from the general population through newspaper advertisements or through the Clinical Research Center Volunteer database. All the participants were over 18 years of age and were included between October 2013 and November 2014.

For all subjects, non-inclusion criteria included pregnancy (urine pregnancy tests were performed for women under 50 at the beginning of each visit), cigarette smoking or any allergies or dermatologic disease of the lower-limb. None of the healthy subjects had any chronic disease or ongoing treatment (except oral contraception for women). For patients, the presence of active diabetic foot ulcers was a non-inclusion criterion.

The investigation conforms to the principles outlined in the Declaration of Helsinki. Grenoble Institutional Review Board (IRB no. 6705) approval was obtained in November 2011, and each subject gave written informed consent before participation. The study was registered at clinicaltrials.gov (NCT01554540).

2.2. Drugs

Treprostinil 1 mg/ml solution (Remodulin[®]) was supplied by Bioprojet Pharma (Paris, France). The commercially available solution was diluted with isotonic sodium chloride (NaCl 0.9%, Aguettant, Lyon, France) to obtain a 0.1 mg/ml (250 μM) solution, which was previously shown to induce sustained vasodilation on the forearm of healthy participants (Blaise et al., 2013). NaCl solution was chosen as placebo and diluent as it has been shown to induce less non-specific axon reflex vasodilation than deionized water (Roustit and Cracowski, 2012). Moreover, we previously showed that iontophoresis of the buffer of the commercially-available solution of treprostinil does modify skin blood flux in animals (Blaise et al., 2011). All solutions were prepared extemporaneously by a pharmacist independent from the study and used double-blinded.

2.3. Study design

This was a double-blind randomized pharmacology study enrolling 12 healthy subjects and twelve type 2 diabetic patients.

Upon arrival at the laboratory, subjects were placed in a temperature-controlled room (23 ± 1 °C). They remained supine for the whole experiment. Blood pressure was recorded on the contralateral arm (Agilent M3, M3046A Monitor, Philips, Boeblingen, Germany) during skin blood flux measurements. Photographs of the skin were taken before the start of iontophoresis and immediately after iontophoresis. The presence of peripheral diabetic neuropathy was tested using Semmes–Weinstein monofilament testing.

2.3.1. Treprostinil iontophoresis protocol

After 30-min acclimatization, two ellipsoidal skin sites (approximately 12 cm²) were chosen and marked using a surgical pencil on the ventral side of the right malleolus area, avoiding visible veins (Fig. 1A). Baseline skin blood flux was recorded during 5 min with laser speckle contrast imaging. Then, two ellipsoid 7.2 cm² Ag–AgCl electrodes (logel, lomed Inc., Salt Lake City, UT, USA) were soaked with either 1.5 ml of treprostinil or NaCl solution (marked as “A” or “B” such that their use was double-blinded). Electrodes



Fig. 1. Experimental setup. (A) Two ellipsoidal skin sites were chosen and marked on the ventral side of the right malleolus area. Microvascular blood flux was recorded using laser speckle contrast imaging. (B) Two iontophoresis electrodes connected to power supplies were placed on the right malleolus area according to the randomization assignment and 40 mC/cm² cathodal iontophoresis of treprostinil and placebo were performed. (C) Cutaneous perfusion recorded with LSCI at 1 h after treprostinil iontophoresis in a diabetic patient. Colors range from dark blue (no perfusion) to yellow and red (high perfusion). (For interpretation of the references to color in this figure legend, the reader is referred to the web version of this article.)

were then placed on the ventral side of the right malleolus area according to a computer randomization plan (Fig. 1B). Electrodes were connected to the cathode, while the anode was connected to dispersive electrodes fixed at a distance of 10 cm. Low-voltage, computer-driven generators were used (PF 751 Perilont USB Power Supply, Perimed, Järfälla, Sweden). Iontophoresis at 40 mC/cm² (20 min at 240 μ A, i.e. 0.033 mA/cm²) was then performed simultaneously at both sites. Voltage was continuously recorded to estimate skin resistance (PF 751 Perilont USB Power Supply, Perimed, Järfälla, Sweden).

2.3.2. Skin microvascular blood flux measurements

Cutaneous blood flux was measured with laser speckle contrast imaging (LSCI) (PeriCam PSI System, Perimed, Järfälla, Sweden) that exhibits an excellent reproducibility when assessing skin blood flux (Roustit et al., 2010). The LSCI wavelength was 785 nm and the laser head was placed 20 cm above the skin (with a resolution of \approx 6.9 pixels/cm). The image size was 12 \times 12 cm and the acquisition rate was 3 s⁻¹ (Fig. 1C). Before recording, the leg was immobilized with a vacuum cushion to avoid movement artefacts. Microvascular blood flux was measured for 5 min before, immediately after the end of iontophoresis, and 15 min, 30 min, 1 h, 2 h, 3 h, 4 h, 5 h and 6 h after the end of iontophoresis.

2.3.3. Plasma concentration of treprostinil following iontophoresis in healthy subjects

Venous blood samples were collected from a catheter inserted in the forearm. Samples were collected after the end of iontophoresis at T0, 15 min, 30 min, 1 h, 2 h, 3 h, 4 h, 5 h and 6 h.

2.4. Data analysis

Data were analyzed with signal processing software (PIMSoft 1.1.1; Perimed, Järfälla, Sweden). Skin blood flux was expressed as cutaneous vascular conductance (CVC), which is the flux in arbitrary perfusion units (PU) divided by the mean arterial pressure (MAP) in mm Hg (Roustit and Cracowski, 2013). We then calculated the percentage change from baseline flux (%BL) and calculated the area under the curve for 6 h (AUC_{0–6 h}) after the end of iontophoresis. The treprostinil hyperemic area was calculated on LSCI maximal perfusion over 3 images transferred to ImageJ 1.44 (NIH software, in the public domain). Then, for each image, the mean value of the control area was used as a cutoff for determining the hyperemic area due to treprostinil in mm².

2.5. Statistical analysis

A sample size of 11 in each group had 80% power to detect a probability of 0.85 that an observation in the treprostinil site is superior to placebo using a Wilcoxon rank-sum test with a 0,050 two-sided significance level (nQuery Advisor 7.0, Statistical Solutions Ltd., Cork, Ireland). In order to take into account potential drop out due to technical problems, we chose to enroll 12 subjects.

Continuous data are reported as mean and standard deviation, and categorical data are reported as numbers. Skin blood flux after treprostinil and placebo iontophoresis simultaneously recorded in the same subject were compared using a Wilcoxon rank test. We considered p-values of \leq 0.05 as significant. Statistical analyses were performed using IBM SPSS Statistics v21.

3. Results

3.1. Study population

Twelve healthy volunteers (5 men and 7 women) were enrolled in this study. Their mean age was 22.4 \pm 1 years and their BMI was 21 \pm 1.8 kg/m². Systolic and diastolic arterial blood pressure was 118 \pm 13 and 67 \pm 10 mm Hg, respectively. Three women were taking oral contraception.

In the second part of this study, 12 type 2 diabetic patients were enrolled (3 women and 9 men). Their mean age was 57.8 \pm 8 years and their BMI was 29 \pm 5.5 kg/m². Systolic and diastolic arterial blood pressure was 132 \pm 12 and 78 \pm 13 mm Hg, respectively. Their mean HbA1c was 7.8 \pm 1.6% and serum creatinine was 89 \pm 21 μ mol/l. The mean duration of diabetes mellitus was 10.3 \pm 9.7 years. Eleven out of 12 patients were being treated with metformin and four of them also received gliclazide and insulin. One diabetic patient was solely on insulin therapy. None of the patients exhibited peripheral diabetic neuropathy.

3.2. Effect of 40 mC/cm² cathodal iontophoresis of treprostinil on skin blood flux in healthy volunteers

Treprostinil 250 μ M induced a significant increase in CVC compared with NaCl (AUC_{0–6 h} was 37781 \pm 24619; versus 2657 \pm 6775%BL.min, respectively; $P=0.002$). The peak flux was obtained 1 h after the end of treprostinil iontophoresis and flux remained higher than baseline up to 6 h after the end of iontophoresis (Fig. 2A). Treprostinil induced hyperemia over an area of 1033 \pm 407 mm². Skin resistance was not different between the two skin sites.

3.3. Plasma concentration of treprostinil after iontophoresis in healthy subjects

The treprostinil plasma concentration was below the quantification threshold of 1.8 pg/ml in 8 out 12 volunteers. We observed low systemic diffusion only in four samples from 4 different subjects with a maximal peak of 11.9 pg/ml measured 15 min after the end of treprostinil iontophoresis.

3.4. Effect of 40 mC/cm² cathodal iontophoresis of treprostinil on skin blood flux in type 2 diabetic patients

Treprostinil 250 μ M induced a significant increase in CVC compared with NaCl (AUC_{0–6 h} was 19970 \pm 8697; versus 2893 \pm 5481%BL.min, respectively; $P=0.002$). The peak flux was obtained between 30 min and 1 h after the end of treprostinil iontophoresis and flux remained higher than baseline up to 6 h after the end of iontophoresis (Fig. 2B). Treprostinil induced hyperemia extended over an area of 724 \pm 315 mm². Skin resistance was not different between the two skin sites.

3.5. Post hoc analysis

We compared treprostinil iontophoresis between healthy volunteers and diabetic patients, which was significantly higher in healthy volunteers in terms of amplitude (AUC_{0–6 h}, $P=0.033$) but not of diffusion area.

3.6. Skin and systemic tolerance of the iontophoresis of treprostinil

No serious side-effect occurred. We observed no significant change in mean arterial pressure after the iontophoresis of treprostinil. As expected skin erythema localized to the probe area was observed after removal of the heating probe, which disappeared in a few hours. No

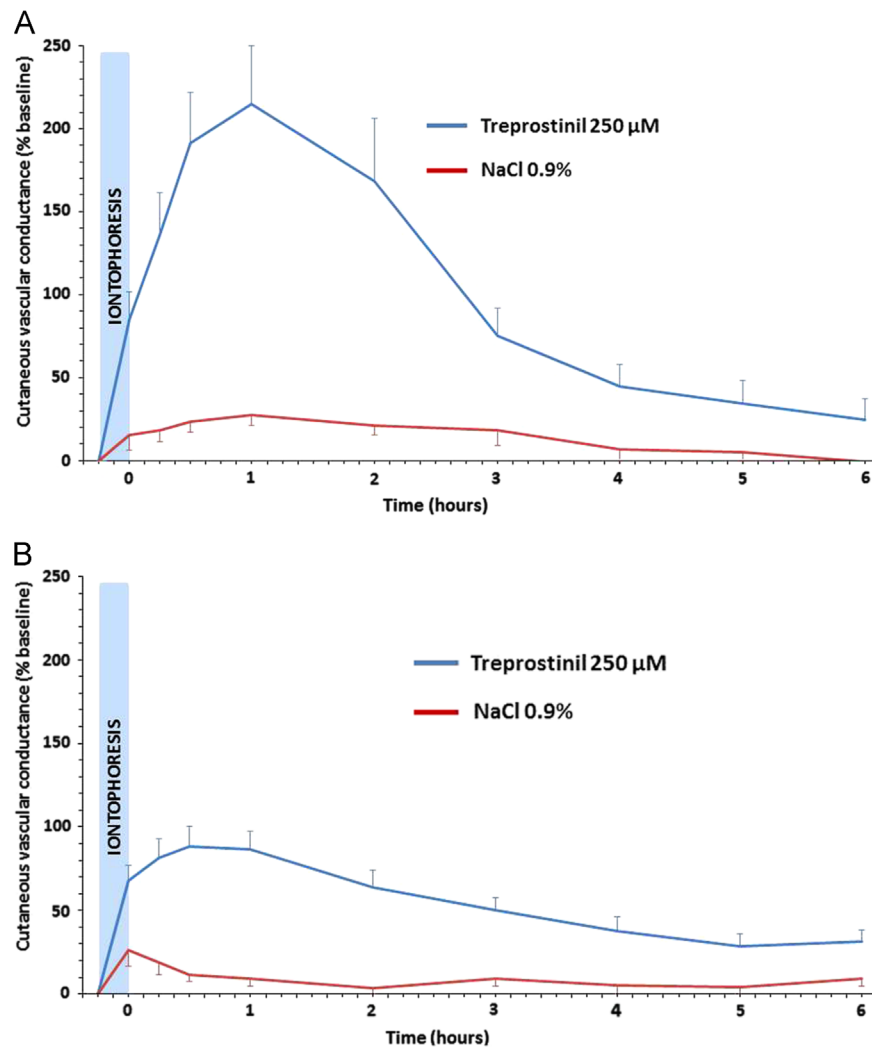


Fig. 2. Effect of 40 mC/cm² cathodal iontophoresis of 250 µM treprostinil versus NaCl 0.9%, on cutaneous vascular conductance (CVC) expressed as a percentage of baseline, recorded over 6 h in healthy subjects (A) and diabetic patients (B).

squamous, vesicular or bullous lesions were observed at the end of the experiment.

4. Discussion

In this study, cathodal iontophoresis of 250 µM treprostinil significantly increased skin microvascular blood flux in the malleolus area in healthy volunteers and in diabetic patients compared to NaCl 0.9%. The peak flux was obtained between 30 min and 1 h after the end of iontophoresis and flux remained higher than baseline up to 6 h after the end of iontophoresis.

Using two-dimensional LSCI, we showed that treprostinil systematically induced a sustained hyperemia in diabetic patients and in healthy subjects, lasting more than 6 h.

Such data are consistent with our previous report on healthy volunteers forearm (Blaise et al., 2013), while on the finger pads of systemic sclerosis patients, the duration of the hyperemia was shorter (Roustit et al., 2014b). Other groups have tested the effects of prostacyclin analogs on skin microcirculation. Beraprost sodium, administered orally, significantly increased microvascular skin blood flux in the feet in healthy subjects and type 2 diabetic patients, skin blood flux being estimated using laser Doppler fluxmetry (Aso et al., 1997). Following

intravenous administration of iloprost, partial or total healing of ischemic tissue lesions in diabetics was reported (Brock et al., 1990).

To our knowledge, only one study has previously investigated the topical effect of prostacyclin analogs on skin healing. Pimilprost ointment used topically in diabetic mice on a full thickness wound created by excising the skin, increased skin blood flux in the center of the wound (Yamamoto et al., 1996). In addition, pimilprost ointment improved wound healing. The authors further noticed that numerous capillaries, endothelial cells and fibroblasts were observed at the edge of the wounds when mice were treated with pimilprost ointment, but not in those treated with placebo ointment alone. They speculated that prostacyclin analogs might stimulate the proliferation of fibroblasts and endothelial cells through the improvement of the blood flux, explaining the improvement of wound healing.

In terms of experimental design we ran an atypical cross over trial, with the specificity that each subject was its own control at the same time, i.e. each subject received simultaneously treprostinil and placebo. The principal drawback of crossover trial is that the effects of one treatment may “carry over” and alter the response to subsequent treatments. Here, our experimental design was very potent given that as it had the advantages of cross over trials, without the major disadvantage, i.e. no carry over effect.

In our study, the treprostinil concentration used was 1/10th of the lowest concentration used for subcutaneous treatment in pulmonary

arterial hypertension. This explains why plasma monitoring showed negligible systemic diffusion of the drug. We used a liquid chromatography – tandem mass spectrometry method that has a very low detection threshold (Roustit et al., 2014b). Indeed, the highest plasma concentration detected, i.e. 11.9 pg/ml was far below the concentrations reached in patients treated with treprostinil for pulmonary hypertension (Laliberte et al., 2004). Considering the negligible concentration observed in the plasma in healthy subjects, the pharmacokinetic study was not performed in subsequently recruited diabetic patients. We observed no local side-effect, including no localized pain often described following subcutaneous infusion. Similarly, we observed no systemic effects, in particular no drop in mean arterial blood pressure.

The peak treprostinil hyperemic area extended over the same area as the electrode surface, and did not significantly differ between healthy controls and diabetic patients. However, the area under the curve was smaller in diabetics, though this result should be taken with caution given that it was a *post hoc* analysis using two groups that were unmatched for sex and age. It could be explained by the decreased microvascular density or function in diabetes mellitus (Ko et al., 2010), but we did not quantify microvascular density in our study.

Although different therapies have been proposed and developed for diabetic wound healing, the treatment of diabetic microvascular ulcers remains challenging. Indeed, wound healing is a complex process which depends on many factors, such as inflammation, proliferation, hemostasis and remodeling. In diabetic patients, it is also impacted by hyperglycemia, sensory neuropathy, macro-circulatory problems and microvascular dysfunction (Baltzis et al., 2014). To date, iontophoresis of vasodilatory drugs has only been used to assess microvascular reactivity and endothelial function in cardiovascular disease, rather than as an alternative local treatment to conventional therapy. It has been suggested that noninvasive vasodilator delivery by iontophoresis could be investigated as a possible method of treatment in diseases affecting the peripheral microcirculation (Murray et al., 2005). Another potential benefit of iontophoresis in the treatment of skin ulcers could be the effect of low-intensity current per se. Indeed, endogenous electrical signals in the wound play a role in healing, by increasing the directed migration of keratinocytes, fibroblasts and neutrophils (Zhao et al., 2006). Exogenous electric stimulation may have a positive impact on wound healing (Baltzis et al., 2014; Huttenlocher and Horwitz, 2007). Indeed, exogenous electric stimulation increases skin perfusion through prostacyclin release (Gohin et al., 2011; Roustit and Cracowski, 2013) and reduces bacterial load (Daeschlein et al., 2007) and the risk of infection that slow down the healing process. Besides avoiding systemic side effects, we indeed hypothesize that the combination of the pharmacological effect of treprostinil with the proper effect of the current enhances wound healing. However, our data do not allow concluding about any effect on wound healing, but they open perspectives as treprostinil iontophoresis has an effect on an intermediate biomarker such as the blood flux. Thus, whether such a treatment may be effective in healing diabetic foot ulcers remains to be confirmed in a future study.

5. Conclusions

In conclusion, cutaneous iontophoresis of 250 μ M treprostinil increases microvascular blood flux in the malleolus area in healthy volunteers and diabetic patients, without inducing systemic or local side-effects. Topical administration of a prostacyclin analog administered through iontophoresis could be a potential innovative, well-tolerated therapy of microvascular skin ulcers, which should be further investigated.

Conflict of interest

M.R. and J.-L.C. hold a patent on treprostinil iontophoresis for the treatment of ulcers. The other authors declared no conflict of interest.

Acknowledgments

This study was funded by grant from the French Ministry of Health (PHRC I 2011). Bioprojet Pharma supplied treprostinil. Marcin Hellmann received a French government scholarship delivered by the French Embassy in Poland (826766J 2014). We thank Alison Foote for critically reading and editing the manuscript and Lucie Ulmer for help with technical measurements.

References

- Aso, Y., Inukai, T., Takemura, Y., 1997. Evaluation of microangiopathy of the skin in patients with non-insulin-dependent diabetes mellitus by laser Doppler fluxmetry; microvasodilatory responses to beraprost sodium. *Diabetes Res. Clin. Pract.* 36, 19–26.
- Baltzis, D., Eleftheriadou, I., Veves, A., 2014. Pathogenesis and treatment of impaired wound healing in diabetes mellitus: new insights. *Adv. Ther.* 31, 817–836.
- Blaise, S., Roustit, M., Millet, C., Ribout, C., Boutonnat, J., Cracowski, J.L., 2011. Cathodal iontophoresis of treprostinil and iloprost induces a sustained increase in cutaneous flux in rats. *Br. J. Pharmacol.* 162, 557–565.
- Blaise, S., Roustit, M., Hellmann, M., Millet, C., Cracowski, J.L., 2013. Cathodal iontophoresis of treprostinil induces a sustained increase in cutaneous blood flux in healthy volunteers. *J. Clin. Pharmacol.* 53, 58–66.
- Brock, F.E., Abri, O., Baitsch, G., Bechara, G., Beck, K., Corovic, D., Diehm, C., Marshall, M., Rahmel, B., Scheffler, P., 1990. Iloprost in the treatment of ischemic tissue lesions in diabetics. Results of a placebo-controlled multicenter study with a stable prostacyclin derivative. *Schweiz. Med. Wochenschr.* 120, 1477–1482.
- Caselli, A., Rich, J., Hanane, T., Uccioli, L., Veves, A., 2003. Role of C-nociceptive fibers in the nerve axon reflex-related vasodilation in diabetes. *Neurology* 60, 297–300.
- Daeschlein, G., Assadian, O., Kloth, L.C., Meinel, C., Ney, F., Kramer, A., 2007. Antibacterial activity of positive and negative polarity low-voltage pulsed current (LVPC) on six typical Gram-positive and Gram-negative bacterial pathogens of chronic wounds. *Wound Repair Regen.* 15, 399–403.
- Gohin, S., Sigaudo-Roussel, D., Conjard-Duplany, A., Dubourg, L., Saumet, J.L., Fromy, B., 2011. What can current stimulation tell us about the vascular function of endogenous prostacyclin in healthy rat skin in vivo? *J. Invest. Dermatol.* 131, 237–244.
- Huttenlocher, A., Horwitz, A.R., 2007. Wound healing with electric potential. *New Engl. J. Med.* 356, 303–304.
- Kalia, Y.N., Naik, A., Garrison, J., Guy, R.H., 2004. Iontophoretic drug delivery. *Adv. Drug Deliv. Rev.* 56, 619–658.
- Ko, S.H., Cao, W., Liu, Z., 2010. Hypertension management and microvascular insulin resistance in diabetes. *Curr. Hypertens. Rep.* 12, 243–251.
- Laliberte, K., Arneson, C., Jeffs, R., Hunt, T., Wade, M., 2004. Pharmacokinetics and steady-state bioequivalence of treprostinil sodium (Remodulin) administered by the intravenous and subcutaneous route to normal volunteers. *J. Cardiovasc. Pharmacol.* 44, 209–214.
- Murray, A.K., Herrick, A.L., Gorodkin, R.E., Moore, T.L., King, T.A., 2005. Possible therapeutic use of vasodilator iontophoresis. *Microvasc. Res.* 69, 89–94.
- O'Meara, S., Cullum, N., Majid, M., Sheldon, T., 2001. Systematic reviews of wound care management: (3) antimicrobial agents for chronic wounds; (4) diabetic foot ulceration. *Health Technol Assess.* 4, 1–237.
- Roustit, M., Millet, C., Blaise, S., Dufournet, B., Cracowski, J.L., 2010. Excellent reproducibility of laser speckle contrast imaging to assess skin microvascular reactivity. *Microvasc. Res.* 80, 505–511.
- Roustit, M., Cracowski, J.L., 2012. Non-invasive assessment of skin microvascular function in humans: an insight into methods. *Microcirculation.* 19, 47–64.
- Roustit, M., Cracowski, J.L., 2013. Assessment of endothelial and neurovascular function in human skin microcirculation. *Trends Pharmacol. Sci.* 34, 373–384.
- Roustit, M., Blaise, S., Cracowski, J.L., 2014a. Trials and tribulations of skin iontophoresis in therapeutics. *Br. J. Clin. Pharmacol.* 77, 63–71.
- Roustit, M., Gaillard-Bigot, F., Blaise, S., Stanke-Labesque, F., Cracowski, C., Seinturier, C., Jourdil, J.F., Imbert, B., Carpentier, P.H., Cracowski, J.L., 2014b. Cutaneous iontophoresis of treprostinil in systemic sclerosis: a proof-of-concept study. *Clin. Pharmacol. Ther.* 95, 439–445.
- Veves, A., Akbari, C.M., Primavera, J., Donaghue, V.M., Zacharoulis, D., Chrzan, J.S., DeGrolami, U., LoGerfo, F.W., Freeman, R., 1998. Endothelial dysfunction and the expression of endothelial nitric oxide synthetase in diabetic neuropathy, vascular disease, and foot ulceration. *Diabetes* 47, 457–463.
- Whittle, B.J., Silverstein, A.M., Mottola, D.M., Clapp, L.H., 2012. Binding and activity of the prostacyclin receptor (IP) agonists, treprostinil and iloprost, at human prostanoid receptors: treprostinil is a potent DP1 and EP2 agonist. *Biochem. Pharmacol.* 84, 68–75.

- Woodward, D.F., Jones, R.L., Narumiya, S., 2011. International union of basic and clinical pharmacology. LXXXIII: classification of prostanoid receptors, updating 15 years of progress. *Pharmacol. Rev.* 63, 471–538.
- Yamamoto, T., Horikawa, N., Komuro, Y., Hara, Y., 1996. Effect of topical application of a stable prostacyclin analog, SM-10902 on wound healing in diabetic mice. *Eur. J. Pharmacol.* 302, 53–60.
- Zhao, M., Song, B., Pu, J., Wada, T., Reid, B., Tai, G., Wang, F., Guo, A., Walczysko, P., Gu, Y., Sasaki, T., Suzuki, A., Forrester, J.V., Bourne, H.R., Devreotes, P.N., McCaig, C.D., Penninger, J.M., 2006. Electrical signals control wound healing through phosphatidylinositol-3-OH kinase-gamma and PTEN. *Nature* 442, 457–460.

Perspectives et conclusion

1. Perspectives physiopathologiques de l'étude de la microcirculation cutanée

En utilisant le *laser speckle contrast imaging* (LSCI) couplé à la microdialyse cutanée, nous avons montré, qu'au-delà de l'implication des nerfs sensoriels dans l'hyperhémie post-occlusive (HPO), les EETs – des métabolites des cytochromes P450 (CYP) époxygénases – jouent un rôle majeur dans l'HPO au niveau de la surface cutanée de l'avant bras (87). Notre équipe avait également montré que la reproductibilité de cet outil pour évaluer des tests dynamiques tels que l'HPO est excellente (88). Plus récemment, l'équipe du Pr Pierre Abraham a montré que le LSCI permet d'obtenir une quantification de l'hyperhémie post-occlusive avec des coefficients de variation excellents, à condition de tirer avantage de l'acquisition bidimensionnelle de cet outil, en sélectionnant des zones d'intérêt de plus de 10 mm (89). Depuis, notre équipe a également testé et évalué la reproductibilité du LSCI développé par la firme *Perimed* et validé la linéarité de son signal (90).

Tout au long de ce travail de thèse, nous avons mis en exergue le fait que l'apport d'outils pharmacologiques était indispensable dans l'étude et la modulation des voies physiologiques, comme celles impliquant les médiateurs de la relaxation endothéliale. En effet, en utilisant des voies d'administration qui font intervenir une distribution systémique permettant ensuite d'atteindre le site cible, outre le risque d'effets systémiques des médicaments administrés, il est difficile de démontrer la diffusion du médicament au niveau de ce site d'intérêt. L'administration topique ou intradermique a donc été proposée en raison de l'accessibilité de la peau, et la possibilité d'utiliser des concentrations élevées avec une exposition systémique limitée. Bien que l'iontophorèse soit proposée comme un outil pharmacologique, ses effets non-spécifiques (comme par exemple la vasodilatation courant-induite) sont des facteurs de confusion. Un autre inconvénient lié à l'utilisation de l'iontophorèse est que la quantité exacte de médicament administrée dans ou à travers la peau ne peut pas être quantifiée avec précision.

Dans une zone cutanée d'intérêt, la microdialyse permet à la fois de prélever en continu et *in vivo* des molécules dans le liquide extracellulaire – par l'insertion d'une membrane semi-perméable dans le derme superficiel – et d'être utilisée comme un outil de délivrance locale de médicaments, au sein de cette même zone d'intérêt (91).

Cependant, la microdialyse ne peut pas être réalisée sur toute la surface cutanée ; les doigts, en particulier, ne sont pas accessibles en raison des saignements et des difficultés techniques d'insertion). Sur ce territoire, la technique alternative est la micro-injection dermique, qui consiste à injecter un volume de l'ordre de la dizaine de microlitre dans le derme. Cette technique de micro-injection digitale a été préalablement utilisée avec cependant des techniques variables (92,93). Cette technique était estimée peu reproductible et déclenchant potentiellement un réflexe axonal. Nous avons récemment mis au point cette technique sur le dos des doigts à l'aide d'une aiguille d'un diamètre de 30 gauges (aiguille 30 G). Cette aiguille présente l'avantage d'être très fine (30 G), permettant de limiter le réflexe axonal (Figures 13 et 14).

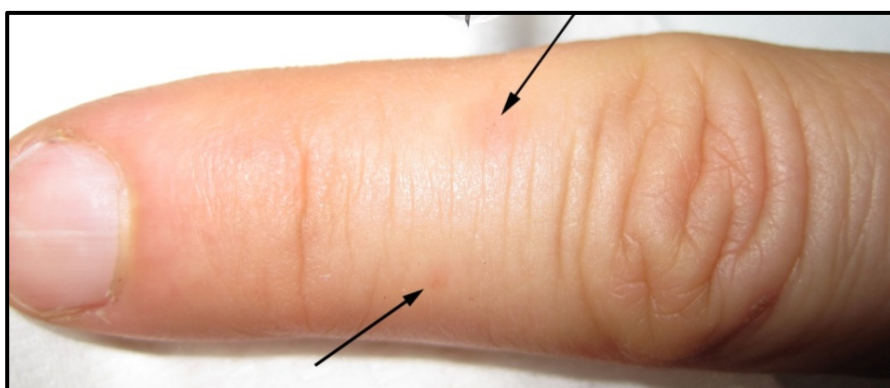


Figure 13. Microinjection de 40 μ L de nitroprussiate de sodium (SNP) à 29 mM (flèche supérieure) et de NaCl à 0,9% (flèche inférieure) réalisée à l'aide d'une aiguille 30 G sur la face dorsale de la seconde phalange de l'index. À l'aide de cette technique, il est difficile de discerner le site de ponction du contrôle, et l'on constate à l'œil nu l'érythème lié à l'effet pharmacologique attendu du SNP (cliché personnel).

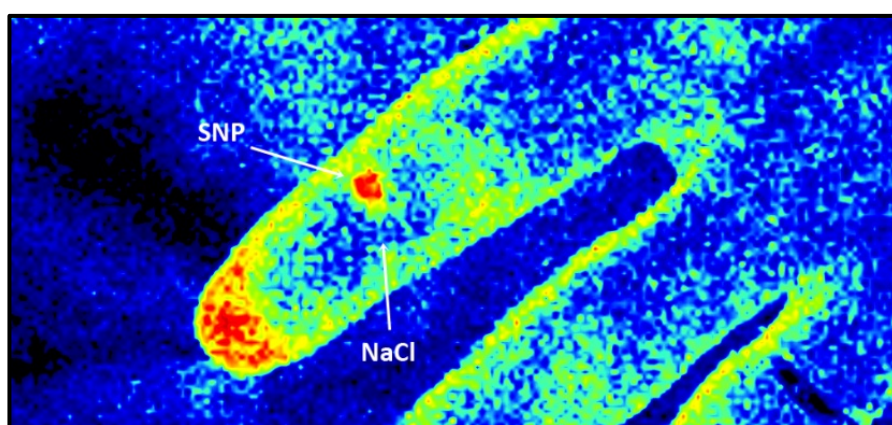


Figure 14. Même expérience : cartographie de flux réalisée 5 minutes après micro-injection de NaCl à 0,9% et de nitroprussiate de sodium (SNP) à 29 mM. Le réflexe axonal observé après l'injection de NaCl est très modeste et transitoire (2 minutes, ayant disparu ici à 5 minutes), alors que l'hyperhémie liée à l'injection du SNP est limitée à la zone entourant le point de ponction et perdure (durée 40 minutes) de façon soutenue (cliché personnel, données non publiées).

En termes de perspectives, nous disposons de tests permettant d'explorer la fonction endothéliale cutanée digitale (HPO) mais aussi permettant d'explorer la réponse au froid (données non développées dans ce travail), dans laquelle des médiateurs endothéliaux sont impliqués sans que les données actuelles ne permettent d'identifier ces médiateurs.

Les objectifs futurs de l'équipe à ce sujet comprennent, à l'aide du couplage du LSCI aux techniques de micro-injection dermique, l'évaluation de l'implication spécifique de deux principaux médiateurs endothéliaux, les EETs et le monoxyde d'azote (NO), dans le phénomène de Raynaud primaire. Il est envisagé d'utiliser et de comparer deux tests : l'HPO – qui permettrait d'étudier spécifiquement ces voies des EETs et du NO – et un test de refroidissement local – pour lequel les médiateurs endothéliaux ne sont pas connus.

Ce faisant, l'on pourrait essayer de déterminer si l'existence d'une anomalie endothéliale peut expliquer la différence de réactivité microvasculaire – telle qu'elle est observée dans le cadre du phénomène de Raynaud – par rapport au volontaire sain, et déterminer si ces anomalies sont exclusivement exprimées en cas de stimulation au froid.

2. Perspectives thérapeutiques de l'iontophorèse de tréprostinil appliquée à la microcirculation cutanée

Comme nous l'avons vu, la SSc est une maladie rare caractérisée par une atteinte microvasculaire et une fibrose cutanée. Les ulcères digitaux sont une complication sévère et très invalidante (Figure 15).



Figure 15. Gauche, Sclérodémie cutanée limitée : Ulcérations digitales ischémiques de l'index et du majeur gauche, ici la plaie n'est pas débridée. Droite, sclérodémie cutanée diffuse : Ulcérations digitales récidivantes (clichés personnels).

La physiopathologie fait intervenir une ischémie vasculaire et des facteurs mécaniques déclenchants liés à une peau scléreuse sous tension, ou bien à des calcinose cutanées, ou encore suite à un traumatisme local. Les ulcérations digitales de la sclérodémie sont le principal facteur de handicap. En effet, cette complication est fréquente, la prévalence variant de 8 à 31 % selon les études. Il est estimé que leur fréquence de survenue est de 43% durant la vie d'un patient dans les formes cutanées limités, et qu'elle est de 51 % dans les formes cutanées diffuses (94). Elle conduit à des amputations digitales dans 4,8 % des cas (Figure 16), (94). Le handicap au travail et dans les activités de la vie quotidienne est par ailleurs corrélé au nombre d'ulcérations digitales (95).



Figure 16. *Sclérodémie systémique diffuse. Ulcérations digitales récidivantes des extrémités de la main gauche ont conduit à l'amputation de la phalange distale de l'index gauche (cliché personnel).*

Comme nous l'avons évoqué précédemment, le paradoxe dans le traitement des ulcérations digitales de la sclérodémie systémique est que la diminution de la densité capillaire et de la réactivité microvasculaire limite la diffusion du médicament au niveau du site d'action recherché lorsqu'il est administré par voie orale ou intraveineuse. Des doses élevées sont alors nécessaires pour atteindre une concentration suffisante au niveau de la plaie, ce qui génère des effets indésirables au niveau systémique.

L'administration locale du médicament pourrait permettre de contourner ce problème et l'iontophorèse apparaît donc comme une nouvelle voie aux potentiels majeurs.

En effet, nous avons démontré, d'abord sur modèle murin, que le tréprostinil est un bon candidat pour une administration topique par iontophorèse (96,97). Dans le cadre des études cliniques précédentes INFLUX-IT (98) et TIPPS (99,100) nous avons montré que l'administration cutanée locale de tréprostinil par iontophorèse dite cathodale est bien tolérée (absence d'effet indésirable local ou systémique chez des volontaires sains, comme chez des patients atteints de sclérodémie systémique ou chez des diabétiques). L'iontophorèse induit une augmentation soutenue du flux sanguin cutané sur les doigts (Figure 17). Nous avons également posé des fibres de microdialyse cutanée et montré que le tréprostinil est détectable dans le derme jusqu'à 8 heures après l'iontophorèse, sans augmentation significative dans le plasma. Une équipe américaine ayant travaillé sur la base de nos travaux, a tout récemment confirmé nos données : l'iontophorèse de tréprostinil est bien tolérée à la concentration de 1 mg/mL et induit une vasodilatation soutenue, sans passage systémique significatif et sans effet de l'excipient (101).

L'iontophorèse apparaît donc particulièrement intéressante car elle permet de délivrer localement le tréprostinil sans observer d'effets secondaires systémiques.

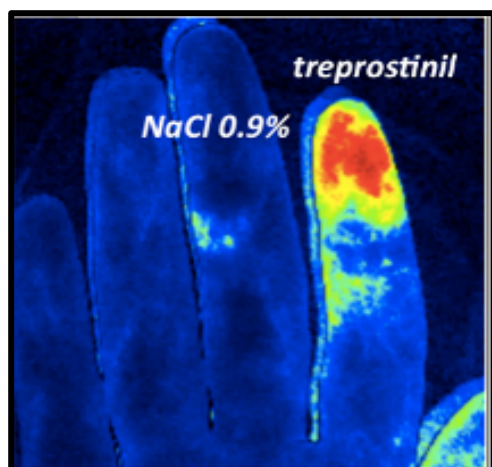


Figure 17. Image obtenue en Laser Speckle Contrast Imaging montrant l'effet vasodilatateur obtenu sur la pulpe de l'index après iontophorèse cathodale de tréprostinil (en bleu : flux faible, en rouge : flux élevé)(99). Cet effet persiste pendant 4 à 6 heures après la fin de l'iontophorèse (d'après Roustit, Clin Pharmacol Ther 2014).

En termes de thérapeutique, l'on imagine des perspectives de l'iontophorèse, qui quotidiennement répétée pendant 10 jours sur des zones ulcérées, pourrait donc permettre d'obtenir des concentrations tissulaires thérapeutiques, et au minimum pendant cette durée d'administration.

Les projets à venir et les résultats attendus

Avant de concevoir une étude de phase IIb/III de démonstration d'efficacité, il existe de possibles difficultés à surmonter. Pour cela, nous avons besoin :

1- D'optimiser la matrice dans laquelle le médicament est situé. Nous avons travaillé avec du tréprostinil en solution. Notre but est de l'utiliser sous une autre forme galénique qui puisse être applicable sur une plaie ; en l'occurrence, un hydrogel. Des travaux préliminaires montrent que cette forme galénique est assez facilement réalisable.

2- De tester cet hydrogel de tréprostinil sur la peau ulcérée.

En cas de succès, l'étape suivante serait de procéder à une étude de phase IIb/III sur un critère clinique intermédiaire de cicatrisation.

Références

1. Gutterman DD, Chabowski DS, Kadlec AO, Durand MJ, Freed JK, Ait-Aissa K, et al. The Human Microcirculation Regulation of Flow and Beyond. *Circ Res*. 2016 Jan 8;118(1):157–72.
2. Davis MJ, Hill MA. Signaling mechanisms underlying the vascular myogenic response. *Physiol Rev*. 1999;79(2):387–423.
3. Charkoudian N. Skin blood flow in adult human thermoregulation: how it works, when it does not, and why. *Mayo Clin Proc*. 2003 May;78(5):603–12.
4. Holowatz LA, Thompson-Torgerson CS, Kenney WL. The human cutaneous circulation as a model of generalized microvascular function. *J Appl Physiol Bethesda Md* 1985. 2008 Jul;105(1):370–2.
5. Khaodhiar L, Dinh T, Schomacker KT, Panasyuk SV, Freeman JE, Lew R, et al. The use of medical hyperspectral technology to evaluate microcirculatory changes in diabetic foot ulcers and to predict clinical outcomes. *Diabetes Care*. 2007 Apr;30(4):903–10.
6. Greenman RL, Panasyuk S, Wang X, Lyons TE, Dinh T, Longoria L, et al. Early changes in the skin microcirculation and muscle metabolism of the diabetic foot. *The Lancet*. 2005 Nov 18;366(9498):1711–7.
7. Abularrage CJ, Sidawy AN, Aidinian G, Singh N, Weiswasser JM, Arora S. Evaluation of macrocirculatory endothelium-dependent and endothelium-independent vasoreactivity in vascular disease. *Perspect Vasc Surg Endovasc Ther*. 2005 Sep;17(3):245–53.
8. Cracowski J-L, Minson CT, Salvat-Melis M, Halliwill JR. Methodological issues in the assessment of skin microvascular endothelial function in humans. *Trends Pharmacol Sci*. 2006 Sep;27(9):503–8.
9. Roustit M, Blaise S, Millet C, Cracowski JL. Reproducibility and methodological issues of skin post-occlusive and thermal hyperemia assessed by single-point laser Doppler flowmetry. *Microvasc Res*. 2010 Mar;79(2):102–8.
10. Roustit M, Maggi F, Isnard S, Hellmann M, Bakken B, Cracowski J-L. Reproducibility of a local cooling test to assess microvascular function in human skin. *Microvasc Res*. 2010 Jan;79(1):34–9.

11. Millet C, Roustit M, Blaise S, Cracowski JL. Comparison between laser speckle contrast imaging and laser Doppler imaging to assess skin blood flow in humans. *Microvasc Res.* 2011 Sep;82(2):147–51.
12. Roustit M, Millet C, Blaise S, Dufournet B, Cracowski JL. Excellent reproducibility of laser speckle contrast imaging to assess skin microvascular reactivity. *Microvasc Res.* 2010 Dec;80(3):505–11.
13. Carpentier PH, Maricq HR. Microvasculature in systemic sclerosis. *Rheum Dis Clin North Am.* 1990 Feb;16(1):75–91.
14. Herrick AL. Vascular function in systemic sclerosis. *Curr Opin Rheumatol.* 2000 Nov;12(6):527–33.
15. Roustit M, Simmons GH, Baguet J-P, Carpentier P, Cracowski J-L. Discrepancy between simultaneous digital skin microvascular and brachial artery macrovascular post-occlusive hyperemia in systemic sclerosis. *J Rheumatol.* 2008 Aug;35(8):1576–83.
16. Kowal-Bielecka O, Landewé R, Avouac J, Chwiesko S, Miniati I, Czirjak L, et al. EULAR recommendations for the treatment of systemic sclerosis: a report from the EULAR Scleroderma Trials and Research group (EUSTAR). *Ann Rheum Dis.* 2009 May;68(5):620–8.
17. Abularrage CJ, Sidawy AN, Aidinian G, Singh N, Weiswasser JM, Arora S. Evaluation of the microcirculation in vascular disease. *J Vasc Surg.* 2005 Sep;42(3):574–81.
18. Sax FL, Cannon RO, Hanson C, Epstein SE. Impaired forearm vasodilator reserve in patients with microvascular angina. Evidence of a generalized disorder of vascular function? *N Engl J Med.* 1987;317(22):1366–70.
19. Feihl F, Liaudet L, Waeber B, Levy BI. Hypertension: a disease of the microcirculation? *Hypertens Dallas Tex* 1979. 2006 Dec;48(6):1012–7.
20. Vincent MA, Clerk LH, Lindner JR, Klibanov AL, Clark MG, Rattigan S, et al. Microvascular recruitment is an early insulin effect that regulates skeletal muscle glucose uptake in vivo. *Diabetes.* 2004 Jun;53(6):1418–23.
21. Levy BI, Schiffrin EL, Mourad J-J, Agostini D, Vicaute E, Safar ME, et al. Impaired tissue perfusion: a pathology common to hypertension, obesity, and diabetes mellitus. *Circulation.* 2008 Aug 26;118(9):968–76.
22. Antonios TF, Singer DR, Markandu ND, Mortimer PS, MacGregor GA. Structural skin capillary rarefaction in essential hypertension. *Hypertens Dallas Tex* 1979. 1999 Apr;33(4):998–1001.

23. Chang CH, Tsai RK, Wu WC, Kuo SL, Yu HS. Use of dynamic capillaroscopy for studying cutaneous microcirculation in patients with diabetes mellitus. *Microvasc Res.* 1997 Mar;53(2):121–7.
24. Yamamoto-Suganuma R, Aso Y. Relationship between post-occlusive forearm skin reactive hyperaemia and vascular disease in patients with Type 2 diabetes--a novel index for detecting micro- and macrovascular dysfunction using laser Doppler flowmetry. *Diabet Med J Br Diabet Assoc.* 2009 Jan;26(1):83–8.
25. Kruger A, Stewart J, Sahityani R, O’Riordan E, Thompson C, Adler S, et al. Laser Doppler flowmetry detection of endothelial dysfunction in end-stage renal disease patients: correlation with cardiovascular risk. *Kidney Int.* 2006;70(1):157–64.
26. Pries AR, Kuebler WM. Normal endothelium. *Handb Exp Pharmacol.* 2006;(176 Pt 1):1–40.
27. Huttner I, Gabbiani G. Vascular endothelium: recent advances and unanswered questions. *Lab Investig J Tech Methods Pathol.* 1982 Nov;47(5):409–11.
28. Félétou M, Vanhoutte PM. Endothelium-derived hyperpolarizing factor: where are we now? *Arterioscler Thromb Vasc Biol.* 2006 Jun;26(6):1215–25.
29. Lüscher TF, Noll G. The pathogenesis of cardiovascular disease: role of the endothelium as a target and mediator. *Atherosclerosis.* 1995 Dec;118 Suppl:S81–90.
30. Davignon J, Ganz P. Role of endothelial dysfunction in atherosclerosis. *Circulation.* 2004 Jun 15;109(23 Suppl 1):III27–32.
31. Sakuma I, Stuehr DJ, Gross SS, Nathan C, Levi R. Identification of arginine as a precursor of endothelium-derived relaxing factor. *Proc Natl Acad Sci U S A.* 1988 Nov;85(22):8664–7.
32. Moncada S, Palmer RM. Biosynthesis and actions of nitric oxide. *Semin Perinatol.* 1991 Feb;15(1):16–9.
33. Förstermann U, Nakane M, Tracey WR, Pollock JS. Isoforms of nitric oxide synthase: functions in the cardiovascular system. *Eur Heart J.* 1993 Nov;14 Suppl I:10–5.
34. Birks EJ, Yacoub MH. The role of nitric oxide and cytokines in heart failure. *Coron Artery Dis.* 1997 Jun;8(6):389–402.
35. Geller DA, Billiar TR. Molecular biology of nitric oxide synthases. *Cancer Metastasis Rev.* 1998 Mar;17(1):7–23.
36. Ignarro LJ. Biological actions and properties of endothelium-derived nitric oxide formed and released from artery and vein. *Circ Res.* 1989 Jul;65(1):1–21.

37. Vanhoutte PM. Vascular biology. Old-timer makes a comeback. *Nature*. 1998 Nov 19;396(6708):213, 215–6.
38. Nagao T, Vanhoutte PM. Characterization of endothelium-dependent relaxations resistant to nitro-L-arginine in the porcine coronary artery. *Br J Pharmacol*. 1992 Dec;107(4):1102–7.
39. Miura H, Gutterman DD. Human coronary arteriolar dilation to arachidonic acid depends on cytochrome P-450 monooxygenase and Ca²⁺-activated K⁺ channels. *Circ Res*. 1998 Sep 7;83(5):501–7.
40. Delpy E, Coste H, Gouville AC. Effects of cyclic GMP elevation on isoprenaline-induced increase in cyclic AMP and relaxation in rat aortic smooth muscle: role of phosphodiesterase 3. *Br J Pharmacol*. 1996 Oct;119(3):471–8.
41. Shimokawa H, Takeshita A. Endothelium-dependent regulation of the cardiovascular system. *Intern Med Tokyo Jpn*. 1995 Oct;34(10):939–46.
42. Bellien J, Iacob M, Gutierrez L, Isabelle M, Lahary A, Thuillez C, et al. Crucial role of NO and endothelium-derived hyperpolarizing factor in human sustained conduit artery flow-mediated dilatation. *Hypertens Dallas Tex 1979*. 2006 Dec;48(6):1088–94.
43. Bellien J, Joannides R, Iacob M, Arnaud P, Thuillez C. Evidence for a basal release of a cytochrome-related endothelium-derived hyperpolarizing factor in the radial artery in humans. *Am J Physiol Heart Circ Physiol*. 2006 Apr;290(4):H1347–1352.
44. Quyyumi AA, Ozkor M. Vasodilation by hyperpolarization: beyond NO. *Hypertens Dallas Tex 1979*. 2006 Dec;48(6):1023–5.
45. Turner J, Belch JFF, Khan F. Current concepts in assessment of microvascular endothelial function using laser Doppler imaging and iontophoresis. *Trends Cardiovasc Med*. 2008 May;18(4):109–16.
46. Cracowski J-L, Lorenzo S, Minson CT. Effects of local anaesthesia on subdermal needle insertion pain and subsequent tests of microvascular function in human. *Eur J Pharmacol*. 2007 Mar 22;559(2-3):150–4.
47. Binggeli C, Spieker LE, Corti R, Sudano I, Stojanovic V, Hayoz D, et al. Statins enhance postischemic hyperemia in the skin circulation of hypercholesterolemic patients: a monitoring test of endothelial dysfunction for clinical practice? *J Am Coll Cardiol*. 2003 Jul 2;42(1):71–7.

48. Dalle-Ave A, Kubli S, Golay S, Delachaux A, Liaudet L, Waeber B, et al. Acetylcholine-induced vasodilation and reactive hyperemia are not affected by acute cyclooxygenase inhibition in human skin. *Microcirc New York N* 1994. 2004 Jun;11(4):327–36.
49. Binggeli C, Spiekler LE, Corti R, Sudano I, Stojanovic V, Hayoz D, et al. Statins enhance postischemic hyperemia in the skin circulation of hypercholesterolemic patients: a monitoring test of endothelial dysfunction for clinical practice? *J Am Coll Cardiol*. 2003 Jul 2;42(1):71–7.
50. Medow MS, Taneja I, Stewart JM. Cyclooxygenase and nitric oxide synthase dependence of cutaneous reactive hyperemia in humans. *Am J Physiol Heart Circ Physiol*. 2007 Jul;293(1):H425–432.
51. Lorenzo S, Minson CT. Human cutaneous reactive hyperaemia: role of BKCa channels and sensory nerves. *J Physiol*. 2007 Nov 15;585(Pt 1):295–303.
52. Larkin SW, Williams TJ. Evidence for sensory nerve involvement in cutaneous reactive hyperemia in humans. *Circ Res*. 1993 Jul;73(1):147–54.
53. Wong BJ, Wilkins BW, Holowatz LA, Minson CT. Nitric oxide synthase inhibition does not alter the reactive hyperemic response in the cutaneous circulation. *J Appl Physiol Bethesda Md* 1985. 2003 Aug;95(2):504–10.
54. Minson CT, Wong BJ. Reactive hyperemia as a test of endothelial or microvascular function? *J Am Coll Cardiol*. 2004 Jun 2;43(11):2147; author reply 2147–2148.
55. Nohria A, Gerhard-Herman M, Creager MA, Hurley S, Mitra D, Ganz P. Role of nitric oxide in the regulation of digital pulse volume amplitude in humans. *J Appl Physiol Bethesda Md* 1985. 2006 Aug;101(2):545–8.
56. Agarwal SC, Allen J, Murray A, Purcell IF. Comparative reproducibility of dermal microvascular blood flow changes in response to acetylcholine iontophoresis, hyperthermia and reactive hyperaemia. *Physiol Meas*. 2010 Jan;31(1):1–11.
57. Clough GF, Church MK. Vascular responses in the skin: an accessible model of inflammation. *News Physiol Sci Int J Physiol Prod Jointly Int Union Physiol Sci Am Physiol Soc*. 2002 Aug;17:170–4.
58. Minson CT, Berry LT, Joyner MJ. Nitric oxide and neurally mediated regulation of skin blood flow during local heating. *J Appl Physiol Bethesda Md* 1985. 2001 Oct;91(4):1619–26.

59. Holowatz LA, Thompson CS, Minson CT, Kenney WL. Mechanisms of acetylcholine-mediated vasodilatation in young and aged human skin. *J Physiol*. 2005 Mar 15;563(Pt 3):965–73.
60. Wilkins BW, Holowatz LA, Wong BJ, Minson CT. Nitric oxide is not permissive for cutaneous active vasodilatation in humans. *J Physiol*. 2003 May 1;548(Pt 3):963–9.
61. McCord GR, Cracowski J-L, Minson CT. Prostanoids contribute to cutaneous active vasodilation in humans. *Am J Physiol Regul Integr Comp Physiol*. 2006 Sep;291(3):R596–602.
62. Chiffлот H, Fautrel B, Sordet C, Chatelus E, Sibilia J. Incidence and prevalence of systemic sclerosis: a systematic literature review. *Semin Arthritis Rheum*. 2008 Feb;37(4):223–35.
63. Gabrielli A, Avvedimento EV, Krieg T. Scleroderma. *N Engl J Med*. 2009 May 7;360(19):1989–2003.
64. LeRoy EC, Black C, Fleischmajer R, Jablonska S, Krieg T, Medsger TA, et al. Scleroderma (systemic sclerosis): classification, subsets and pathogenesis. *J Rheumatol*. 1988 Feb;15(2):202–5.
65. LeRoy EC, Medsger TA. Criteria for the classification of early systemic sclerosis. *J Rheumatol*. 2001 Jul;28(7):1573–6.
66. Poormoghim H, Lucas M, Fertig N, Medsger TA. Systemic sclerosis sine scleroderma: demographic, clinical, and serologic features and survival in forty-eight patients. *Arthritis Rheum*. 2000 Feb;43(2):444–51.
67. Trojanowska M. Cellular and molecular aspects of vascular dysfunction in systemic sclerosis. *Nat Rev Rheumatol*. 2010 Aug;6(8):453–60.
68. Thompson AE, Shea B, Welch V, Fenlon D, Pope JE. Calcium-channel blockers for Raynaud’s phenomenon in systemic sclerosis. *Arthritis Rheum*. 2001 Aug;44(8):1841–7.
69. Kowal-Bielecka O, Fransen J, Avouac J, Becker M, Kulak A, Allanore Y, et al. Update of EULAR recommendations for the treatment of systemic sclerosis. *Ann Rheum Dis*. 2017 Aug;76(8):1327–39.
70. Black CM, Halkier-Sørensen L, Belch JJ, Ullman S, Madhok R, Smit AJ, et al. Oral iloprost in Raynaud’s phenomenon secondary to systemic sclerosis: a multicentre, placebo-controlled, dose-comparison study. *Br J Rheumatol*. 1998 Sep;37(9):952–60.

71. Scorza R, Caronni M, Mascagni B, Berruti V, Bazzi S, Micallef E, et al. Effects of long-term cyclic iloprost therapy in systemic sclerosis with Raynaud's phenomenon. A randomized, controlled study. *Clin Exp Rheumatol*. 2001 Oct;19(5):503–8.
72. Hachulla E, Clerson P, Launay D, Lambert M, Morell-Dubois S, Queyrel V, et al. Natural history of ischemic digital ulcers in systemic sclerosis: single-center retrospective longitudinal study. *J Rheumatol*. 2007 Dec;34(12):2423–30.
73. Wigley FM, Korn JH, Csuka ME, Medsger TA, Rothfield NF, Ellman M, et al. Oral iloprost treatment in patients with Raynaud's phenomenon secondary to systemic sclerosis: a multicenter, placebo-controlled, double-blind study. *Arthritis Rheum*. 1998 Apr;41(4):670–7.
74. Matucci-Cerinic M, Denton CP, Furst DE, Mayes MD, Hsu VM, Carpentier P, et al. Bosentan treatment of digital ulcers related to systemic sclerosis: results from the RAPIDS-2 randomised, double-blind, placebo-controlled trial. *Ann Rheum Dis*. 2011 Jan;70(1):32–8.
75. Nguyen VA, Eisendle K, Gruber I, Hugl B, Reider D, Reider N. Effect of the dual endothelin receptor antagonist bosentan on Raynaud's phenomenon secondary to systemic sclerosis: a double-blind prospective, randomized, placebo-controlled pilot study. *Rheumatol Oxf Engl*. 2010 Mar;49(3):583–7.
76. Kalia YN, Naik A, Garrison J, Guy RH. Iontophoretic drug delivery. *Adv Drug Deliv Rev*. 2004 Mar 27;56(5):619–58.
77. Singh S, Singh J. Transdermal drug delivery by passive diffusion and iontophoresis: a review. *Med Res Rev*. 1993 Sep;13(5):569–621.
78. Turrell WJ. The Therapeutic Action of the Constant Current. *Proc R Soc Med*. 1921;14(Electro Ther Sect):41–52.
79. Sloan JB, Soltani K. Iontophoresis in dermatology. A review. *J Am Acad Dermatol*. 1986 Oct;15(4 Pt 1):671–84.
80. Leduc S. Introduction of medicinal substances into the depth of tissues by electric current. *Ann d'electrobiol*. 1900;(3):545–60.
81. Leduc S. Electric ions and their use in medicine. 1908;
82. Costello CT, Jeske AH. Iontophoresis: applications in transdermal medication delivery. *Phys Ther*. 1995 Jun;75(6):554–63.
83. Dixit N, Bali V, Baboota S, Ahuja A, Ali J. Iontophoresis - an approach for controlled drug delivery: a review. *Curr Drug Deliv*. 2007 Jan;4(1):1–10.

84. Singh J, Bhatia KS. Topical iontophoretic drug delivery: pathways, principles, factors, and skin irritation. *Med Res Rev.* 1996 May;16(3):285–96.
85. Tesselaar E, Sjöberg F. Transdermal iontophoresis as an in-vivo technique for studying microvascular physiology. *Microvasc Res.* 2011 Jan;81(1):88–96.
86. Holbrook KA, Odland GF. Regional differences in the thickness (cell layers) of the human stratum corneum: an ultrastructural analysis. *J Invest Dermatol.* 1974 Apr;62(4):415–22.
87. Cracowski JL, Gaillard-Bigot F, Cracowski C, Sors C, Roustit M, Millet C. Involvement of cytochrome epoxygenase metabolites in cutaneous postocclusive hyperemia in humans. *Journal of applied physiology.* 2013 Jan 15;114:245–51.
88. Roustit M, Millet C, Blaise S, Dufournet B, Cracowski JL. Excellent reproducibility of laser speckle contrast imaging to assess skin microvascular reactivity. *Microvasc Res.* 2010 Dec;80(3):505–11.
89. Rousseau P, Mahé G, Haj-Yassin F, Durand S, Humeau A, Leftheriotis G, et al. Increasing the “region of interest” and “time of interest”, both reduce the variability of blood flow measurements using laser speckle contrast imaging. *Microvasc Res.* 2011 Jul;82(1):88–91.
90. Millet C, Roustit M, Blaise S, Cracowski JL. Comparison between laser speckle contrast imaging and laser Doppler imaging to assess skin blood flow in humans. *Microvasc Res.* 2011;82(2):147–51.
91. Cracowski JL, Minson CT, Salvat-Melis M, Halliwill JR. Methodological issues in the assessment of skin microvascular endothelial function in humans. *Trends Pharmacol Sci.* 2006 Sep;27:503–8.
92. Cankar K, Finderle Z, Strucl M. The effect of alpha-adrenoceptor agonists and L-NMMA on cutaneous postocclusive reactive hyperemia. *Microvasc Res.* 2009;77(2):198–203.
93. Lenasi H. The role of nitric oxide- and prostacyclin-independent vasodilatation in the human cutaneous microcirculation: effect of cytochrome P450 2C9 inhibition. *Clin Physiol Funct Imaging.* 2009 Jul;29:263–70.
94. Hachulla E, Clerson P, Launay D, Lambert M, Morell-Dubois S, Queyrel V, et al. Natural history of ischemic digital ulcers in systemic sclerosis: single-center retrospective longitudinal study. *The Journal of rheumatology.* 2007 Dec;34:2423–30.

95. Guillevin L, Hunsche E, Denton CP, Krieg T, Schwierin B, Rosenberg D, et al. Functional impairment of systemic scleroderma patients with digital ulcerations: results from the DUO Registry. *Clin Exp Rheumatol*. 2013 Apr;31(2 Suppl 76):71–80.
96. Kotzki S, Roustit M, Arnaud C, Godin-Ribuot D, Cracowski J-L. Effect of continuous vs pulsed iontophoresis of treprostinil on skin blood flow. *Eur J Pharm Sci Off J Eur Fed Pharm Sci*. 2015 May 25;72:21–6.
97. Blaise S, Roustit M, Millet C, Ribuot C, Boutonnat J, Cracowski JL. Cathodal iontophoresis of treprostinil and iloprost induces a sustained increase in cutaneous flux in rats. *Br J Pharmacol*. 2011 Sep 22;162:557–65.
98. Blaise S, Roustit M, Hellmann M, Millet C, Cracowski JL. Cathodal iontophoresis of treprostinil induces a sustained increase in cutaneous blood flux in healthy volunteers. *Journal of clinical pharmacology*. 2013 Jan;53:58–66.
99. Roustit M, Gaillard-Bigot F, Blaise S, Stanke-Labesque F, Cracowski C, Seinturier C, et al. Cutaneous iontophoresis of treprostinil in systemic sclerosis: a proof-of-concept study. *Clin Pharmacol Ther*. 2014 Apr;95(4):439–45.
100. Hellmann M, Roustit M, Gaillard-Bigot F, Cracowski J-L. Cutaneous iontophoresis of treprostinil, a prostacyclin analog, increases microvascular blood flux in diabetic malleolus area. *Eur J Pharmacol*. 2015 Jul 5;758:123–8.
101. Tonelli AR, Ahmed MK, Alkukhun L, Cikach F, Aulak K, Dweik RA. Treprostinil Iontophoresis in Idiopathic Pulmonary Arterial Hypertension. *Am J Respir Crit Care Med*. 2015 Oct 15;192(8):1014–6.